TRIUMF

ISAC

ISAC-II
A PROJECT FOR HIGHER ENERGIES AT ISAC

TRI-99-1

TRI–99–1

TRIUMF ISAC

ISAC–II
A PROJECT FOR HIGHER ENERGIES AT ISAC

Contents

1 Executive Summary

In the field of nuclear physics it is generally acknowledged that a new frontier will be probed when radioactive ion beams of sufficient intensity and quality become available. With the ISAC facility, TRIUMF has positioned itself as offering the best possible source of exotic beams in the world for many years to come. Based upon the ISOL method of production with a 100 μA, 500 MeV proton beams incident on thick targets, the production source has been built and is starting to operate. The intensity of the proton beam will be progressively increased as the commissioning of the remote handling facilities and the production target development proceed.

While the source will produce any elements within the constraints of target/ion source efficiencies, the initial facility, ISAC-I, has been optimized for the requirements of the nuclear astrophysics program ($A \leq 30$ and $E \leq 1.5$ MeV/u) as far as the accelerator systems are concerned. The scientific program has been initiated and is catering to precision tests of the Standard Model, static properties of exotic nuclei, and opportunities in condensed matter research.

ISAC-II is a project that will extend the reach of ISAC-I both in energy and mass. The demands of the nuclear-structure community, in Canada and worldwide, would be largely satisfied by raising the final energy for all masses up to $A = 150$ to 6.5 MeV/u; an energy sufficient to overcome the Coulomb barrier for all possible target nuclei. Current interests focus on nuclear-structure physics from heavy-ion fusion-evaporation reactions with proton- or neutron-rich projectiles, the spectroscopy of exotic nuclei with resonance reactions, studies of shell structures near the limits of stability, the exploitation of the isospin degree of freedom to study heavy-ion reaction dynamics, Coulomb excitation of neutron-rich nuclei relevant to astrophysical processes and reaction-mechanism studies with neutron-rich projectiles leading to the production of heavy elements. While some of the instruments, which were dispersed after the closure of TASCC, would be reconfigured for a new life at ISAC, some more modern spectrometers would also be built.

The accelerator complex would be modified by increasing the energy at which the initial stripping occurs (from 150 keV to 400 keV) by the addition of a short DTL linac section after the present RFQ accelerator. It will be followed by a superconducting linac based upon existing technologies (Legnaro or Argonne). A modular cavity configuration will be used to reach 6.5 MeV/u for $A = 150$ (and higher energies for lower masses) while maintaining very high transport efficiency throughout the accelerator. The extended mass range is obtained by introducing a state-of-the-art charge-state boosting system between the present ion source/separator system and the RFQ.

It is anticipated that an initial configuration giving energies in the 5 MeV/u range for masses up to $A = 60$ would be available in the latter part of the year 2003.

The ISAC experimental complex will require additional buildings to provide space for the new accelerator and their ancillary services as well as a new experimental area for the research program. In the planning, further improvements are anticipated to allow for the possibility of servicing several users concurrently by increasing the number of sources of radioactive ions.

With its ISAC-II extension, TRIUMF will provide a truly unique radioactive beam facility, which will meet the demands of a large segment of the community worldwide as was recommended by the Working Group in Nuclear Physics of the OECD Megascience Forum.

2 Introduction

In June 1995, the Canadian government funded the construction of a new exotic beam facility at TRIUMF called ISAC (Isotope Separator and ACcelerator), which will provide intense beams of accelerated radioactive isotopes by the fall of the year 2000 with energies up to 1.5 MeV per atomic mass unit (u). This document describes a proposed extension to the TRIUMF-ISAC facility, which will provide exotic beams at energies above the Coulomb barrier, opening up new research opportunities in nuclear physics. The intent is to exploit the unique high intensity source of exotic ions with masses $A \leq 150$ u, which has been developed at ISAC, and accelerate them with only minimal losses of intensity up to energies of 6.5 MeV/u. As such ISAC-II will be one of the first of a new generation of facilities the need for which has been identified by nuclear physicists worldwide (see OECD Megascience Forum working group on nuclear physics [1]), and will provide Canadian physics with a unique tool for many years to come.

After a brief review of the characteristics of ISAC-I, the physics topics that could be addressed at ISAC-II are discussed in Section 4 with a particular emphasis on the Canadian community's interest. Some of the experimental equipment needed to support this range of physics is described in Section 5. In Section 6 the concept for an experimental facility is developed that will provide initial beams of higher energy as early as 2003. Beam energies, intensities and mass range will be upgraded in the following two years. In Section 7, safety issues are discussed while in Section 8, an outline of the schedule and cost estimates is given. Other possible future developments are discussed in Section 9.

3 ISAC-I

ISAC produces radioactive beams by the ISOL method using intense beams of protons at 500 MeV to bombard thick isotope production targets. The facility is being constructed with a capability to handle proton beam intensities on target of up to 100 μA. Protons from the TRIUMF main cyclotron are extracted into a new beam line that feeds into the new ISAC building. In the target hall, two target stations will receive the proton beam alternatively to increase the efficiency of ion beam delivery. Having two target stations will allow efficient use of different targets, an important feature since the success of the facility depends crucially on target technology. The artist's conceptual view of the new ISAC facility at TRIUMF is presented in Fig. 1.
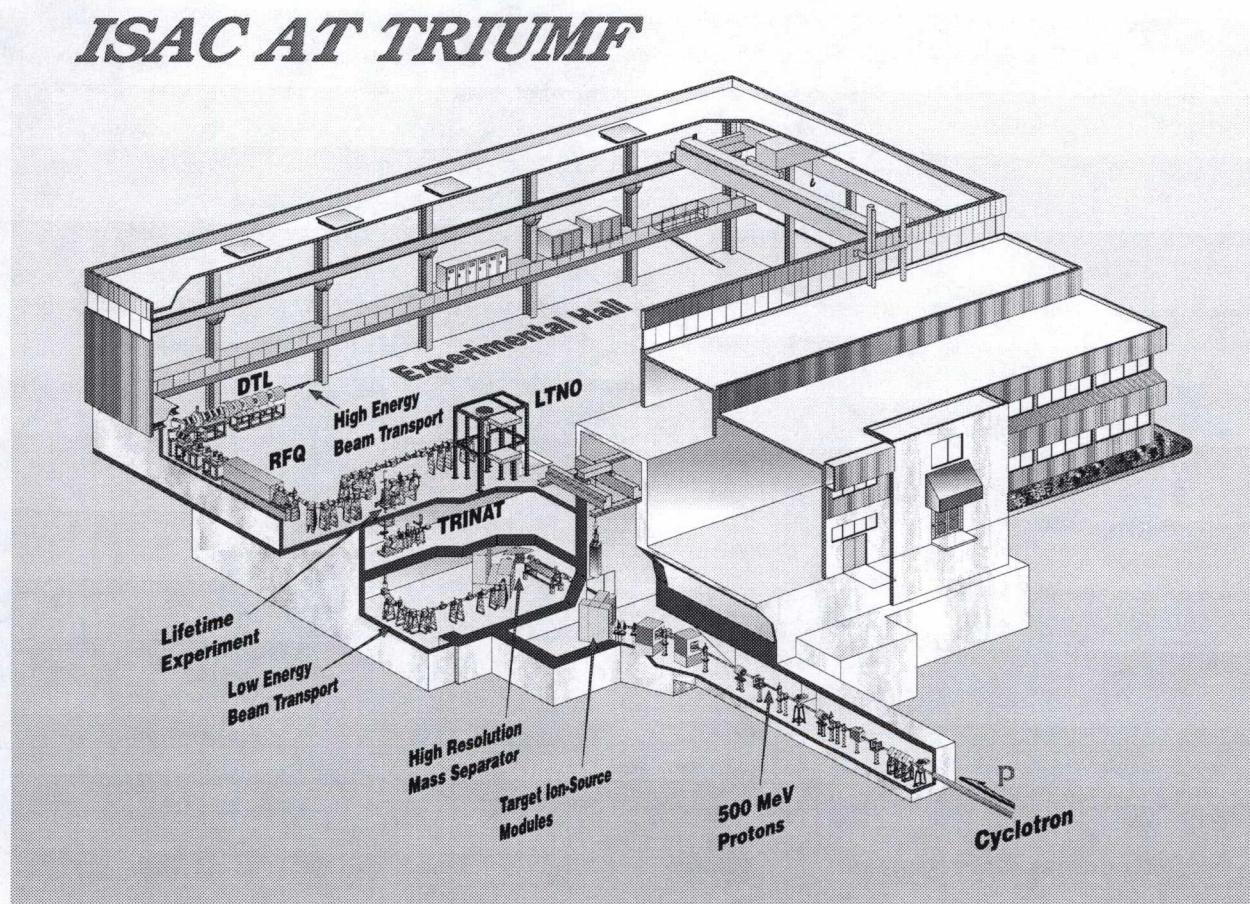
Figure 1: Sketch of the ISAC-I building layout.

The target is coupled to the ion source via a small transfer tube. Several types of ion sources will be available; the first operation uses a surface ionization source to produce beams of alkali elements. In addition, this ion source should also produce beams of elements such as Sr, Ga, Yb, and others. Development has started on a compact microwave ECR ion source to produce beams of volatile elements. At present there are conceptual plans to develop other sources, such as FEBIAD

or Laser ion sources.

The target area will be the most activated location of the new ISAC facility. To handle the components of the proton beam line near the production target and the first elements of the ion beam production, it was decided to use the concept of a double vacuum enclosure with a shielding plug (2 m in height) above each component. Services, connections and vacuum couplings are outside the high radiation field region where a hands-on operation is possible. The replacement of components can be done remotely via a high-precision crane and through an appropriate hot cell.

After exiting the ion source, the ion beam is mass analyzed, by a low-resolution pre-separator followed by a high acceptance mass analyzer with a resolving power of $\Delta M/M \simeq 1/10000$. The high-resolution separator sits on a HV platform to allow the operation of the mass separator at constant momentum, independent of the actual beam energy. The mass separated beam is then directed vertically from the underground mass separator floor, up approximately 8 m to the experimental hall located at the ground level. Alternatively, the beam can be deflected to the TRINAT (TRIUMF Neutral Atom Trap) facility, located on a well-shielded intermediate floor. Once at ground level in the new ISAC experimental hall, the beam will be directed either to the radiofrequency quadrupoles/drift-tube linac (RFQ/DTL) accelerators for experiments with accelerated beam (HE), or to the experimental areas planning to use the unaccelerated radioactive beams at 60 keV (LE). The 35 MHz cw RFQ accelerator will take a singly charged ion beam with $q/A > 1/30$ from 2 keV/u to 150 keV/u. After the RFQ, the beam will be stripped, and the selected charge directed to a cw DTL which will accelerate an ion beam with $q/A > 1/6$ to the desired energy in the range from 0.15 to 1.5 MeV/u. The entire acceleration system including matching sections between the RFQ and DTL are expected to be ready for commissioning by the beginning of 2000. It is anticipated that radioactive beams at full energy will be available in the HE experimental area by the fall of 2000.

3.1 Experimental Program

A wide range of radioactive beams at low energy ($\leq$ 60 keV) will be provided for a number of experimental programs including: 1) the test of weak interaction symmetries by trapping radioactive atoms in a magneto-optic trap; 2) tests of the conserved-vector current (CVC) hypothesis and the Standard Model from precise measurements of the intensities for superallowed Fermi $0^+ \rightarrow 0^+$ β-decay; 3) a systematic study of ground state moments for nuclei far from stability using low-temperature nuclear orientation methods; 4) condensed matter studies of small structures and interfaces in semiconductors and superconductors by β-NMR with a polarized ^{8}Li beam; and 5) the production of pure radionuclides of importance in nuclear medicine.

The accelerated radioactive ion beams with masses $A < 30$ and energies from $0.15 - 1.5$ MeV/u will be used primarily for research in nuclear astrophysics. The HE experimental area will house a state of the art recoil separator (DRAGON) and a general purpose scattering facility. Figure 2 gives a general layout of the planned experimental facilities in the ISAC hall.

For more details on the ISAC-I facility and its initial scientific program, the reader is referred to references [2, 3, 4].
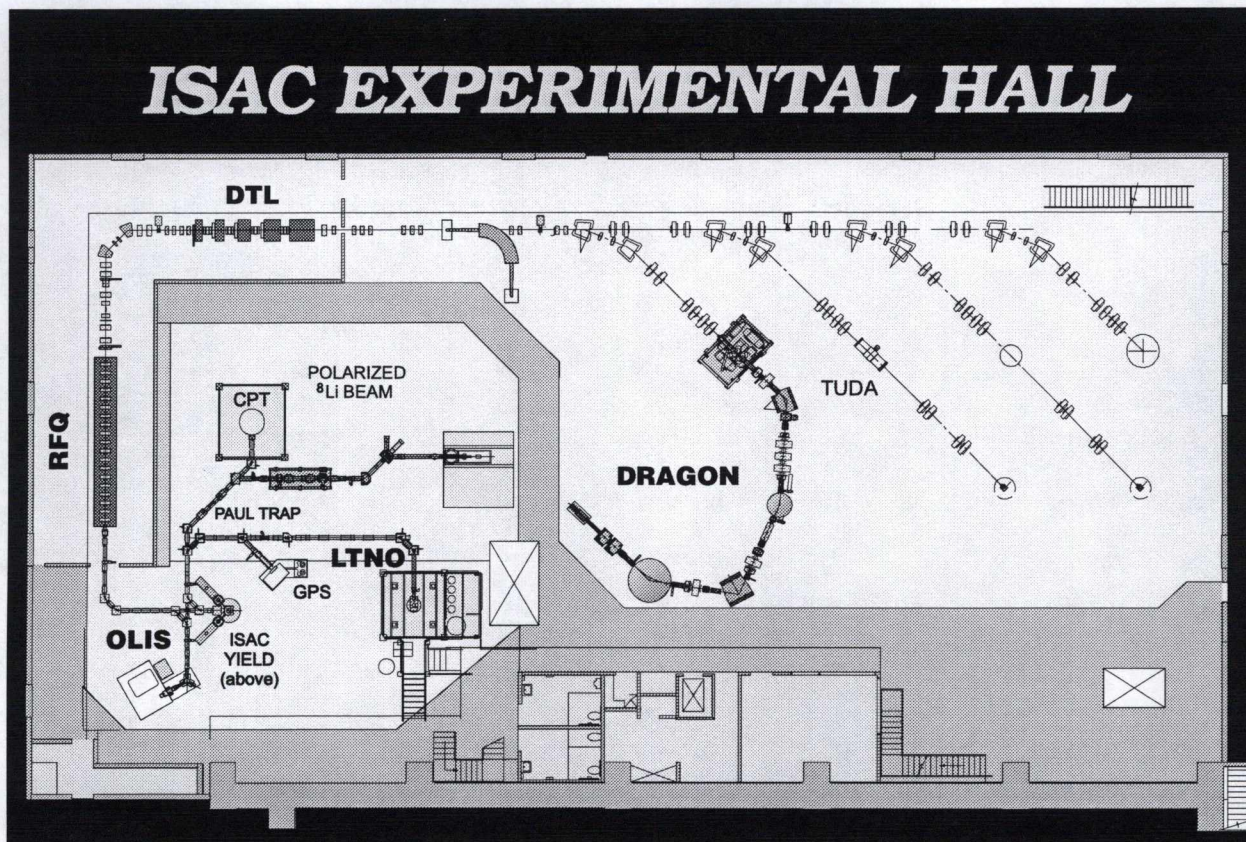
Figure 2: Planned layout of scientific stations in the ISAC experimental hall.

3.2 Radioactive Beam Intensities

A key part of any radioactive beams facility is the intensity of the available radioactive beam. At ISAC, spallation, fission or fragmentation of the target using 500 MeV protons will produce the desired radioactive beam. The final radioactive beam intensity, I, is given by

$$I = \phi \sigma N_\alpha \epsilon_1 \epsilon_2 \eta,$$

where σ is the production cross section, ϕ is the proton beam intensity, N_α is the target thickness, ϵ_1 is the combined efficiencies for diffusion of the wanted species in the thick matrix of the target and the effusion of the species from the target matrix to the ion source, ϵ_2 is the efficiency for ionization in the selected ion source, and η is the overall efficiency for any transmission in the isotope separator and any further acceleration stage. A more complete discussion can be found in the ISAC-I proposal document [2] and references therein.

It is a difficult task to predict precisely the final intensities that can be obtained, mainly because of the uncertainty in ϵ_1. Fortunately, the operation of thick target on-line isotope separators has been studied in detail for over 30 years at various laboratories including at the TISOL facility at TRIUMF and a great deal of information is available. Projected beam intensities for ISAC based primarily on calculations but also tempered by such experiences of the field were presented in the

Table I: Projected Beam Intensities (particles/s) at ISAC for 1 μA of Protons on Target

Beam	$T_{\frac{1}{2}}$	Calculated Isotope Production Rate			Best Observed Ion Yields at 0.5 GeV			Transmission to 1.5 MeV/u
		Target	Thickness (g/cm^2)	Rate (p/s/μA)	Target	Thickness (g/cm^2)	Yield (p/s/μA)	(%)
^{8}He	122 ms	UC$_2$	58	6.9×10^6	ThC	55	$^I 6.6 \times 10^5$	90
^{8}Li	842 ms	Ta	121	2.2×10^9	Ta	122	$^I 3.9 \times 10^8$	85
^{11}Li	9 ms	Ta	121	2.1×10^6	–	–	–	85
^{7}Be	53.3 d	C	45	9.3×10^{10}	–	–	–	70
^{11}C	20 m	MgO	29	4.1×10^{10}	MgO	3	$^I 6.8 \times 10^5$	60
^{16}C	747 ms	MgO	29	4.7×10^7	CaO	6.5	$^I 4.0 \times 10^3$	60
^{13}N	10 m	Zeolite	33	2.0×10^{11}	CaO	6.5	$^I 2.4 \times 10^4$	55
^{18}N	624 ms	Zeolite	33	4.1×10^8	Zeolite	13.1	$^T 3.4 \times 10^3$	40
^{14}O	71 s	Zeolite	33	6.7×10^{10}	Zeolite	4.4	$^T 8.5 \times 10^4$	50
^{15}O	2.0 m	Zeolite	33	2.1×10^{11}	–	–	–	50
^{22}O	2.3 s	Pt	27	1.9×10^6	Pt	27	$^I 4.5 \times 10^2$	40
^{17}F	65 s	SiC	19	1.1×10^{10}	SiC	19	$^I 1.1 \times 10^7$	48
^{19}Ne	17 s	Zeolite	33	1.0×10^{10}	Zeolite	13.1	$^T 3.3 \times 10^8$	45
^{26}Ne	162 ms	UC$_2$	58	2.7×10^8	–	–	–	35
^{20}Na	446 ms	SiC	8.1	7.7×10^9	SiC	8.1	$^T 1.2 \times 10^6$	43
^{30}Na	53 ms	UC$_2$	58	1.9×10^7	UC	4	$^I 1.4 \times 10^4$	35
^{26m}Al	6 s	SiC	45	2.5×10^{11}	UC	9.7	$^I 4.0 \times 10^4$	38
^{34}Ar	884 ms	Ti	65	8.7×10^7	Nb	47	$^I 5.5 \times 10^6$	–
^{46}Ar	88 s	VC	62	7.6×10^6	CaO	5	$^I 3.0 \times 10^4$	–
^{37}K	1.2 s	TiC	50	6.0×10^8	CaO	36	$^T 2.9 \times 10^7$	–
^{64}Ge	64 s	ZrO$_2$	80	4.6×10^6	–	–	–	–
^{73}Se	7 h	ZrO$_2$	80	2.2×10^{10}	ZrO$_2$	6.3	$^I 2.1 \times 10^8$	–
^{74}Kr	12 m	ZrC	80	4.5×10^8	Nb	50	$^I 2.0 \times 10^6$	–
^{91}Kr	8.6 s	UC$_2$	58	1.9×10^9	ThC	55	$^I 1.5 \times 10^8$	–
^{105}Cd	56 m	Sn	108	1.0×10^{10}	Sn	120	$^I 3.5 \times 10^8$	–
^{111}In	2.8 d	Sn	108	1.2×10^{11}	Ta	122	$^I 5.3 \times 10^7$	–
^{108}Sn	10 m	TeCl$_4$	61	1.4×10^8	TeCl$_4$	–	$^I 5.0 \times 10^6$	–
^{132}Sn	40 s	UC$_2$	58	1.0×10^8	UC$_2$	9.7	$^I 3.0 \times 10^7$	–
^{119}Xe	5.8 m	LaC$_2$	103	2.5×10^9	La	124	$^I 4.1 \times 10^5$	–
^{142}Xe	1.2 s	UC$_2$	55	1.9×10^9	ThC	55	$^I 4.2 \times 10^6$	–
^{121}Cs	2.3 m	La	140	1.2×10^{10}	La	140	$^I 7.3 \times 10^9$	–
^{160}Yb	4.8 m	Ta	122	9.9×10^9	Ta	130	$^I 4.0 \times 10^9$	–
^{210}Fr	3.0 m	ThC	55	7.0×10^8	ThC	55	$^I 1.9 \times 10^9$	–

I = ISOLDE Data from CERN SC T = TISOL Data from TRIUMF

6

ISAC-I proposal document [2] and an updated version is reproduced here as Table I. The isotopes listed in this table were chosen partially as a result of the interests of the scientific program planned for ISAC-I and partially as a result of the comparison presented in the NUPECC report of European facilities. Accelerator efficiencies for species heavier than $A = 30$ were not considered since they could not be accelerated with the ISAC-I accelerators. It is also assumed that the appropriate ion source will be made available to ionize the required species. Present plans at ISAC include a heated surface ion source, an RF-plasma, ECR-like ion source and a laser ion source. Table I can still be used to indicate projected intensities for a wide range of isotopes in the low-energy and high-energy experimental regions of ISAC-I for production beam intensities of 1 μA.

3.3 Development of ISAC-I Towards High Intensities and Higher Masses

The accelerated beam of ISAC-I, up to 1.5 MeV/u will be available by the end of 2000 when experiments in nuclear astrophysics can start with the DRAGON recoil spectrometer. Although ISAC-I will be completed at that point as far as energy is concerned, much development work will have to take place on ion sources and targets as the complex moves towards operation at 100 μA. From the point of view of shielding, activation handling, and remote manipulation, every system has been built with the requirement for 100 μA proton current operation in mind. R&D on targets capable of sustaining the power deposition of a 100 μA proton beam has started but will be intensified during the next few years. To produce a wide variety of isotopes it is envisaged that a laser ionization system will be built as demonstrated by the CERN-ISOLDE collaboration. The simplicity of these type of sources and the specificity of the ionization process makes them ideal candidates for high current operation.

The next logical step to increase the available mass range of accelerated ion beams at ISAC is to increase the charge-state of ions entering the RFQ. Electron-cyclotron-resonance (ECRIS) and electron beam (EBIS) ion sources easily reach the required $q/A = 1/30$ for masses up to $A = 150$ and are under intensive development (GANIL, Grenoble). Sufficient space has been reserved in the low-energy beam transport system to install ion sources such as ECRIS or EBIS. A charge booster producing a q/A of at least 1/30 would allow acceleration of all masses up to an energy of 1.5 MeV/u provided that additional stripping is used after the RFQ to bring q/A to 1/6 or greater.

A charge-booster system, which would produce efficiently $q/A=1/6$ for any mass, would eliminate the need for additional stripping.

4 ISAC-II – An Advanced Nuclear Physics Research Facility

4.1 Global Perspective

With the development of a new generation of facilities capable of providing intense beams of radioactive ions (RIB), new opportunities are opening up in nuclear physics research at both the fundamental and applied level. There is a worldwide interest in radioactive nuclear beams, which has been documented in several recent studies and reports.

For example, the study conducted under the aegis of the OECD Megascience Forum Nuclear Physics Working Group (1996 - 1998) identified RIB as an area of the highest scientific interest. The scientific issues of this new field have been documented in the following recent publications:

- ISAC-I proposal (Canada, 1993) [5]

- "RIKEN proposal for a RI Beam Facility" (Japan, 1994) [6]

- "Long Range Plan" of the "Nuclear Science Advisory Committee" (USA, 1996) [7]

- "Scientific Opportunities with an Advanced ISOL Facility", Columbus white paper (USA, 1997) [8]

- "Proposal for Japan Hadron Facility" (Japan, 1997) [9]

- "Nuclear Physics in Europe: Highlights and Opportunites", report from the "Nuclear Physics European Collaboration Committee" (Europe, 1997) [10]

- Report of the Study Group on Radioactive Nuclear Beams (OECD Megascience Working Group on Nuclear Physics, 1999) [1]

- SIRIUS Science (CLRC, U.K., 1999) [11]

While ISAC-I has been designed to address issues in a varity of fields, nuclear astrophysics, fundamental opportunities, condensed matter physics, nuclear medicine and applied engineering, ISAC-II with increased energy and mass range will open up many more exciting areas of research in nuclear physics, for example, in nuclear structure and nuclear reactions studies.

In 1997, a study in the United States concluded that radioactive ion beams with $A \leq 150$ and energies ≤ 15 MeV/u are required to investigate many of the exciting nuclear-structure and nuclear-reaction physics currently open. This conclusion is documented in the US White Paper "Scientific Opportunities with an Advanced ISOL facility" [8]. The physics reach of this study is summarised in Fig. 3 and Table II taken from that report. ISAC-II would be a world-class facility capable of accessing most of this physics. The choice of topics to be pursued would depend on the interests of the Canadian nuclear physics community and the international users of ISAC-II and on the availability and/or development of the instrumentation required to exploit these exotic beams.

Presently our understanding of the nucleus is based primarily on the relatively small number of isotopes near the valley of stability that can be produced with stable beams. Upgrading ISAC-I would allow physicists to study nuclei with unusual ratios of proton number Z to neutron number
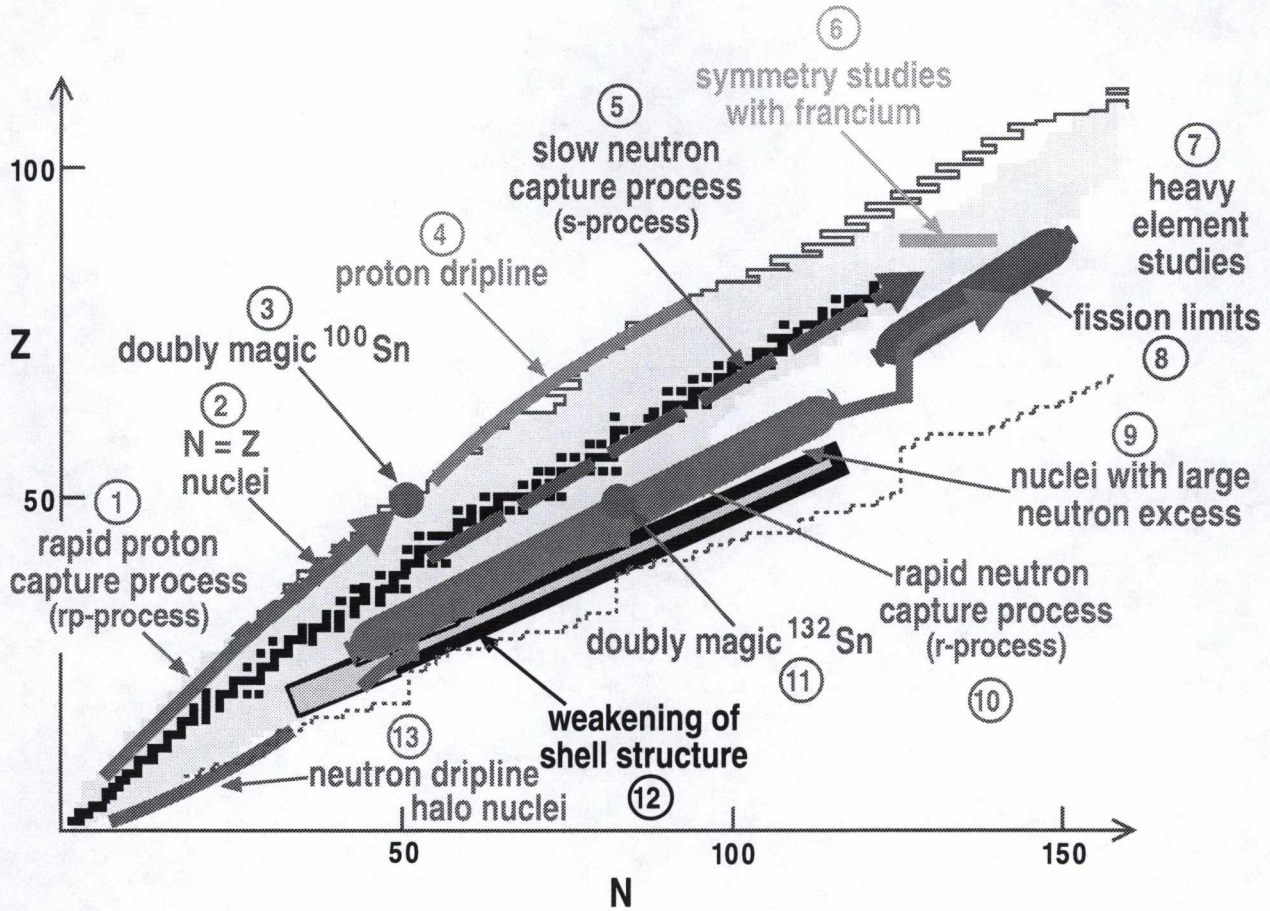
Figure 3: Illustration of research opportunities with beams of short-lived nuclei produced at ISAC. The circled numbers correlate with the entries in Table II.

N, providing access to physics that cannot be studied with normal stable beams and targets. Many physics topics could be explored using the full range of nuclear techniques developed for studies with stable beams. Of particular interest are the loosely bound nuclei near the limits of nuclear existence, which are expected to exhibit new shell structure and new collective modes. Accelerated radioactive ion beams will allow these nuclei to be studied in detail and provide answers to questions such as: how do extremes of isospin and neutron density affect the nucleon-nucleon and spin-orbit forces; what is the form of the pairing interaction for weakly-bound nuclei; how does the nuclear shell structure evolve with N/Z; and what, if any, are the magic numbers at the limits of stability. These are all questions of key importance to an understanding of the nucleus as a many-body quantum system.

The single-particle energies and the effective interaction of exotic nuclei near closed shells, e.g., ^{132}Sn could be studied by single-nucleon transfer reactions such as (d, p) and (p, d), in inverse kinematics with beams of $6 - 10$ MeV/u. The low-lying collective properties of nuclei and the coupling to single-particle degrees of freedom can be explored by the Coulomb excitation of radioactive projectiles.

Table II: Representative examples of beam requirements for the general research areas discussed in the US White Paper "Scientific Opportunities with an Advanced ISOL facility" and schematically illustrated in Fig. 3. Only a few typical ion species are shown for each entry to exemplify the intensity and energy ranges needed for performing experiments in these areas.

Physics Topics[a]	Reactions and Techniques	Beams	Desired Intensities [particles/s]	Energy Range [MeV/u]
1. Rapid proton capture (rp-process)	transfer, elastic, inelastic radiative capture, Coulomb dissociation	^{14}O, ^{15}O ^{26}Si, ^{34}Ar, ^{56}Ni	$10^8 - 10^{11}$ $10^5 - 10^{11}$	0.15−15
2. Reactions with and studies of $N = Z$ nuclei, symmetry studies	transfer, fusion, decay studies	^{56}Ni, ^{62}Ga, ^{64}Ge, ^{68}Ge, ^{67}As, ^{72}Kr	$10^4 - 10^9$	0.1−15
3. Decay studies of ^{100}Sn	decay	^{100}Sn	1−10	low
4. Proton dripline studies	decay, fusion, transfer	^{56}Ni, ^{64,66}Ge, ^{72}Kr	$10^6 - 10^9$	5
5. Slow neutron capture (s-process)	capture	^{134,135}Cs, ^{155}Eu	$10^8 - 10^{11}$	0.1
6. Symmetry studies with francium	decays, traps	^{A}Fr	10^{11}	low
7. Heavy element studies	fusion, decay	$^{50-52}$Ca, ^{72}Ni ^{84}Ge, ^{96}Kr	$10^4 - 10^7$ $10^6 - 10^8$	5−8
8. Fission limits	fusion-fission	$^{140-144}$Xe, $^{142-146}$Cs ^{142}I, $^{145-148}$Xe, $^{147-150}$Cs	$10^7 - 10^{11}$ $10^4 - 10^7$	5
9. Rapid neutron capture (r-process)	capture, decay, mass measurement	^{130}Cd, ^{132}Sn, ^{142}I	$10^4 - 10^9$	0.1−5
10. Nuclei with large neutron excess	fusion, transfer, deep inelastic	$^{140-144}$Xe, $^{142-146}$Cs ^{142}I, $^{145-148}$Xe, $^{147-150}$Cs	$10^7 - 10^{11}$ $10^2 - 10^7$	5−15
11. Single-particle states, effective nucleon-nucleon interactions	direct reactions, nucleon transfer	^{132}Sn, ^{133}Sb	$10^8 - 10^9$	5−15
12. Shell structure, weakening of gaps, spin-orbit potential	mass measurement, Coulomb excitation, fusion, nucleon transfer, deep inelastic	^{A}Kr, ^{A}Sn, ^{A}Xe	$10^2 - 10^9$	0.1−10
13. (Near) neutron-dripline studies, halo nuclei	mass measurement, nucleon transfer	^{8}He, ^{11}Li ^{29}Ne, ^{31}Na, ^{76}Cu	$10^6 - 10^8$ $10^3 - 10^6$	5−10

[a] The numbers 1-13 refer to the corresponding labelling in Fig. 3

Radioactive beams have already been used to study light neutron-rich nuclei. Near the drip-line the weakly-bound valence neutrons have been found to occupy orbits at large distances outside the nuclear core (i.e., halo nuclei). This property of halo nuclei could significantly alter the cross sections for sub-Coulomb barrier reactions and might lead to an oscillation of the weakly-bound neutrons against the core. In addition, the low Q-values for multi-neutron transfer would permit the study of neutron-rich heavy nuclei. Heavier neutron-rich nuclei near the drip-line are predicted also to have an excess of neutrons at large distances (i.e., neutron skin), which will strongly affect nuclear interactions in this region.

Proton radioactivity will play an important role in the study of extremely proton-rich nuclei. Since the proton drip-line lies much closer to the valley of stability it should be possible to investigate the structure of these nuclei up to $Z \sim 82$ using short-lived radioactive beams and new experimental techniques such as recoil-decay tagging.

The nuclei near the $N = Z$ line are predicted to exhibit a wide variety of shape transformations and collective/non-collective transitions as a function of angular momentum. The study of mirror nuclei can be used to investigate the charge independence of the strong force. Neutron-proton ($S = 1$, $T = 0$) pairing is expected to occur for $N = Z$ nuclei with $A > 60$. The ultimate goal is to study the properties of ^{100}Sn, the heaviest particle-stable $N = Z$ closed-shell nucleus.

The synthesis of heavy elements beyond uranium using heavy-ion fusion reactions has been studied for decades and remains an exciting frontier of nuclear stability. Sophisticated detection techniques have been developed that have led to the discovery of elements up to Z=112, (and possibly elements Z=118, 116 and 114 [12]). Current models predict a spherical doubly magic nucleus with 184 neutrons and 114 (126) protons. Radioactive beams of neutron-rich nuclei such as $^{90-96}$Kr would provide a method to explore neutron-rich isotopes of heavy elements not accessible with stable beams. They would also provide new information on the reaction mechanism, in particular, the effect of a neutron skin on the enhancement of the fusion process.

Resonance reactions such as elastic and inelastic proton scattering, (p, α), (p, n) and (α, p) etc., are an incisive spectroscopic tool for the study of particle-unstable discrete states. Early experience with radioactive beams has demonstrated the potential for such studies which would generally require beams of $A < 60$ at continuously variable energies of $E \leq 3$ MeV/u. This program would have a strong overlap with the interests of nuclear astrophysics.

Finally, nuclear reaction mechanisms can be studied in new and more specific ways with radioactive ion beams, which remove the limitations of target/projectile combinations with stable beams (e.g., exploitation of the isospin degree of freedom). In addition, the structure of the weakly-bound proton/neutron-rich nuclei could have a profound effect on many reaction processes.

4.2 Canadian Perspective

The Canadian nuclear physics community made a strong submission to have ISAC-I extended. ISAC-I is arguably the best facility of its kind in the world and would continue to be so, well into the 21st century provided the maximum energy and mass ranges were increased. This upgrade is called ISAC-II. The recent (November, 1997) report "Scientific Opportunities with an Advanced ISOL Facility" [8], illustrates the excitement in the US for such an accelerated radioactive beam facility. From a Canadian perspective, it was clear that although Canada has been a world leader in

nuclear physics for much of this century, its future capability could be jeopardized unless a facility for world-class scientific research is provided promptly.

To reach these goals, the Canadian community has identified some generalized facility specifications. There are few requests for accelerated masses above mass number, $A = 150$. In general a maximum energy of 6.5 MeV/u is acceptable, although there are requests for greater than 10 MeV/u for some lighter masses. The users were not prepared to consider a pulsed accelerator because the loss in beam intensity is deemed unacceptable. The community also emphasized the advantages of having higher mass and/or energy beams available from ISAC-II before 2005. In particular, if by 2003 a wide range of light (A≤60) radioactive ion beams were available from ISAC-II at full intensity for energies ≤5 MeV/u, Canadian physicists would have the opportunity to begin this exciting research at a facility that would remain unique in the world for several years. New physics results would be obtained immediately. In addition, the experience gained would be invaluable in developing new techniques and experimental apparatus required to exploit the full range of exotic beams from ISAC-II in 2005.

The initial experimental program at ISAC-II will be constrained by the instrumentation available. Present instruments will need upgrades and new ones are planned. They are either gamma arrays, charge-particle detector arrays, or recoil separators.

In this section, some of the scientific issues that would be addressed with these facilities are described while more details on these instruments is given in Section 5.

Letters of intent have already been submitted to the TRIUMF experimental evaluation committee (EEC) to relocate two Canadian experimental facilities at ISAC-II, namely: the 8π spectrometer and the HÉRACLÈS 4π multi detector array. The ISAC-II physics interests of Canadian and international collaborations include: 1) nuclear structure physics from heavy-ion fusion-evaporation reactions with proton and neutron-rich projectiles; 2) spectroscopy of exotic nuclei with resonance reactions; 3) nuclear shell structure of nuclei far from stability from one and two-nucleon transfer reactions with radioactive beam in inverse kinematics; 4) exploiting the isospin degree of freedom in the study of heavy-ion reaction dynamics with light ($A < 40$) ions at $E \geq 6.5$ MeV/u; 5) Coulomb excitation of neutron-rich nuclei of importance to the rapid neutron capture (r-) process and where the weakening of the shell structure of nuclei is predicted; 6) the mechanism of heavy-ion reactions with neutron-rich projectiles leading to the production of heavy elements; and 7) an extension of the ISAC-I nuclear astrophysics program to higher masses using the DRAGON recoil separator and general purpose scattering facility, TUDA, currently under development.

4.3   Spectroscopy of Exotic Nuclei in Gamma-Ray Studies

A primary motivation for the construction of an accelerated radioactive beam facility is to provide unique opportunities for the study of specific nuclei away from the valley of stability. The interest arises largely from the desire to achieve a deeper understanding of nuclear structure but also from the need to determine the properties of specific levels of importance in other fields, particularly nuclear astrophysics.

A variety of models of nuclear structure have been developed to account for the diverse properties measured for those nuclei currently accessible to experiment, which tend to be concentrated near the valley of beta stability. The limited experimental data so far available for the exotic nuclei

far from stability already reveal striking new features such as the existence of neutron halos and possibly a related low-lying collective $E1$ mode of excitation. Also of note are the apparent collapse of the $N = 20$ shell closure for $Z = 10 - 12$ and strong quadrupole deformation of the ground states of nuclei in the region $Z = N \sim 40$. Moreover, analyses with existing theories suggest one should expect other important new features to be seen in the properties of nuclei far from stability.

While there are many exciting possibilities for experiments with the radioactive beams from ISAC-II, the experimental techniques required will be varied and difficult. Many of these experiments will require highly advanced detection systems. In this section the emphasis will be on γ-ray studies, while in Section 4.4 the emphasis will be on reaction studies.

4.3.1 Nuclear Pairing

Just as closely linked pairs of electrons lead to superconductivity in solids, pairs of neutrons or protons result in increased stability in nuclei. Our knowledge of nuclear pairing is almost completely restricted to nuclei along the valley of stability. However, very different physics may result if we can study pairing in systems with extreme Z/N ratios. Very neutron-rich nuclei are only weakly bound and neutron-neutron pairing can in some cases tip the balance and make a nucleus particle-stable that otherwise would be unbound. Information on pairing in diffuse neutron-rich nuclei may yield information on the density dependence of the pairing interaction. This could be of importance in understanding the superfluidity of neutron stars. On the proton-rich side, protons and neutrons occupy the same orbitals and can pair in ways not seen before. The most unusual predicted form of pairing is the $T = 0$, $S = 1$ non-spherical Cooper pair that should be important in $N = Z$ nuclei with $A > 60$ (see Fig. 4). This new phase of superconductivity might be observed as an energy gap in odd-odd nuclei and through blocking of alignments at high spin. Radioactive beams will be needed to populate the extreme nuclei that we expect will exhibit these new manifestations of the nuclear pairing interaction.

4.3.2 Breakdown of Mirror Symmetry

Isospin symmetry results from the nuclear force being largely charge independent. Mirror pairs of nuclei that have interchanged numbers of protons and neutrons have spectra that are virtually identical. Conventional spectroscopy has proven this symmetry for near-stable nuclei to mass 56. However, more extreme cases will provide information about the breakdown of this isospin symmetry in heavy nuclei. These Coulomb energy differences in the energy spectra may be studied as a function of spin yielding insight into the process of angular-momentum generation in nuclei.

4.3.3 Nuclear-Shell Structure

It is expected that the well known magic numbers may be drastically changed or be eliminated entirely as one moves away from the valley of stability. Neutron-rich nuclei will have a very diffused surface and the spin-orbit splitting will be reduced. Knowledge of the quenching of the shell structure is important in understanding the processes of stellar nucleosynthesis. Although we do not know the structure of neutron drip-line nuclei, the separation energies, neutron capture cross sections and decay rates of these nuclei are required to make predictions of the r-process. Many of the most interesting cases are far removed from the stability line and it will not be possible to make them in large quantities. However, the relevant information needed to test models is particularly
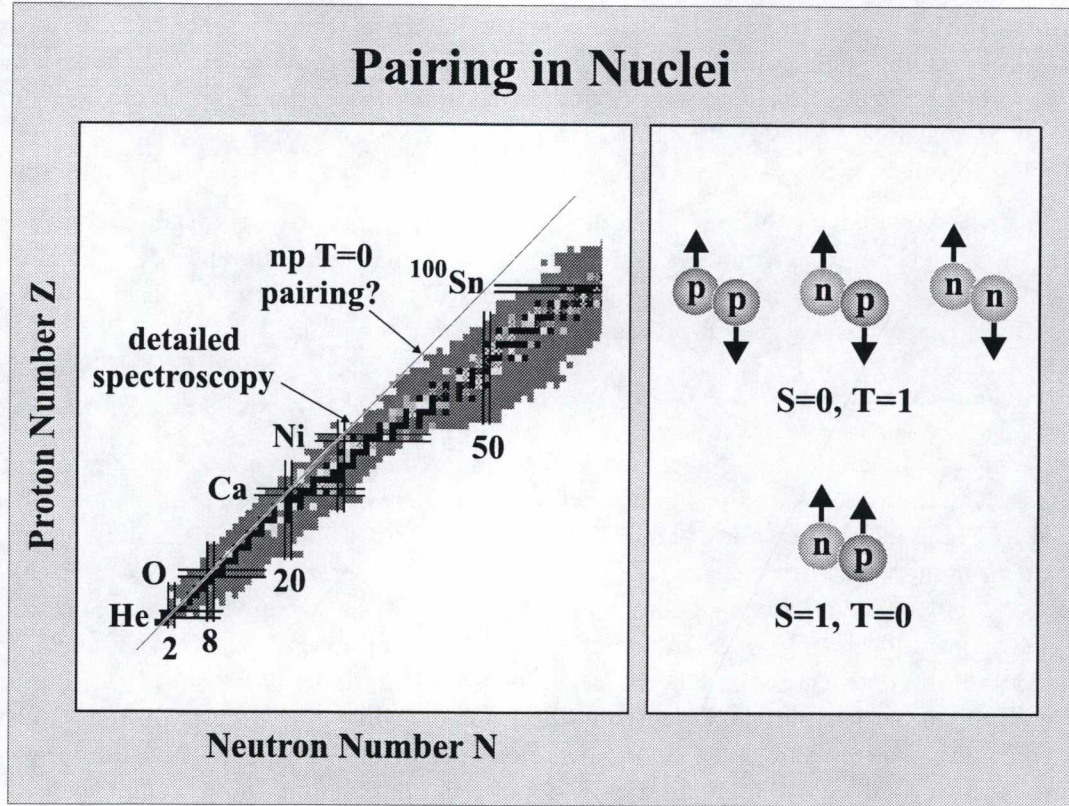
Figure 4: Pairing correlations have been observed in nuclei near the valley of stability for pairs of nucleons coupled to spin zero (i.e. proton-proton, neutron-neutron and neutron-proton $T=1$, $S=0$ pairing). These correlations are expected to be very important for loosely bound proton- and neutron-rich nuclei where the pairing force can no longer be treated as a small residual interaction. Since the neutrons and protons in $N = Z$ nuclei occupy the same shell-model orbitals, these nuclei have a special symmetry that results in a unique type of pairing correlation (i.e., neutron-proton $T=0$, $S=1$ pairing, analogous to the deuteron) that is predicted to become important for heavy $N = Z$ nuclei. So far the only evidence for np pairing comes from the increased binding energy observed for $N = Z$ nuclei (the so-called Wigner energy) that can only be explained if shell-model calculations include $T=0$, $S=1$ pairing [13]. A key issue is the extent to which the Wigner energy dominates the structure of heavy $N \sim Z$ nuclei. Possible experimental signatures of this phenomenon include: 1) an energy gap in the levels of odd-odd nuclei, similar to that observed in even-even nuclei; 2) enhanced probabilities for deuteron transfer in two-nucleon pick-up and stripping reactions; and 3) the absence of the irregularities commonly observed in states at high angular momentum that are associated with the breaking of a $T=1$, $S=0$ pair of nucleons. At the present time our knowledge of the properties of $N \sim Z$ above $A=70$ is very limited. The heaviest bound $N = Z$ nucleus is expected to be ^{100}Sn. The nuclear landscape in this mass region is shown on the left in the figure. Stable nuclei are shown in black, all known nuclei with halflives less than 1 day are shown in red and the black lines correspond to the magic numbers known around the valley of stability. Heavy-ion fusion and transfer reactions with radioactive beams will be essential to study the properties of these nuclei.

simple in these cases and it may be derived from knowledge of only the first few states of exotic even-even nuclei.

The understanding of the shell structure of the heaviest $N = Z$ nucleus ^{100}Sn is an important physics goal. Although it is possible to make this nucleus with stable beams, cross sections for its production with radioactive beams will be many orders of magnitude larger than those with stable beams.

4.3.4 Nuclear-Structure Properties and Reaction Rates Important to γ-Ray Astronomy

Clues to the nature of explosive nucleosynthesis are obtained from the observation of gamma-rays from the decay of unstable nuclei released in stellar explosions. Recent experiments that measured the half-life of ^{44}Ti will greatly assist in the understanding of supernova explosions. A number of further crucial experiments will require radioactive beams. ISAC-II will offer the possibility of increased understanding of the important reaction rates for the heavier systems which ISAC-I cannot measure. In particular, the role of the rp-process in the explosive nucleosynthesis of nuclei up to ^{56}Ni or even ^{96}Cd could be addressed. Fusion-evaporation reactions with radioactive beams will be required to determine the decay schemes of many nuclei of interest. At present very little is known about the nuclear structure of $N = Z$ nuclei above $A \sim 70$. This results primarily from the lack of suitable stable targets and/or projectiles.

4.3.5 Nuclear Structure at the Limits of Angular Momentum with Neutron-Rich Radioactive Beams

Radioactive beams in the mass region $^{126-138}$Sn and $^{138-150}$Xe, which will be available from ISAC-II, offer unique opportunities to study nuclei at the extremes of angular momentum. This comes about in several ways. The fission barrier, which sets one limit on how much angular momentum can be sustained, is significantly raised with neutron excess. One way to see this is to note that the fissibility parameter, X, which determines the barrier, is itself determined by the ratio of the disruptive Coulomb force to the cohesive surface tension. Any neutron excess then adds to the cohesive force without increasing the disruptive force. The gain in angular momentum sustainable can not be quantified accurately in a general way, and needs to be calculated in a case-by-case basis; but very crudely it amounts to a gain of $1\hbar$ per excess neutron, or a gain of more than $10\hbar$ with the most exotic beams. This is just the kind of gain needed to populate hyperdeformed shapes and to explore Jacobi instabilities in nuclei.

Aside from the intrinsic interest in exploring nuclei on the neutron-excess side of stability, it is noted that there are some phenomena that occur only there, or reach their fullest expression there. For example, high-K isomers have provided a very rich field of study in the region around ^{180}Hf, however the most extreme examples are predicted to occur just a few neutrons richer than can be reached with stable beams and targets. Similarly, many exotic nuclear shapes are predicted to occur just beyond today's reach, but would be within grasp with heavy Sn and Xe beams available from ISAC-II.

4.3.6 Experimental Considerations

Initially, radioactive beams with $N = Z - 2$ (such as ^{34}Ar and ^{36}K) available in 2003 with the completion of the first phase of ISAC-II will be used to study proton-rich nuclei formed through

compound-nucleus reactions. Energies sufficient to overcome the Coulomb barrier will allow access to many nuclei at and beyond the $N = Z$ line and detailed investigations of their structure will be possible. When heavier beams such as ^{56}Ni and ^{64}Ge are accelerated in 2005 all of the $N = Z$ nuclei up to ^{100}Sn will become accessible. The neutron rich Sn and Xe beams available from ISAC-II will be used to bombard a ^{48}Ca target to study nuclei at high angular momentum and the most extreme high-K isomers in the W, Ta and Hf nuclei. Extremely neutron-rich beams will be provided in low intensity. These can be used to form other nuclei far from stability and to learn the energies of their first few excited states (information needed to understand shell structure far from stability). Some rare species will be accelerated and then Coulomb excited to obtain this information. Similarly, inverse kinematics experiments will be used to study reaction rates in important specific cases.

4.4 Spectroscopy of Exotic Nuclei in Reaction Studies

One of the primary goals of ISAC-I is to elucidate the vital role of nuclear reactions involving unstable isotopes in nuclear astrophysics. In several aspects the specific objectives in this field coincide with those dedicated to a more general understanding of the structure of nuclei far from stability. The reactions of interest for proton-rich nuclei of $Z < 50$ generally involve states in nuclei with $Z > N$ which are therefore isobaric analogues of states in the usually better-known mirror nuclei. To this end, a better understanding of the breaking of isospin symmetry, including Coulomb displacement energies based on new experimental data, would be a very important element in predicting the properties of the relevant nuclei near the proton drip line for $Z < 50$. Nuclear reactions such as those in the rapid neutron capture (r-) process require knowledge of the properties of very neutron-rich nuclei.

Interest in the properties of a specific nucleus far from stability usually extends well beyond the simple question of the mass, half-life and decay modes of the ground state. An understanding of the nucleus as a many-body quantum system requires knowledge of the spins and parities of these states as well as those of the low-lying excited states; information ideally augmented by measurements of other spectroscopic properties such as γ-ray transition probabilities and spectroscopic factors for one- and two-nucleon transfer. It is not realistic to anticipate that, for nuclei far from stability, one can duplicate the rich detail of the spectroscopic information currently available for nuclei closer to stability but ISAC offers unique opportunities to obtain such information in selected cases.

A very significant part of the detailed spectroscopic information we currently have, particularly for the lighter nuclei ($A \leq 40$), has been obtained from the study of nuclear reactions involving stable targets and relatively low-energy ($E \leq 10$ MeV/u) beams of protons, deuterons, ^{3}He and ^{4}He. For the purpose of the present discussion attention is focussed specifically on:

a) resonance reactions involving protons, which normally would be studied at energies below the Coulomb barrier; and

b) transfer reactions, particularly those involving one- and two-nucleon stripping from deuterons, ^{3}He and ^{3}H. Specifically, the neutron transfer reactions (d, p) and (t, p) allow one to probe farther towards the neutron drip line and could provide important information for (n, γ) reactions rates in explosive astrophysical scenarios.

4.4.1 Resonance Reactions

The study of resonance reactions, particularly the elastic scattering of protons on stable targets is a well-established tool of nuclear spectroscopy. The important extension of these studies to reactions of direct significance in nuclear astrophysics using accelerated radioactive beams of proton-rich nuclei has been pioneered at Louvain-la-Neuve [e.g., Ref. [14] and references cited therein] and will be pursued at ISAC using the general purpose scattering facility, TUDA, (see Section 5.3.1). Most relevant to the present discussion has been the development of a technique for one-step energy scanning of an elastic scattering resonance using a relatively thick polyethylene target. Accurate values of the energy and width of the resonant state, as well as a unique determination of the spin can be derived by observing the energy spectrum of the recoil protons at specific angles. In the broader context of nuclear structure, similar techniques involving hydrogen targets and low-energy $(0.2 < E < 4$ MeV/u) radioactive beams could have a significant impact on the study of nuclei away from the valley of stability in the following three categories.

a)   Nuclei beyond the proton drip line

A variety of techniques have been used to identify with one or two exceptions, all the proton-rich nuclei with $Z < 28$ which are stable with respect to proton emission. With the exception of ^{4}Li and ^{5}Li, none of the nuclei beyond the proton drip line can be formed as a compound nucleus using protons and a non-radioactive target. However, the properties of the ground and low-lying excited states of many of these nuclei could be investigated as compound nuclear resonances with a hydrogen target and beams of proton-rich radioactive isotopes (see Fig. 5). In general the lifetime of these unbound states is too short for them to be of direct significance even in the most explosive stellar environments but the properties of these very proton-rich nuclei are of interest in connection with such topics as: mass models of nuclei, the systematics of Coulomb energies over large isobaric multiplets, the influence of extended unbound proton orbitals, and the general question of isospin purity.

b)   Specific excited states in proton-rich nuclei

The study of the 5.17 MeV state in ^{14}O at Louvain-la-Neuve [16] is an example of the detailed nuclear spectroscopy motivated by nuclear astrophysics. In this particular case, the important cross section for radiative proton capture is unusually large and hence well suited to a first-generation experiment with a radioactive beam. Unfortunately, most of the other experiments of greatest interest in the field of explosive stellar burning involve much smaller yields and hence present serious challenges even for a second-generation facility such as ISAC. The 5.17 MeV state in ^{14}O is, however, quite typical of many unbound states in nuclei with $Z > N$ for which unique spectroscopic information could be derived by the study of proton-induced resonances involving radioactive beams. It is important to emphasize that in many cases the states of greatest interest for nuclear structure are those with large reduced widths, which consequently appear as strong resonances. In these experiments the inelastic scattering from low-lying states of the projectile must also be considered, both as a source of background and as a means of obtaining detailed spectroscopic information of the radioactive projectile itself.

c)   Isobaric analogue states in neutron-rich nuclei

The determination of spins, parities and other detailed spectroscopic properties of even the lowest
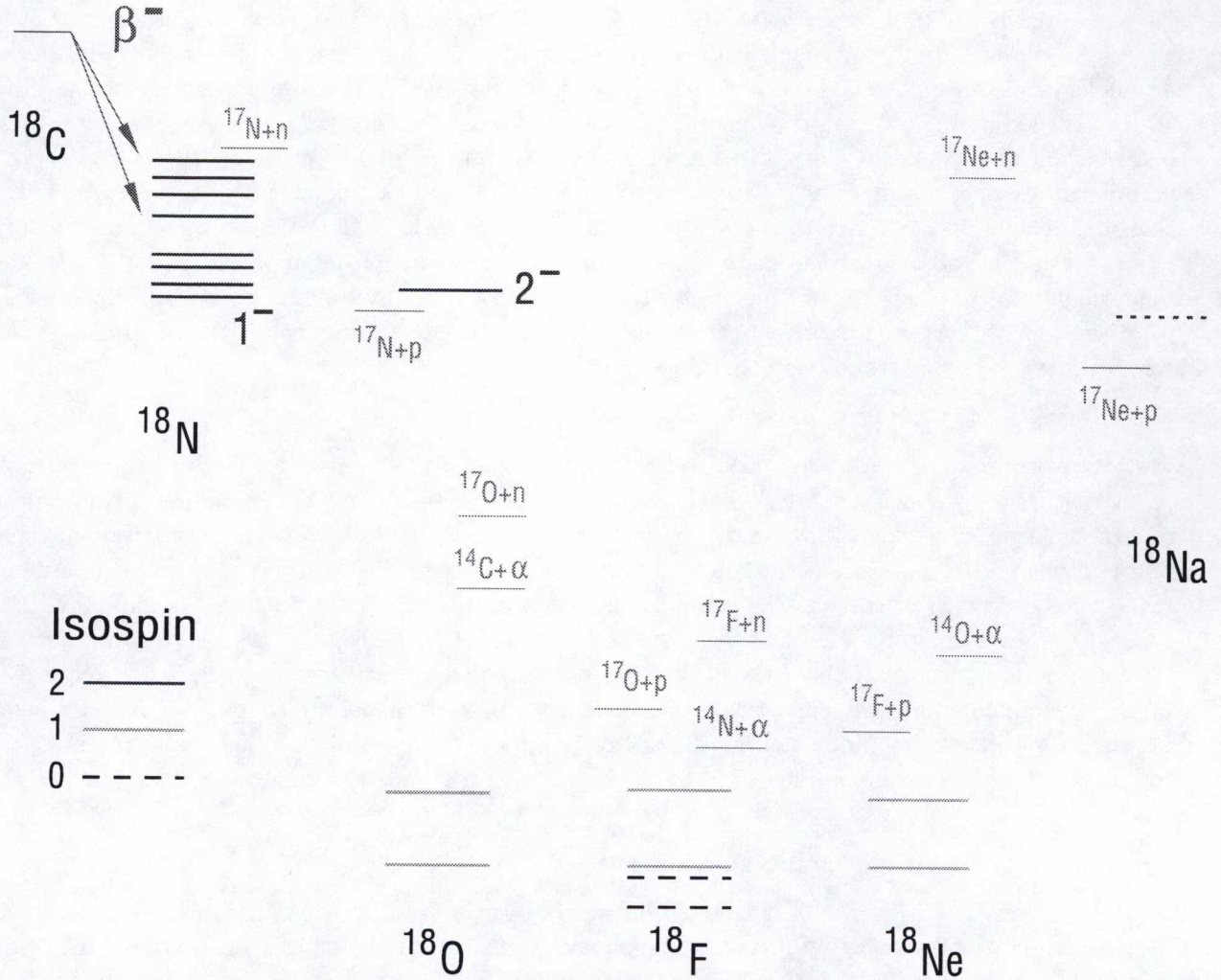
Proton Resonances: A=18, T=2

Figure 5: Resonant reactions using radioactive beams will have a significant impact on the study of isobaric multiplets in light ($A \leq 40$) nuclei. This is illustrated for the A=18, T=2 states. Shown are the lowest known T=0, 1, 2 and 3 states in A=18 nuclei [The diagrams for individual isobars have been shifted vertically to eliminate the neutron-proton mass and Coulomb energy differences [15]] together with the relevant p, n and α binding energies (only the lowest two T=0, 1 states are shown). For the T=2 states, values of J^π have been assigned to two of the eight known levels in ^{18}N and the only one yet identified in ^{18}O. No levels are known for ^{18}Na; the ground state is predicted to be unstable to proton emission by 1.6 MeV. A search for resonances in the elastic scattering of ^{17}Ne on a hydrogen target at E_p(cm)$\leq$ 5 MeV could uniquely determine the mass, width and J^π for the lowest states in ^{18}Na. Similarly, the ^{17}N+p reaction provides the only isospin-allowed resonant channel for forming the analogue T=2 states in ^{18}O. Here the isospin-forbidden n- and α-decays would provide insight into the nature of isospin mixing and possibly help determine the most promising means to identify the T=2 states in ^{18}F and ^{18}Ne.

lying states in a specific nucleus (Z, N) near or beyond the neutron drip line is in general very difficult. Studies of resonance reactions induced by radioactive beams incident on hydrogen could in many cases be used to determine the corresponding properties of the isobaric analogue states in the $(Z + 1, N - 1)$ nucleus (see Fig. 5). The isobaric analogue resonances will be characterized by large reduced widths for the isospin-allowed formation channel (p_0) and very small reduced widths for isospin-forbidden neutron emission. However, the IAS of a level beyond the neutron drip line (i.e., where the neutron separation energy, S_n <0) will also have an isospin-allowed decay by low-energy neutron emission. The simplest cases for which the study of isobaric analogue resonances could be used to make unique spin assignments for very neutron-rich nuclei would involve the use of accelerated beams of even-even nuclei for which $J^\pi = 0^+$.

4.4.2 Transfer Reactions

The study of one- and two-nucleon transfer reactions with light $(A \leq 6)$ projectiles on stable targets is also a well-established spectroscopic tool. The extension of this technique to the study of exotic nuclei using radioactive projectiles in inverse kinematics will provide a powerful method of determining the nuclear shell structure far from stability. In particular, by measuring the excitation energies, spins and/or parities, and spectroscopic factors for the levels populated in pick-up and stripping reactions it is possible to obtain information on single-particle energies, effective inter-actions and pairing correlations. Of special interest are those nuclei near the doubly magic nuclei ^{56}Ni, and ^{132}Sn.

Transfer reactions with radioactive projectiles are also important for astrophysics. Recently, the inverse $d(^{56}$Ni$,p)^{57}$Ni reaction was studied using a radioactive ^{56}Ni beam to determine the spectroscopic factors of the low-lying states in ^{57}Ni [17]. The data was used to predict the strength of the ^{56}Ni(p, γ) reaction leading to the mirror nucleus ^{57}Cu, which is crucial for the production of heavier proton-rich nuclei in explosive nucleosynthesis. Other key reactions of interest for the Hot CNO-cycle and the rp-process include the proton transfer reaction $(^3$He$,d)$ on ^{13}N, ^{19}Ne and ^{72}Kr. A challenging, though not first generation, experiment would be the α-transfer on ^{15}O with the ^{6}Li$(^{15}$O$,d)^{19}$Ne reaction.

The radioactive beams available from ISAC-II are well suited to the study of one- and two-nucleon stripping reactions and one-nucleon pick-up reactions involving small negative Q-values. For stripping reactions such as (d, p) in inverse kinematics, the forward angles in the center of mass correspond to backward angles in the laboratory. As a result, the light reaction products are well separated from the elastic scattering of the light target atoms, which are confined to laboratory angles < 90°. However, if the radioactive beam contains a small isobaric impurity it may also be necessary to detect the heavy recoil. At ISAC-II laser ion-sources will be used to avoid this difficulty.

4.5 Coulomb Excitation in Inverse Kinematics at ISAC-II

The Coulomb excitation of radioactive projectiles provides a powerful method to measure the low-lying collective properties of nuclei far from stability (see Fig. 6). Recently, experiments conducted at projectile-fragmentation facilities have demonstrated the usefulness of intermediate-energy ($\sim$50 MeV/u) Coulomb excitation for the study of light neutron-rich nuclei near the $N = 20$ shell closure. In these experiments, the measurements are restricted to projectiles scattered from
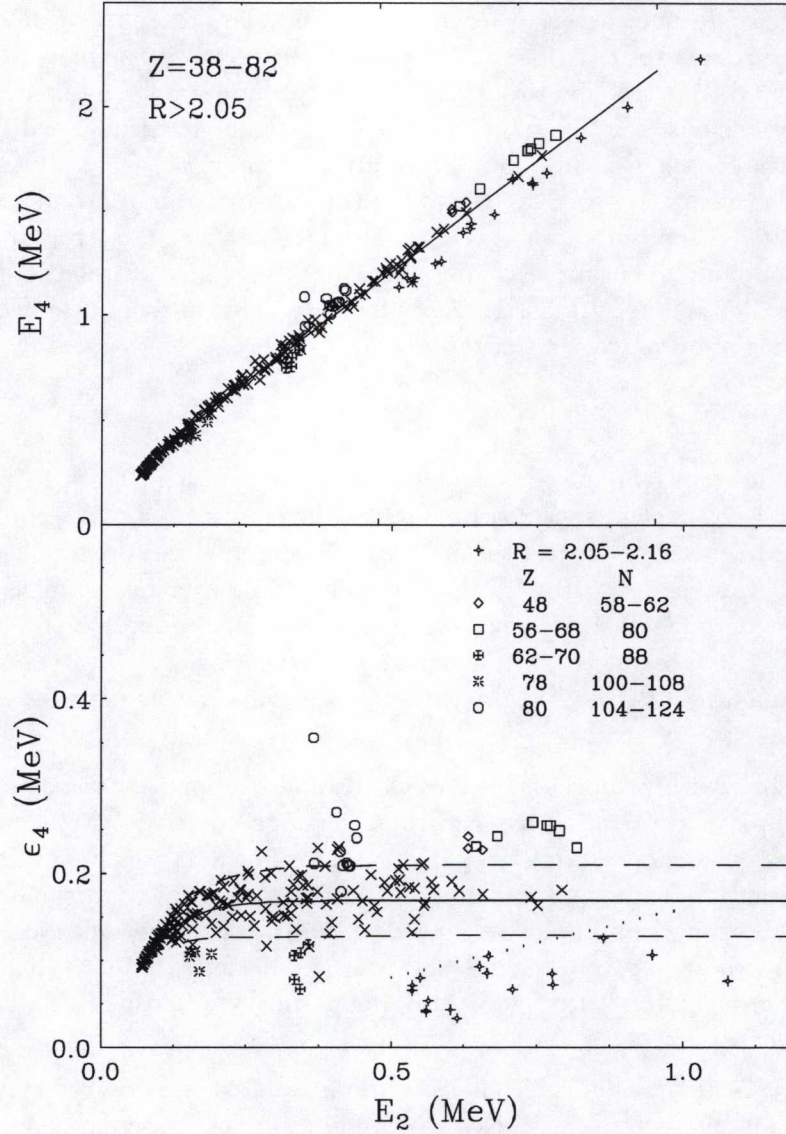
Figure 6: Correlations between collective observables can be a powerful tool to elucidate nuclear structure with only a minimum of data. This is illustrated in the upper half of the figure where the energy of the lowest 4_1^+ state is plotted versus the energy of the lowest 2_1^+ level for all known collective, but nonrotational, even-even nuclei with $Z = 38 - 82$. The data can be fitted with the expression $E(4_1^+) = 2E(2_1^+) + \varepsilon_4$. This equation, which is valid for an extremely large range of nuclei, is that of an anharmonic vibrator with a constant anharmonicity, ε_4. The deviations of $E(4_1^+)$ from $2E(2_1^+)$ are plotted in the lower part of the figure. Although there is some scatter in the data points, over 90% of the ε_4 are between 90 and 210 keV whereas the 4_1^+ energies range from 270 to 1800 keV. Of particular interest are those nuclei that deviate from the normal behaviour namely, those with large values of ε_4, which are known to have two holes relative to a closed shell, and many of the nuclei with low values of ε_4, which are found in spherical-deformed shape-transition regions. Such simple structural signatures will be useful in determining the low-lying structure of nuclei far from stability [From Ref. [18]].

a heavy (e.g., Au foil) target at angles of less than 4° to ensure that Coulomb excitation is the dominant excitation process.

Traditionally, Coulomb excitation studies with stable beams were performed at incident energies well below the Coulomb barrier to avoid the influence of excitations via the strong interaction. The ISAC-II facility is ideal to perform such studies with the full range of radioactive beams. Of particular interest are the neutron-rich nuclei of importance to the rapid neutron capture (r-) process and where the weakening of the shell structure of nuclei is predicted. The optimum energy range for these experiments is $2-4$ MeV/u and the required intensities are $\sim 10^3$-10^6 s^{-1}. It is important to note that Coulomb excitation studies of light ($A < 50$) radioactive beams was the main experimental justification for the new REX-ISOLDE facility.

The initial Coulomb excitation experiments proposed for ISAC-II [Ref. [19]] would use an apparatus designed to measure $B(E2 : 0_1^+ \to 2_1^+)$ values by the Coulomb excitation of radioactive beams in inverse kinematics using a thin, low-Z target. The Coulomb excited projectiles decay in flight downstream of the target. Two methods have been developed to measure the γ-rays from these excited nuclei: 1) the lifetime method for long-lived (~ 1 ns) states; and 2) the integral method for shorter lifetimes. In the lifetime method a linear array of NaI (Tl) detectors is used to measure the decay curve of the excited state. This method is feasible for beam intensities $\sim 10^6$ s^{-1}. In the integral method the $B(E2)$ value is determined by measuring the total Coulomb excitation cross section using a large "through-well" Na (Tl) detector to surround the target. In this case beam intensities as low as 10^3 s^{-1} are adequate.

This program is ideal for the first experiments with ISAC-II. The measurements are simple but they promise to provide new and very exciting results on the structure of nuclei far from stability.

4.6   Nuclear Astrophysics Experiments at ISAC-II

ISAC-I provides a unique opportunity to measure the rates of nuclear fusion reactions considered important in the production of elements in explosive astrophysical phenomena such as novae or X-ray bursts. It is currently believed that given the relatively high temperatures occurring in explosive phenomena combined with high hydrogen and helium densities, radiative proton and alpha capture reactions can occur with radioactive species. In order to obtain quantitative confirmation of this hypothesis, it is critically important to measure the rates of key reactions expected to play a role in the various paths leading to the production of heavy elements. These paths generally follow along the proton rich side of the $N = Z$ line of isotopes and in its earliest stages involve nuclei with masses $A < 30$. Of particular importance is the radiative alpha capture on ^{15}O which is believed to be the key reaction leading to a break-out from the so-called Hot CNO cycle to the rapid proton capture (rp-) process along the proton-rich side of the $N = Z$ line of stability. The time scale for the rp process outburst varies from 10 to 100 second and within this time period nuclei up ^{56}Ni or even ^{96}Cd can be synthesized (see Fig. 7). Waiting points in the rp process occur at ^{14,15}O, ^{24}Si, ^{34}Ar, ^{56}Ni, ^{64}Ge, ^{68}Se, and ^{72}Kr where the sequence is delayed until either β-decay or a nuclear reaction in which an α-particle or two protons are captured, has occurred. Above $A = 72$ the rp path is unknown because of a lack of information on the masses, decay schemes and level structures of the relevant nuclei near the $N = Z$ line. The study of the structure of these nuclei is one of the important areas of research that will be pursued with radioactive beams from ISAC-I and II.

The beams from ISAC-II will also greatly extend the ISAC-I nuclear astrophysics program

- temperature:

- energy production:

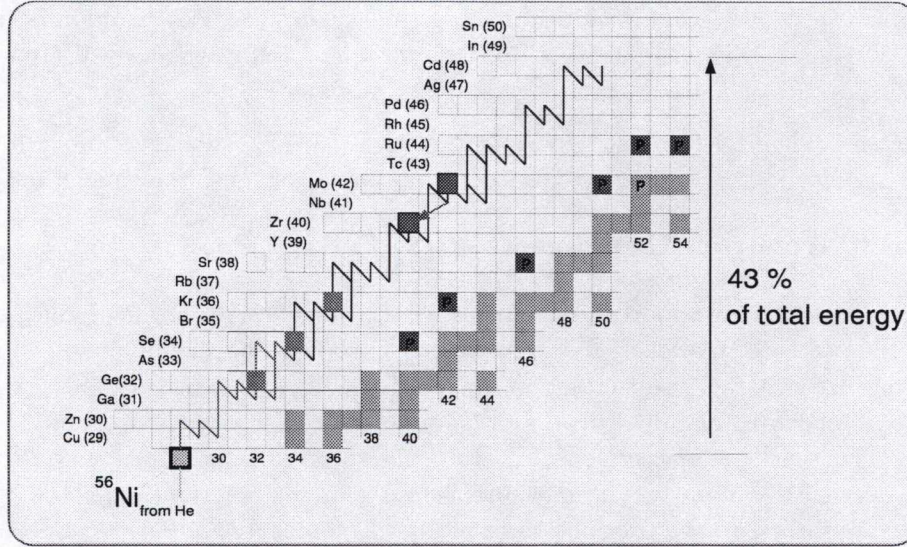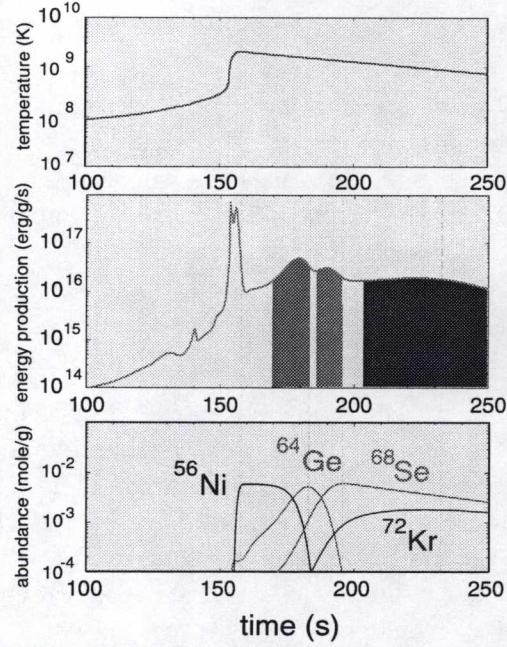- abundances of waiting point nuclei:

Figure 7: A portion of the *rp*-process reaction sequence path along the proton rich side of the valley of stability from ^{56}Ni up to ^{96}Cd. During an X-ray burst, at temperatures up to $\sim 2 \times 10^9$K nearly half the energy production comes from the synthesis of elements above ^{56}Ni where the lack of experimental data results in large uncertainties in the reaction path and time scale. For example, when the reaction path encounters the unbound nucleus ^{69}Br, it can only proceed by waiting for the β-decay of ^{68}Se or via a sequential pair of proton capture reactions that converts ^{68}Se into ^{70}Kr. The rate of the latter process depends on the unknown decay energy for ^{69}Br $\rightarrow$ ^{68}Se+p. Theoretical estimates vary by ~ 1.5 MeV corresponding to a variation in the stellar lifetime of the ^{68}Se waiting point of 10^4. Best estimates of the temperature, energy production and the abundance of the waiting point nuclei up to ^{72}Kr are shown as a function of time in seconds. Above ^{72}Kr the waiting path is virtually unknown [From Ref. [20]].

to higher masses using the same experimental apparatus. For example, radiative proton capture reactions of considerable interest for the rp process that could be measured with the DRAGON facility include ^{34,35}Ar$(p,\gamma)^{35,36}$K, and ^{39}Ca$(p,\gamma)^{40}$Sc. In addition, the ^{45}V$(p,\gamma)^{46}$Cr reaction cross section is crucial to our understanding of the production of ^{44}Ti in supernova explosions.

The general purpose scattering facility, TUDA, which will be built to study elastic, inelastic, transfer and fusion reactions of relevance to nuclear astrophysics complements the DRAGON recoil separator by concentrating on charged particle reactions in the outgoing channel. This facility will be highly utilized with beams from ISAC-I and II both for nuclear astrophysics and nuclear structure physics (see Section 4.4). For example, at temperatures $>10^9$ K the (α,p) reactions on waiting point nuclei (most with masses >30) in the rp process may play an important role in the synthesis of proton-rich nuclei. Further, where high precision and a detailed understanding of the reaction mechanism is required, radioactive beam energies >1.5 MeV/u are needed. In particular, for the ^{7}Be$(p,\gamma)^8$B reaction an extension of both the capture and elastic scattering measurements to energies of ~ 3 MeV/u are needed to resolve problems encountered in interpreting the data obtained at lower energies and in determining the astrophysical S-factor at zero energy.

Most nuclei with masses $A >80$ are formed by slow neutron capture (s-process), which occurs in red giant stars, and rapid neutron capture (r-process), which occurs in supernova explosions. In addition to measuring the masses, decay schemes and low-lying level structures of the neutron-rich nuclei relevant to the r-process with low-energy radioactive beams from ISAC-I, (d,p), (t,d), $(^7$Li,^{6}Li) and similar transfer reaction studies with higher energy beams from ISAC-II could be used to deduce the neutron capture cross sections at the waiting points of the r-process associated with nuclei near the magic neutron numbers 50 and 82 (see Section 4.4). In these regions the level densities for neutron capture are expected to be low and therefore statistical models are not applicable. In addition, if the predictions of shell softening are correct then the actual level densities will be very different. Finally, heavy-ion fusion reactions with radioactive beams at $5-6$ MeV/u are needed to produce and measure the masses and decay properties of heavy $A >180$ neutron-rich nuclei in the r-process path (see Section 4.3).

4.7   A Program in Heavy-Element Synthesis at ISAC-II

The search for new elements and the study of their properties have been active areas of research since the beginning of modern science. While all stable elements have now been found, intensive efforts continue to explore the predicted limits of nuclear stability by producing new elements/isotopes in heavy-ion fusion reactions. For many years these studies, involving state of the art chemistry and physics facilities, were performed at the Lawrence Berkeley National Laboratory at the University of California. Over the last 15 years the search for and production of new superheavy elements has also been pursued successfully at the GSI Laboratory in Darmstadt, Germany and the JINR institute in Dubna, Russia.

Elements up to $Z=112$ have now been discovered using sophisticated detection techniques. For example, the successful discovery of element $Z = 112$ at the GSI facility in Germany involved using such heavy-ion reactions as ^{208}Pb$(^{70}$Zn,$n)$ ^{277}112 [21]. Two events corresponding to element 112 were detected in the large background of reaction products observed with the upgraded velocity filter SHIP coupled with a new alpha-correlation detection system. This facility has a detection sensitivity of one decay chain in 10 days, which is equivalent to a cross section of 1 pb. The beam

energy was 5 MeV/u and the intensity was 0.5 particle-μA. It is important to emphasize that these experiments were successful because the researchers performed systematic studies of the excitation functions for the types of reactions they planned to use to produce these new elements. It is just these types of studies that are now required with radioactive projectiles, such as very neutron-rich beams or nuclei with neutron density distributions (halos) that extend relatively far outside the nuclear core, to explore new ways to increase the cross section for producing superheavy elements.

Quite recently, there have been two unconfirmed announcements of new element discoveries. In January, 1999 researchers from Dubna and Livermore claimed that they had produced element 114. This atomic number is in the vicinity of the magic numbers associated with increased stability, according to most theoretical calculations. The alleged lifetime, while only 30 seconds, is still orders of magnitude greater than the lifetimes of isotopes produced to date in the atomic number range $109 - 112$. Reactions to the announcement [12] are tempered by the need to confirm the result. The Dubna-Livermore group has seen only one atom. Moreover, the researchers produced it in an unexplored region of the chart of nuclei, so one cannot link the daughters and granddaughters of its decay chain to any known isotopes.

In June, 1999 researchers from Lawrence Berkeley National Laboratory reported the discovery of element 118 produced in the reaction ^{86}Kr+^{208}Pb at 449 MeV. In this experiment three events were observed each consisting of a series of six alpha decays leading to new elements or isotopes of element 116, 114, 112, 110, Hs and Sg. Since the decay chain did not include any known isotopes it was not possible to assign unambiguously the decay to ^{293}118. However, the measured alpha energies and reaction energetics are consistent with the $1n$ reaction channel. At GSI experiments have already begun in an attempt to confirm the result. The cross section for the production of element 118 was found to be $\sim$2 pb. This is a factor $10 - 100$ larger than that predicted by the cold-fusion reaction systematics leading to the synthesis of element 112. However, this surprising result is more in accord with a recent theoretical prediction, which suggested even bigger cross sections. This result also increases the importance of pursuing the study of heavy-element synthesis with more neutron-rich projectiles.

These recent observations have re-energized the entire field of heavy-element research as there seems to be a true new region of nuclear stability. However, it is evident that further progress towards producing and studying the properties of the heaviest, spherical, doubly-magic nucleus (i.e., with 184 neutrons and 114 (126) protons) will only be possible with new approaches as these recent discoveries demonstrate. At the present time, radioactive beams cannot be used to produce these new elements given the limited beam intensities available at first-generation facilities, although with higher than expected cross sections this may not hold true. Nevertheless, radioactive beams can be used to study the mechanisms of new reaction paths and provide important guidance on the choice of stable beam-target combinations to produce superheavy elements.

The advantages in using radioactive beams arise from the fact that more neutron-rich projectiles can be used to reach the expected region of stability in the heavy-element regime. Equally important, there is some expectation that the cross section for reactions involving very neutron-rich projectiles, which have extended neutron distributions, are enhanced by one to two orders of magnitude. It is for these reasons that investigations are now beginning elsewhere and for which ISAC-II is ideally suited.

Theoretical calculations predict that there should be large enhancements in sub-Coulomb barrier
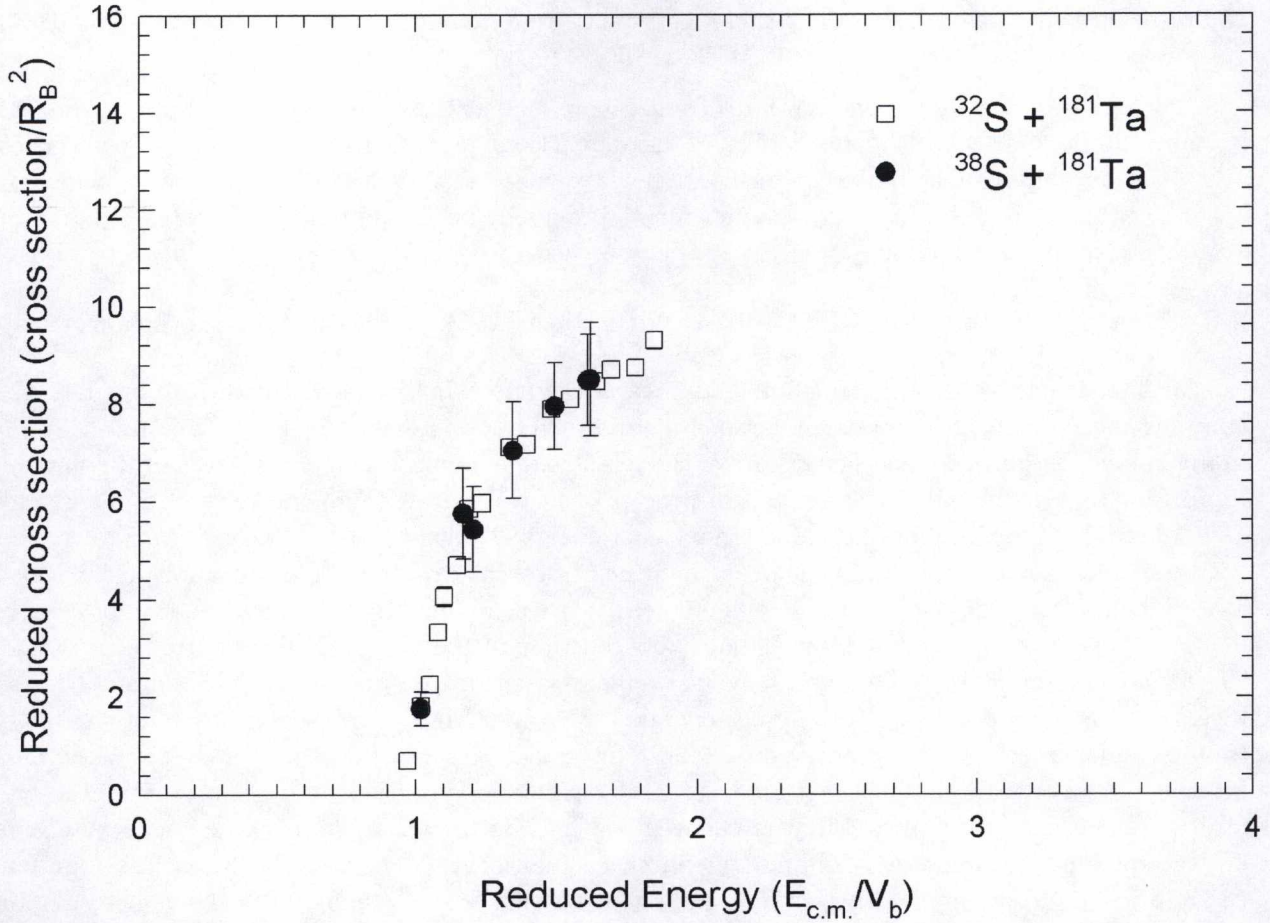
Figure 8: The projectile-fragmentation facility at MSU was used to measure the fusion excitation functions for the reaction ^{38}S+^{181}Ta. These data were compared with those obtained at ATLAS for the ^{32}S+^{181}Ta reaction. In both cases, calculations indicate that $\sim 99\%$ of the products formed in the reaction fission so the fission-fusion excitation function should be equivalent to the fusion excitation function. After correcting the data for contributions resulting from quasi-fission, the fusion barrier height for the ^{38}S+^{181}Ta reaction was found to be reduced by 6.9 MeV relative to that for ^{32}S+^{181}Ta. This energy shift, which corresponds to about one neutron binding energy, could affect the production rates of new heavy nuclei by a factor of $10 - 1000$. The reduced excitation functions for the two systems are shown in the figure. Within the uncertainties in these data, there is no evidence for anything other than a simple shift in the height of the fusion barrier [From Ref. [23]].

fusion cross sections using a ^{11}Li beam as compared to a ^{6}Li beam [22]. However, experiments have not performed satisfactorily so far given the limited intensities of low-energy ^{11}Li beams presently available but it is clear that such studies will be pursued at the new REX-ISOLDE facility. Recently, the cross section for the fusion of a very neutron-rich ^{38}S beam with a Ta target was found to be enhanced relative to the value measured with a stable ^{32}S beam. This was attributed to the reduced Coulomb barrier for fusion (see Fig. 8). The experiment was limited because of the properties of

the radioactive beam and it is clear that this type of study could be pursued successfully and in a very systematic fashion at the new ISAC-II facility.

A program in heavy-element synthesis could be pursued at ISAC-II. In the initial phase, the program would be focused on the mechanism of fusion reactions involving very neutron-rich projectiles. With the development of higher intensity radioactive beams, this program could be expanded to actually attempt to produce very heavy elements provided the appropriate sophisticated detection systems were made available.

4.8 Heavy-Ion Reaction Mechanisms with the HÉRACLÈS 4π Multidetector Array

Despite considerable experimental and theoretical effort in the past decade to elucidate the complex mechanism of heavy-ion reactions at intermediate energies (i.e., $10 < E < 100$ MeV/u) many open questions remain. For example, there is strong evidence that reaction dynamics plays an important role in the multi fragmentation process of heavy ions at these energies. The persistence of final-state configurations having a binary character well into the Fermi energy range even for very central or violent collisions has been confirmed in recent experiments but cannot be explained theoretically. Another observed phenomenon, still not well understood, is the formation of a neck-like structure, with a velocity intermediate between that of the projectile-like emitter and that of the target-like emitter, analogous to the participant-spectator or fireball models commonly used to explain heavy-ion collisions at higher energies ($E > 100$ MeV/u). In collisions between heavy targets and projectiles the production of most intermediate-mass fragments (IMF's), with mass intermediate between that characteristic of light-particle evaporation and fission, originate from multiple neck rupture, akin to what is believed to occur with low probability in low-energy fission and predicted by Boltzmann-Uehling-Uhlenbeck calculations. Moreover, the fragments found in the mid-velocity region are substantially more neutron-rich than those found in the velocity region dominated by the emission from the projectile. Evidence for neckline emission has also been observed in collisions between light ($A < 60$) heavy ions (see Fig. 9).

The availability of light ($A \leq 60$) radioactive ion beams at energies $E \geq 6.5$ MeV/u from ISAC-II will allow heavy-ion reaction dynamics to be studied in new and more specific ways by removing the limitations of target/projectile combinations with stable beams. In particular, the variation of the overall isospin ratio as well as the respective isospin ratio of the projectile, target and therefore of the neck between them, opens up a new dimension in the study of nuclear matter. Theoretical effort is also required to define those signals that will carry the information after the cooling process.

Two examples of possible experiments are: 1) a comparison of the reactions ^{13,18}N+^{12,13}C $\rightarrow$ ^{25,31}Al, where the charge of the projectile and target are fixed but the N/Z ratio of the total system varies by a factor of 1.5; and 2) a study of the reactions ^{24}Mg+^{24}Mg $\rightarrow$ ^{48}Cr, ^{20,30}Na+^{27}Al $\rightarrow$ ^{47,57}Cr and ^{34,46}Ar+^{12,13}C $\rightarrow$ ^{46,59}Cr where both the charge and N/Z ratios of the projectile/target combinations vary but the charge of the total system remains constant.
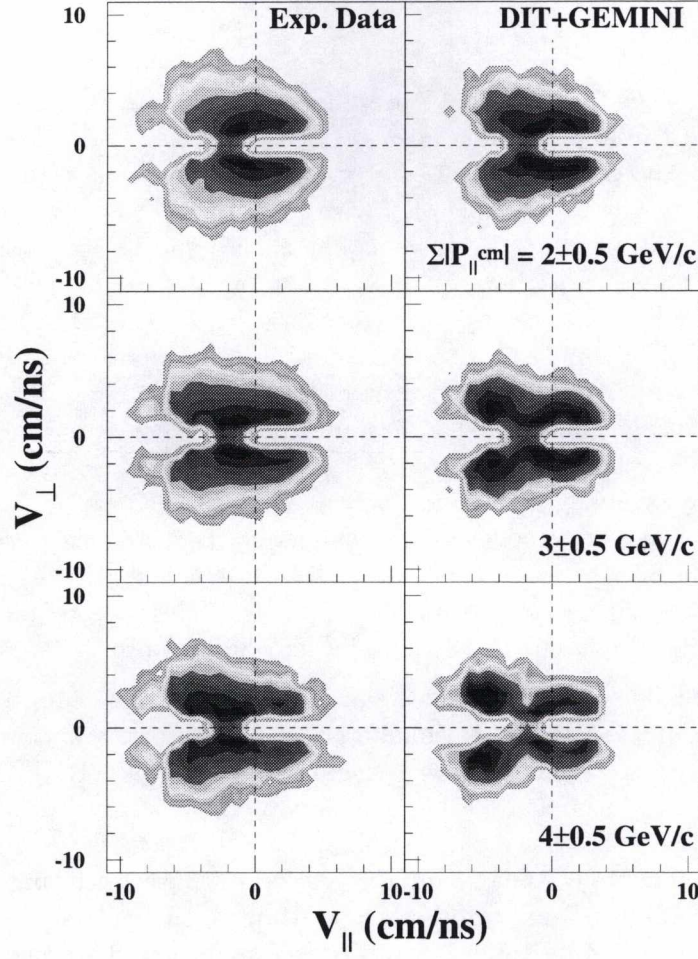
Z=2 Particles

Figure 9: Evidence for the formation of a necklike structure in the reaction ^{58}Ni+^{12}C at 34.5 MeV/u has been obtained using the HÉRACLÈS 4π multidetector array [24]. Galilean-invariant centre-of-mass velocity plots are shown on the left for $Z=2$ particles observed for central, intermediate and peripheral collisions characterized by the total absolute parallel momentum in the centre-of-mass frame of all charged particles emitted in the collision. Theoretical simulations were obtained by treating the reaction in two steps, namely: 1) the interaction stage evaluated (using a Deep Inelastic Transfer (DIT) code) in the framework of a stochastic nucleon transfer model leading to energy and angular momentum dissipation; and 2) the break up of excited nuclei formed in the interaction stage through statistical sequential binary decays calculated with the GEMINI code; these are shown on the right. For peripheral collisions, (i.e. high total parallel momentum), the particle velocity distributions are strongly elongated towards the beam direction and two emission components associated with quasi-particle and quasi-target sources are observed. The relative velocity separation between the two sources decreases for more central collisions (i.e., lower total parallel momentum). A feature present in the data that is not predicted by the simulation is the persistent mid-rapidity emission consistent with the break-up of a necklike structure (or pre-equilibrium emission from a participant zone) formed between the two principal reaction partners.

27

5 Experimental Facilities for ISAC-II

5.1 Introduction

As discussed previously, the radioactive beam intensities available at ISAC-II will cover a much larger range compared to those of stable beams. While ion beams of certain nuclei near the valley of stability will be produced with intensities of $10^{10} - 10^{11}$ particles/s, more exotic nuclei located at the limits of stability will be available only with rates of $1 - 10$ particles/s or less. In addition, many of the reactions will be studied in inverse kinematics and in some cases the beams will also have contaminants from other isobars, which are produced with higher yields, and can not be completely removed with a high-resolution mass separator. The decay of the scattered radioactive beam particles will produce a high background counting rate in particle and gamma-ray detectors. For these reasons the experimental equipment at ISAC-II has to fulfill additional requirements compared to conventional experiments with stable beams. For experiments with low-intensity beams high efficiency detector systems covering a large fraction of the full solid angle are essential. The inverse kinematics in many of the experiments calls for high granularity detectors to define the reaction kinematics and to compensate for Doppler shifts in gamma-ray experiments. To select a particular reaction of interest in experiments with beams of several isobars, coincident detection of the outgoing particles with good mass and charge identification is required. Finally, segmented detector systems are needed to handle the high background rate from the radioactive beam itself.

Following is a discussion of the first-phase experimental facilities required to pursue the physics interests of Canadian and international collaborations in nuclear science with ISAC-II. As mentioned in Section 4.2, letters of intent have been submitted to the TRIUMF EEC to relocate two Canadian experimental facilities at ISAC-II, namely: the 8π spectrometer and the HÉRACLÈS 4π multidetector array. Both of these facilities will need to be upgraded for physics with radioactive beams. The recoil separator, DRAGON, and the general purpose scattering facility, TUDA, will be used to extend the ISAC-I nuclear astrophysics program to higher masses. Additional scattering chambers and/or silicon strip detector arrays will be required to meet the needs for nuclear-structure studies using resonance and few-nucleon transfer reactions. Finally, two new facilities are needed to exploit fully the exotic beams from ISAC-II: $i)$ a new segmented Ge detector array optimized for ISAC-II physics that can be easily reconfigured for a wide variety of experiments with radioactive beams, and $ii)$ a gas-filled separator suitable for heavy-element synthesis and other fusion reaction studies.

5.2 Gamma-Ray Detectors

5.2.1 The 8π Spectrometer

The 8π spectrometer [25] is a second-generation instrument comprised of 20 Compton-suppressed Ge detectors, a 4π BGO gamma-ray calorimeter and a multi-element charged-particle array. All of these features will prove valuable for some of the experiments proposed. Much bigger spectrometers are now available elsewhere and others are planned. However, the 8π has a number of features that will prove crucial in some of these experiments. The so-called third-generation gamma-ray arrays were designed primarily to obtain their greatest sensitivity in high-fold experiments in which many gamma-rays are detected in coincidence. Most of the experiments that will be done with radioactive beams will be low fold. Given sufficient statistics the 8π is actually more sensitive than

the third-generation arrays for low-fold situations. However, with low-beam intensities it will often not be possible to obtain sufficient statistics with the 8π spectrometer. For these experiments a new high-efficiency array is proposed (see Section 5.2.3).

5.2.2 Target Chamber for Radioactive Beam Experiments

One of the major technical difficulties that must be overcome in order to perform in-beam gamma-ray spectroscopy experiments with radioactive beams is the very large background of gamma rays from the beta decay of scattered beam particles. This is especially true for proton-rich beams because of the 511 keV gamma rays produced with every β^+ decay. To overcome this difficulty, a unique tape-transport system is being designed by the McMaster group, which will rapidly and continuously remove the vast majority of the scattered beam from the vicinity of the array. Although this system will be technically complex and will require substantial engineering expertise, time, and funds to develop, it will be by far the most cost-effective means of dealing with the severe background of gamma rays from the scattered beam. Initial tests of this system will require only a small number of gamma-ray detectors (one or two of the 8π detectors) and 1.5 MeV/u accelerated beams that will be available from ISAC-I. Development of the system can thus begin as early as 2000 so that a fully operational target chamber system would be ready to begin experiments immediately with the $4 - 5$ MeV/u beams from the first stage of ISAC-II in 2003.

5.2.3 New High Efficiency Gamma Array

The 8π spectrometer was primarily designed and optimized for high-spin nuclear-structure studies with stable beams. Therefore typical experiments performed with the 8π involved high gamma-ray multiplicities and beam currents of the order of a few particle-nanoamperes. At the time of the construction of the spectrometer, the largest available germanium detectors had a relative efficiency of 25%. The 8π spectrometer comprises 20 of these detectors covering a total solid angle of 5% of 4π steradians. The total photo-peak efficiency of the germanium array is about 0.8%. Since then, the technology has evolved and it is now possible to grow much larger germanium crystals. Typical experiments with radioactive beams will involve small beam intensities and in most cases the gamma-ray multiplicity will be relatively low. Therefore it would be extremely useful to build a gamma-ray spectrometer with a large total photo-peak efficiency. Such a large efficiency could be achieved by positioning a few large germanium detectors very close to the target. However, all the experiments with accelerated radioactive ion beams will have to measure the gamma-ray energies for gamma rays emitted by nuclei in motion because the beam, and therefore the recoiling nuclei, cannot be stopped at the target position. The velocity of the emitting nuclei would induce a large Doppler broadening of the photo-peaks for germanium crystals subtending a large solid angle. Furthermore, the pile-up problem (more than one gamma ray firing the same detector) would be important for moderate gamma-ray multiplicities. It is therefore essential to use highly segmented germanium detectors.

In some situations the 8π spectrometer has remained competitive with the more expensive third-generation arrays. It was over-subscribed by a factor of 2.5 in the latest beam time competition at the Lawrence Berkeley National Laboratory. One of the features of the 8π that is responsible for this is the 72 element BGO ball, which measures the total gamma-ray energy and multiplicity for each event. The BGO ball will also be very useful for many experiments with radioactive

beams such as the study of nuclear structure at the limits of angular momentum with neutron-rich projectiles. However, for low-multiplicity experiments that require high-resolution and high gamma-ray detection efficiency the most cost-effective way to make the necessary major improvement in efficiency is not to modify the 8π spectrometer but to build a new modular, segmented germanium detector array.

A new germanium array optimized for ISAC-II physics must satisfy a number of criteria. First of all, it should have a large photo-peak efficiency and be highly segmented. Second, it must be competitive with the instruments being built in other countries while being cost effective. It should also be highly versatile with the possibility of optimizing the configuration for each experiment. The Compton-suppressed segmented clover detector is a very attractive design. Some of these detectors are being built for the EXOGAM (a gamma spectrometer for exotic beams) array at Spiral (system de production d'ions radioactifs et d'acceleration en ligne at GANIL in France). They consist of four germanium crystals forming a square cross section like a four-leaf clover. Each crystal has a relative efficiency of 41% and they are electronically segmented into four quadrants. Each clover detector is therefore segmented into 16 individual elements. The EXOGAM array will consist of 16 clover detectors and it is being built for a cost of approximately \$8M. The recoil velocities will generally be smaller at ISAC-II than at Spiral and the detectors could therefore be positioned closer to the target without losing too much in spectrum quality due to Doppler broadening. Fewer clover detectors would therefore be required to cover the same solid angle. A very efficient, flexible and competitive gamma-ray array can be built for about \$4M.

A modification of the EXOGAM clover array provides a good starting point for the design of a new gamma array for ISAC. These clovers consist of four 41% detectors originally 6 cm across. When arranged as a clover they have a 22.5° taper (over 3 cm) and are approximately a total distance of 9 cm across the front face. A sphere may be tiled with ten squares and eight triangles with the squares covering 80% of 4π. If detectors similar to those of EXOGAM are used but tapered at 30° for 2 cm, the front face would be approximately the same size as those of EXOGAM. Allowing for the size of the detector cans the inscribed sphere would be approximately 17 cm diameter. The suppressors would begin behind the taper.

At this distance the array would only be useful for low multiplicity events. The total expected undegraded photopeak efficiency for eight detectors would be $> 16\%$ for 1.33 MeV gamma rays, (compared with 11% for Gammasphere). This would result in a gamma-gamma coincidence efficiency of 400 times that of the 8π spectrometer. Since many of the radioactive beams will be very weak, such an array will greatly increase the number of useable radioactive species. If a gamma-ray hit can be localised to a single segment, the Doppler broadening will be worse than that of the 8π spectrometer, whose detector opening half angle is 8.0° compared with 6.1°. This may be recovered if the hit can be located to better than one segment. Simulations on the performance of such an array are in progress.

Smaller clover detectors ($4 \times 25\%$) might be borrowed to complement the array. For moderate-to high-multiplicity experiments or experiments that require a larger inner volume, the detectors could be moved out radially. The Compton suppression could be increased in this situation. If fewer detectors are available and summing is not a problem then the clovers could be used for source experiments in other configurations, (for example two clovers close to the source, four to six on the faces of a cube, etc.).

5.3 Particle Detectors

5.3.1 The TUDA Facilty

The studies of resonant and transfer reactions of interest to nuclear structure and nuclear astrophysics span both the mass and energy ranges of ISAC-I and II. Presently, an Edinburgh/TRIUMF collaboration is constructing a general purpose scattering facility to enable the study of reactions of interest to nuclear astrophysics with radioactive beams from ISAC-I. The facility is named TRIUMF-U.K.-Detector Array (TUDA); the U.K. funding council approved funding for TUDA in May 1999. The facility will consist of specialized scattering chambers and large arrays of silicon strip detectors instrumented with microelectronics. The hardware will be designed to be highly versatile and easily reconfigured to suit a wide variety of experiments. This facility would be ideal for the study of a wide variety of charged-particle reactions with ISAC-II.
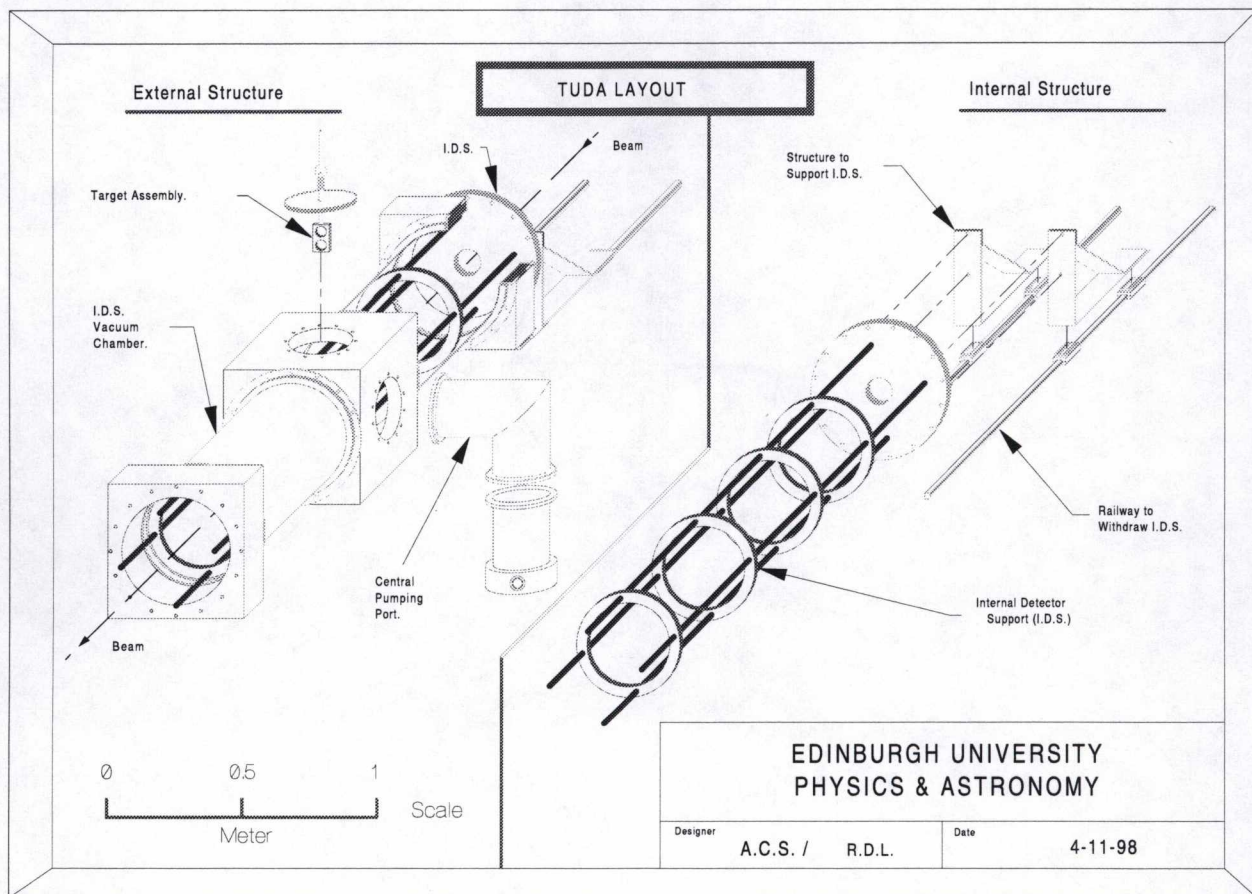
Figure 10: Mechanical assembly of the TUDA facility.

TUDA consists of an extended scattering chamber, the length of which can be changed, with the target in the centre and several large arrays of silicon detectors both in the forward and backward hemisphere. Fig. 10 shows an overview of the mechanical assembly of the chamber. These large silicon arrays, which are part of the facility, were developed by the University of Edinburgh group

31

and are extended annular counters (other highly segmented square detectors will also be used). The largest array detector (LEDA, 26 cm outer diameter with a 10 cm inner borehole) is segmented in eight (removable) pieces in ϕ direction with each (pie) segment divided into 16 concentric (θ) rings. Two of the major segments can be removed to fold the detector and cover a large solid angle at large angles θ (LAMP configuration). Meanwhile another version with smaller area (CD) is available with about equal pixalation in both θ and ϕ direction. Such a segmentation is essential, if either the count rate is very high (forward direction), or if in a multiple-particle breakup, θ, ϕ angular information of the particles is sought. In addition, a wire chamber based ΔE gas detector for LEDA is under development (SWAN). Fig. 11 shows layouts of the three detectors.
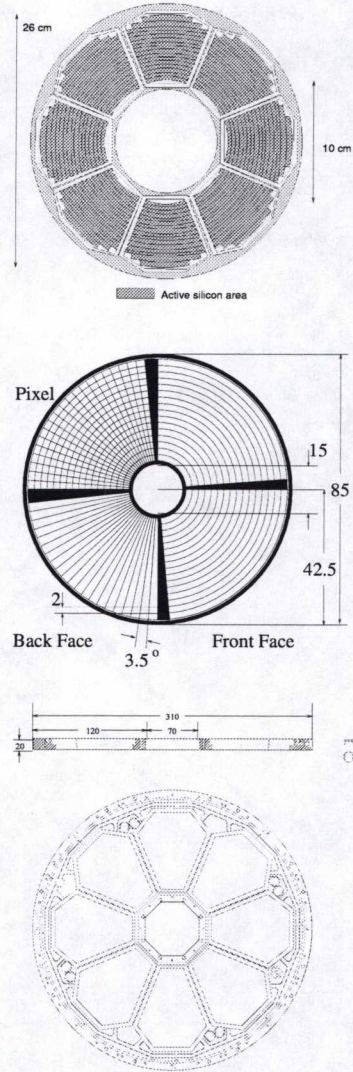
Figure 11: Edinburgh detectors designed for radioactive-beam experiments. LEDA (top), CD (middle) and SWAN (bottom).

Together with the detectors, 300 electronic channels of spectroscopic quality have been approved for funding. This electronics has been developed by the University of Edinburgh in collaboration with the Rutherford Appleton Laboratory and is now also commercially available. The facility is expected to be operational in August 2000 for ISAC-I.

5.3.2 Auxiliary Particle Detectors

In addition to the general purpose scattering facility, TUDA, a second scattering chamber and additional fully-instrumented and highly-pixelated silicon detector arrays will be required for nuclear-structure studies with radioactive beams with ISAC-II. Further, the development of a windowless gas-jet target will probably be required for some transfer reaction studies.

Finally, an array of neutron detectors is essential for the study of proton-rich nuclei, where the detection of evaporation neutrons in addition to the charged particles emitted in heavy-ion fusion reactions with radioactive projectiles would provide an effective tool to select very proton-rich residues.

5.4 Recoil Separators

5.4.1 DRAGON

The DRAGON is a state of the art recoil mass fragment separator designed for the study of proton- and alpha-capture reactions in inverse kinematics by bombarding a high-pressure windowless gas target with radioactive beams from ISAC-I. The separator consists of four alternating magnetic and electrostatic dipole magnets designed to separate the recoils from the primary beam at the level of one part in 10^{15}. A layout of the device is shown in Fig. 12. As mentioned in Section 4.6 the beams from ISAC-II will greatly extend the ISAC-I nuclear astrophysics program to higher masses using both DRAGON and TUDA. For some experiments it might be required to increase the maximum beam available at the DRAGON location to ~ 2 MeV/u but no upgrades to the experimental apparatus are anticipated.

5.4.2 Gas-Filled Separator

The search for and the study of the properties of very heavy new elements will require special techniques given the small cross sections for their production. One approach, which has had considerable success for such studies, is the use of a gas-filled magnetic separator. Since the full momentum of the projectile is transferred in complete fusion reactions used to produce very heavy elements, the heavy recoils emerging from the target have a well defined velocity with a narrow distribution. In contrast, reaction products from transfer reactions have smaller masses and larger velocities while the beam itself has a much smaller mass. Ions passing through a magnetic field will follow a trajectory determined by their charge to momentum ratio. Heavy ions penetrating a gas-filled region are slowed down, undergo atomic charge-changing collisions and follow a trajectory determined by the mean value of their charge to momentum ratio. This trajectory is independent of the initial charge state of the recoil. Gas-filled separators therefore are ideal to search for and study the heavy element products of fusion reactions. They have demonstrated high transport efficiency, excellent suppression of the beam and unwanted reaction products, and reasonable collection spot sizes. In fact, the recent observation of new elements at the Lawrence Berkeley National Laboratory
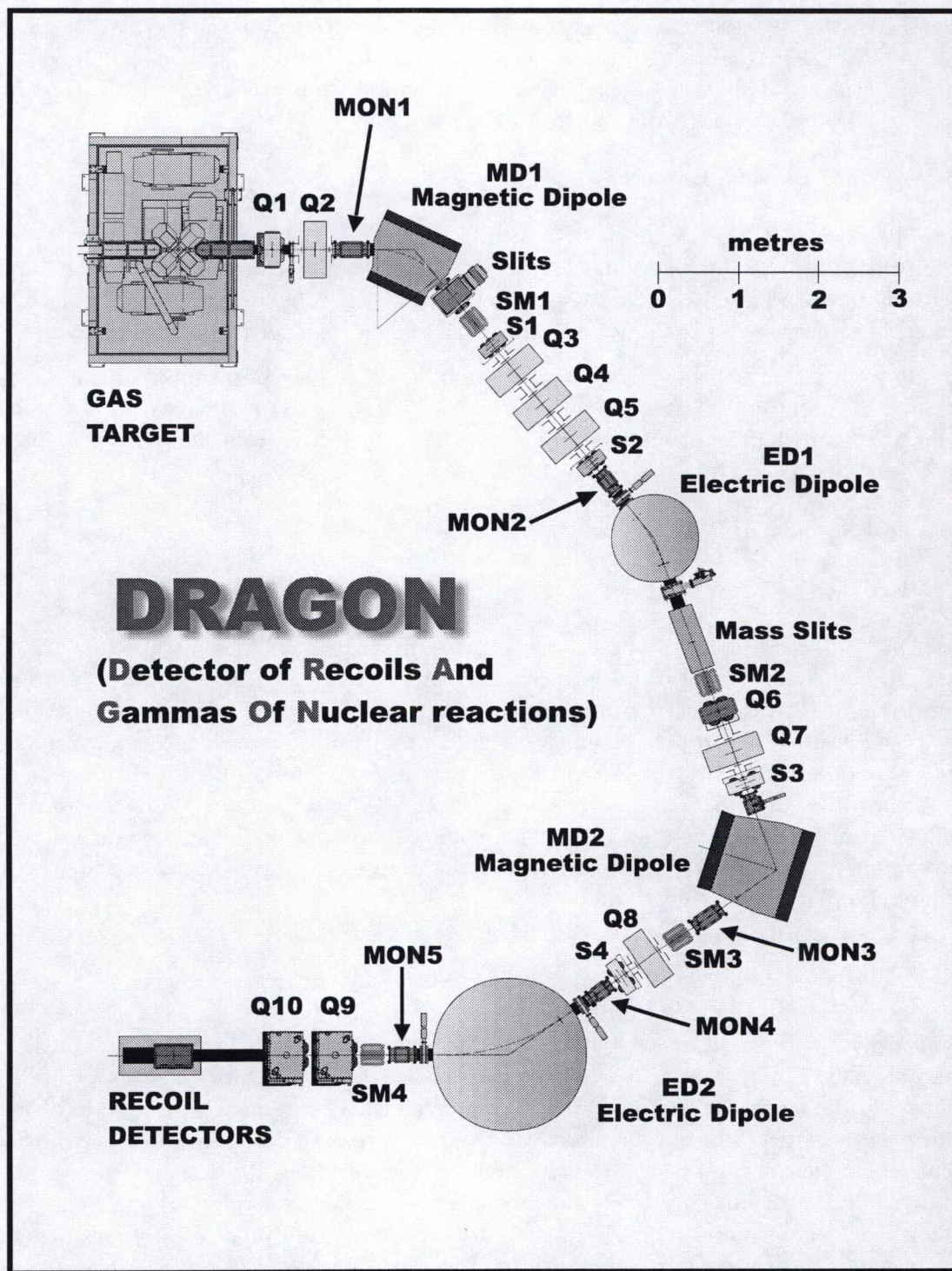
Figure 12: Layout of the DRAGON facility.

were performed with such a device in a QQD configuration. However, since gas-filled separators have very poor mass resolution, sophisticated auxiliary detectors positioned at the focal plane are required to provide the necessary mass identification and to detect all radiation emitted by the desired reaction products[26, 27, 28].

5.5 HÉRACLÈS 4π Multidetector Array

The HÉRACLÈS 4π Multidetector Array has been used to study a variety of heavy-ion reaction phenomena with stable beams up to $A \sim 60$ and energies $E \leq 50$ MeV/u. It is presently installed at the Cyclotron Institute, Texas A&M University and would be moved to ISAC-II when beams become available. The array consists of 144 charged-particle detectors covering the angular range from $3.3°$ to $140°$. Four rings of 16 plastic phoswich detectors subtend the region from $3.3°$ to $24°$ followed by two rings of 16 CsI detectors coupled to phototubes and a 48 element CsI ball coupled to photodiodes. A layout of the device is shown in Fig. 13. Modifications to the array will be required to optimize the performance for the lower energy beams from ISAC-II. In addition, different detectors will be needed to detect residues and slow moving fragments. The facility includes a large 2 m diameter scattering chamber and a 1 m extension at forward angles suitable for time of flight measurements. Finally, because the array has a high efficiency, modest beam intensities $10^6 - 10^8$ s^{-1} should be sufficient for most experiments.
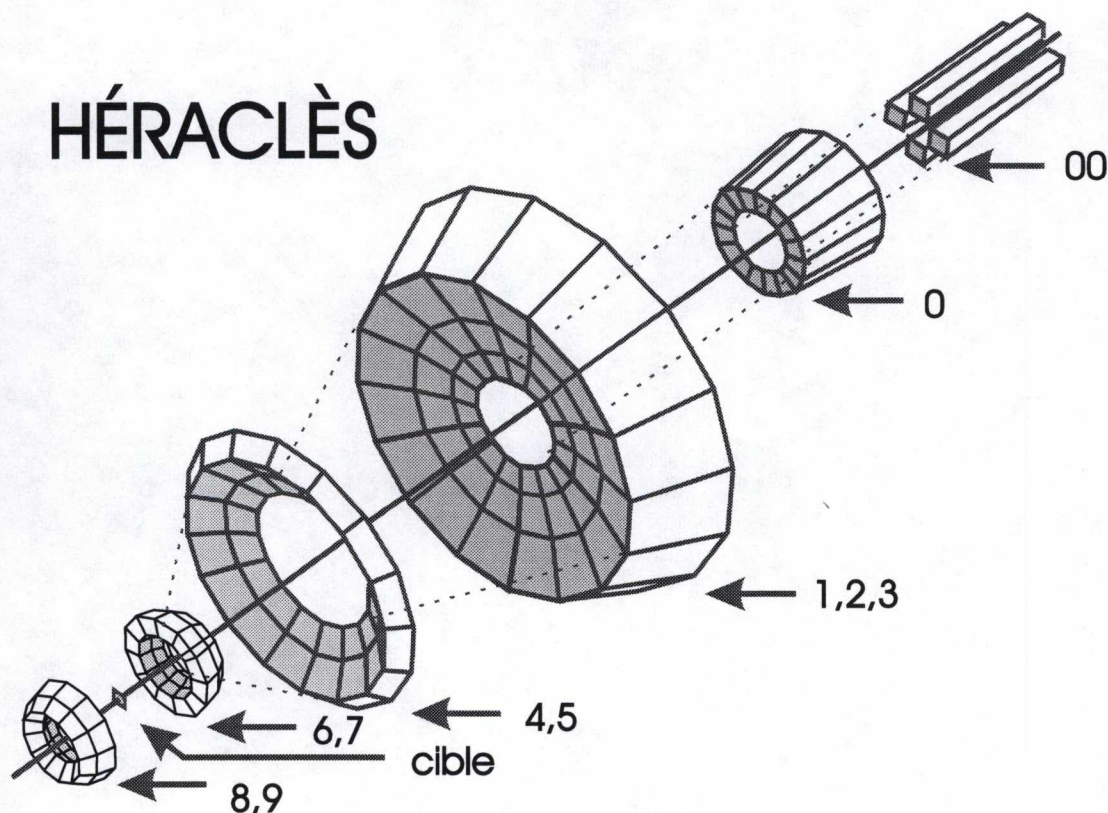

Figure 13: Layout of the HÉRACLÈS facility.

5.6 Summary

Table III summarizes the estimated cost for the experimental facilities required to exploit the exotic radioactive beams at ISAC-II. Also given in Table III is the ideal funding scenario that would allow for the experimental apparatus to be designed and constructed in time for first beams available from ISAC-II in 2003 and from the full facility in 2005. The choice of facility and the priorities for funding are subject to change, however, depending on the needs identified by the Canadian and international users of ISAC-II.

Table III: ISAC-II Detector Facilities (cost in FY98 dollars).

Instrument	Optimum funding scenario (Year)	Estimated Cost [M$]
8π Spectrometer Upgrade	2001 − 2002	0.2
Gamma-ray target chamber	2001 − 2002	0.2
New Gamma Array	2001 − 2004	4.5
Gas Filled Separator	2004 − 2005	2.0
Auxiliary Particle Detectors	2003 − 2006	1.0
HÉRACLÈS Array Upgrade	2002 − 2004	0.5
TOTAL		8.4

6 ISAC-II Facility

6.1 Introduction

The ISAC facility now under construction will provide ions of mass $A \leq 30$ up to energies of 1.5 MeV/u. The post-accelerator (Fig. 14) consists of a 35 MHz RFQ to increase the energy of ions with $A/q \leq 30$ from 2 keV/u to 150 keV/u and a 105 MHz drift-tube linac (DTL) to accelerate ions with $A/q \leq 6$ to a final energy fully variable between $0.15 - 1.5$ MeV/u. The two linacs are connected by a Medium Energy Beam Transport (MEBT) where the beam is stripped to increase the charge state and then matched into the DTL. All linac components operate cw to maintain the intensity of the ions.
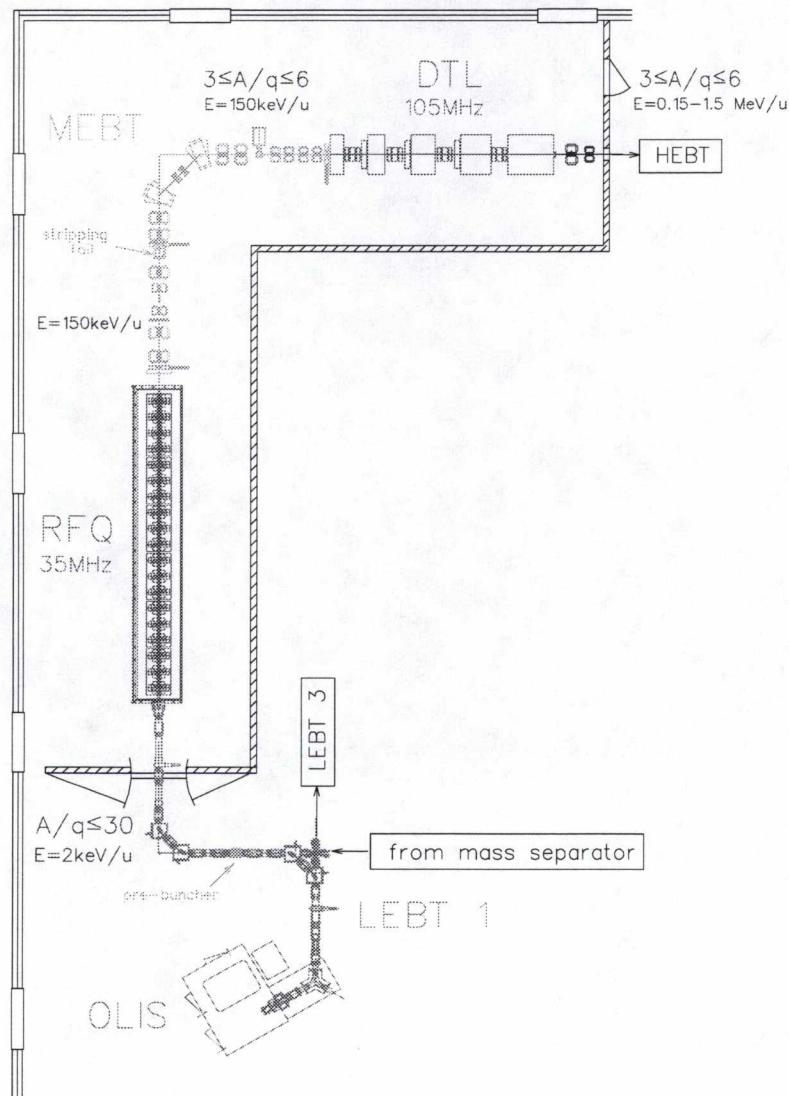
Figure 14: The ISAC-I linear accelerator.

In the ISAC-II facility, the accepted mass range is extended up to 150 and the final energy is increased above the Coulomb barrier ($E \sim 6.5$ MeV/u). The ISAC-II acceleration scheme utilizes the existing RFQ and a new pre-stripper DTL. A superconducting linac is proposed for the post-stripper section of the accelerator chain.

6.2 Overview of Scheme

A schematic of the proposed ISAC-II linear accelerator complex is shown in Fig. 15.

ISAC-II will utilize the existing ISAC-I RFQ for low-energy acceleration and therefore requires that the ion charge from the source obeys $A/q \leq 30$. Recent advances in charge-state booster (CSB) development [29] make this choice feasible. A CSB will be added after the mass separator to increase the charge state of ions with $A > 30$. To minimize the total acceleration voltage required
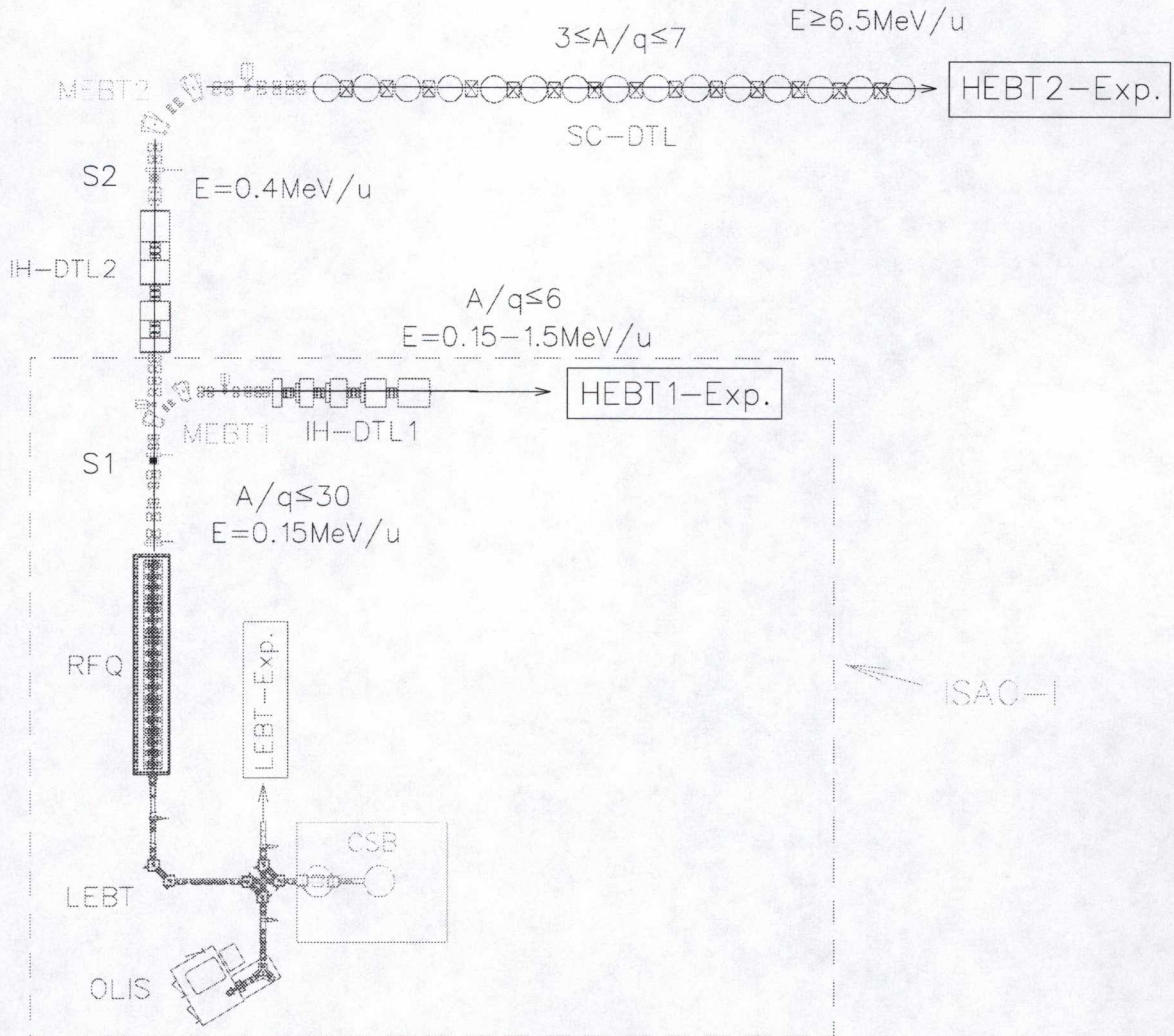
Figure 15: The ISAC-II linear accelerator complex.

the optimum stripping energy for masses of $A \leq 150$ and for $E_{\text{final}} = 6.5$ MeV/u is ~ 400 keV/u (see Section 6.3).

An effective configuration to reach 400 keV/u is to continue the acceleration straight north of the RFQ–MEBT line. This will require a grade-level addition to the north of the present building. A DTL will be placed downstream of the existing MEBT bender after a short matching section. A room-temperature interdigital H-mode (IH) structure operating in cw mode will be used to accelerate the ions of $A/q \leq 30$ from $0.15 - 0.4$ MeV/u. The beam then is stripped and the ion charge selected in a new MEBT2 that bends the beam through $90°$ to a line parallel to the ISAC-I DTL line. Ions of mass to charge ratio $3 \leq A/q \leq 7$ are matched into a superconducting DTL on this line and accelerated to at least 6.5 MeV/u and then transported to the experimental stations.

The short independently phased cavities that make up the post-stripper linac have a wide velocity acceptance and so the ions do not have to follow a fixed velocity profile rigorously to stay in phase with the rf. Consequently the maximum velocity of a particle depends on its charge to mass ratio. In this case the final energy per nucleon for light ions could be more than double that for the high-mass particles. Even for the highest masses, higher energies will be possible at a cost in intensity with the addition of an intermediate stripping station. A summary of the linac specifications is shown in Table IV.

Table IV: Summary of ISAC-II linac specifications.

Device	E_{in} (MeV/u)	E_{out} (MeV/u)	A/q	ΔV_{max} (MV)
CSB	–	0.002	≤ 30	0.06
RFQ1	0.002	0.15	≤ 30	4.44
IH-DTL2	0.150	0.40	≤ 30	7.50
strip				
SC-DTL	0.40	6.5	$3 \rightarrow 7$	42.7

The flexibility of short superconducting modules has other advantages as well. Since they have a wide velocity acceptance, they can be built and utilized in a preliminary configuration. Higher-energy experiments could therefore start in as little as 2.5 years after the beginning of the next Five-Year Plan (i.e., by 2003). Masses up to 30 and energies up to ~ 5 MeV/u would then become available. With the implementation of the charge-state booster, masses up to $A = 60$ would also become available.

6.3 Design Choices

6.3.1 Charge-State Booster

The CSB would take the singly charged radioactive beam from the mass separator and boost the charge state to be compatible with $A/q \leq 30$ for the RFQ. Electron-cyclotron-resonance (ECRIS) and electron-beam (EBIS) ion sources can easily reach the required charge, q. ECRIS charge-state boosters are under intensive development at GANIL and Grenoble. For example, from a beam of singly-charged ions these groups have already demonstrated Kr^{9+} with an efficiency of 9% and Zn^{7+} with an efficiency of 2%. The REX-ISOLDE collaboration is developing an EBIS to convert a dc beam of singly-charged ions to a pulsed beam of multiply-charged ions. There is sufficient space on the accelerator floor in the low-energy transport system (LEBT) for either CSB approach.

An attractive option is to develop a charge-state booster that would give $A/q \leq 7$. This would obviate the need for any stripping and the inherent loss of intensity. However, there is currently no guarantee that such high charge states (e.g., $q = +25$ for $A = 150$) can be obtained efficiently. Moreover, the higher the charge state, the longer the 'cooking' time needed in the charge booster; e.g., up to 100 ms for very high charge states. This rather lengthy charge breeding time would make it difficult to obtain reasonable intensities for short-lived isotopes far from stability.

As a rough rule recent results suggest that efficiencies of 2% are possible in this latter mode and from $10-20\%$ in the low-q mode [29]. The estimated cost of upgrading to higher charge state is 2 M$.

6.3.2 One Stripping Stage

The total voltage required to reach a given energy is dependent on the charge of the ion being accelerated. It is a common practice in accelerators to introduce a stripping foil at some stage in the acceleration process to increase the charge state of the ions and therefore reduce the size and cost of the accelerator. Each stripping stage however will result in a reduction in intensity since only a fraction of the beam (typically $15\%-40\%$) will be in the charge state of choice. When an ion passes through a stripping medium the emerging ions will have a charge state with a population that can be approximated by the Gaussian distribution

$$F(Q) = \frac{1}{\sqrt{2\pi}d} e^{-\frac{(Q-\overline{Q})^2}{2d^2}},$$

where d is the width of the distribution and $\overline{Q}$ is the most probable charge state after stripping. It is the width d that defines the sharpness of the Gaussian distribution and hence the efficiency of populating the most probable charge state.

GANIL has published [30] an approximation for d as follows:

$$d = 0.5\sqrt{\overline{Q}\left(1 - \left(\frac{\overline{Q}}{Z_p}\right)^{5/3}\right)},$$

where Z_p is the proton number of the projectile.

The stripping energy should be chosen carefully since the most probable charge state increases with the energy of the ions, decreasing the length of the post-stripper accelerator at the expense of a longer pre-stripper linac. An optimum can be calculated knowing the energy range of the acceleration and the ions to be accelerated.

In the case of ISAC-II the goal is to accelerate ions of $A/q \leq 30$ and $A \leq 150$ from 0.002 to 6.5 MeV/u. The total accelerating voltage required for no stripping and for one-stripper and two-stripper stages are given in Table V. The table shows how a single stripping stage has a benefit in cost that compensates for the reduction in final intensity; that is, each are affected by roughly a factor of four. It is also clear that a second stripper stage does not offer a similar cost/benefit solution. For this reason a single stripping stage is adopted for ISAC-II. As an aside, there may be certain ions whose initial charge can be efficiently boosted such that $A/q \leq 7$. In this case the ion would be accelerated without stripping.

Table V: The total voltage and associated costs and acceleration efficiency for no stripping stage and one and two stripping stages.

Strippers	ΔV_{max}	Cost	Efficiency
–	(MV)	(M$)	(%)
none	190	60	~80
one	50	15	~20
two	37	11	~5

Assuming a single stripping stage the total voltage required to reach 6.5 MeV/u from 2 keV/u is given by

$$V_{tot} = \frac{A}{q_i}(E_s - 0.002) + \frac{A}{q_s}(6.5 - E_s),$$

where q_i is the initial charge injected into the RFQ, q_s is the charge state after stripping and E_s is the stripping energy. The total voltage required for accelerating several different ions to 6.5 MeV/u as a function of stripping energy is given in Fig. 16. The results assume that the initial $A/q_i \leq 30$ and that $q_s = \overline{Q}(E_s)$ the most probable charge state for a given ion and E_s. The plot shows that the optimum energy for stripping is ~ 400 keV/u.

Data relevant to stripping heavy ions at an energy of 400 keV/u are summarized in Fig. 17 [31] as a function of the proton number of the projectile. In Fig. 17(a), the most probable charge state, $\overline{Q}$, is plotted. The efficiency of stripping into the most probable charge state is reflected in Fig. 17(b). The mass to charge values after stripping (for stable ions) is shown in Fig. 17(c). This leads to the design choice of $3 \leq A/q \leq 7$ for the post accelerator linac with associated stripping efficiencies varying from 50% for the lightest ions to 15% for $A = 150$.
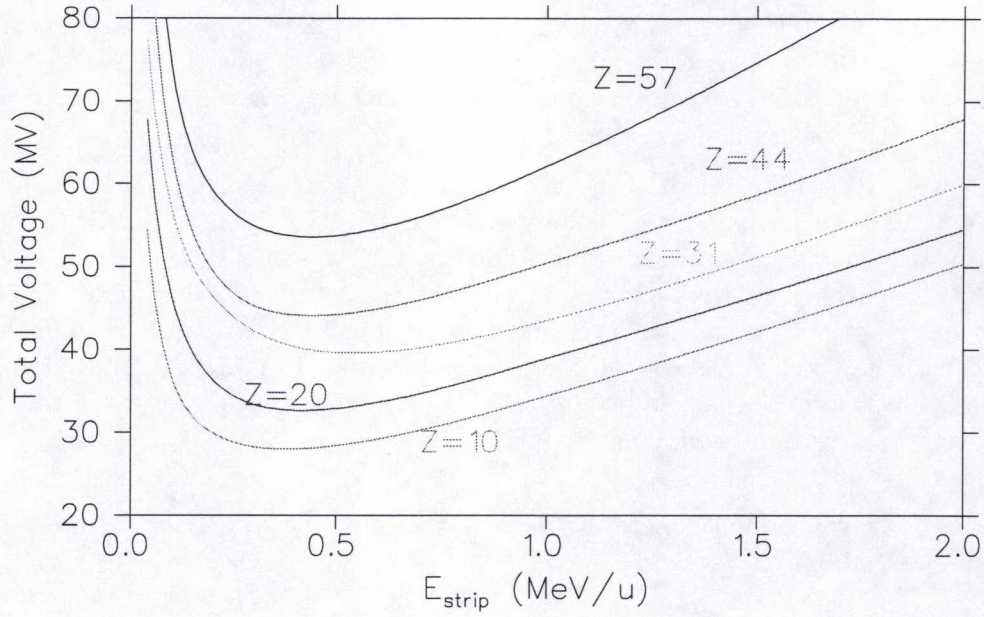
Figure 16: The total voltage required to accelerate various ions from 0.15 to 6.5 MeV/u as a function of stripping energy.

6.4 The ISAC-II Accelerator

A schematic of the proposed ISAC-II linear accelerator complex is shown in Fig. 15. Details of the various sub-components are described below.

6.4.1 RF Quadrupole

The 8 m long 35 MHz ISAC RFQ (Fig. 18) is a four-rod split ring structure designed to accelerate ions of $A/q \leq 30$ from 2 keV/u to 150 keV/u operating at a peak voltage of 74 kV. To date, a 2.8 m long section of the RFQ has been operated at full voltage in cw mode with predicted beam performance. High power tests have confirmed that while operation at peak voltage is relatively routine, operation at even 10% higher voltages (for a 10% increase in A/q) may require some development. Therefore, although the design choices of the RFQ were conservative, they were also realistic and the Charge-State Booster will be employed for masses above $A \sim 30$.

6.4.2 LMEBT

A short transport section is needed after the existing MEBT 45° dipole to match the 150 keV/u beam from the RFQ to the new IH-linac. The section (Fig. 19) will consist of a 35 MHz rebuncher and six quadrupoles.

6.4.3 Pre-Stripper Linac

The IH linac structure [32] offers very high shunt impedance values making cw operation at room temperature possible. The structure is used in the ISAC DTL1 variable energy linac design [33]
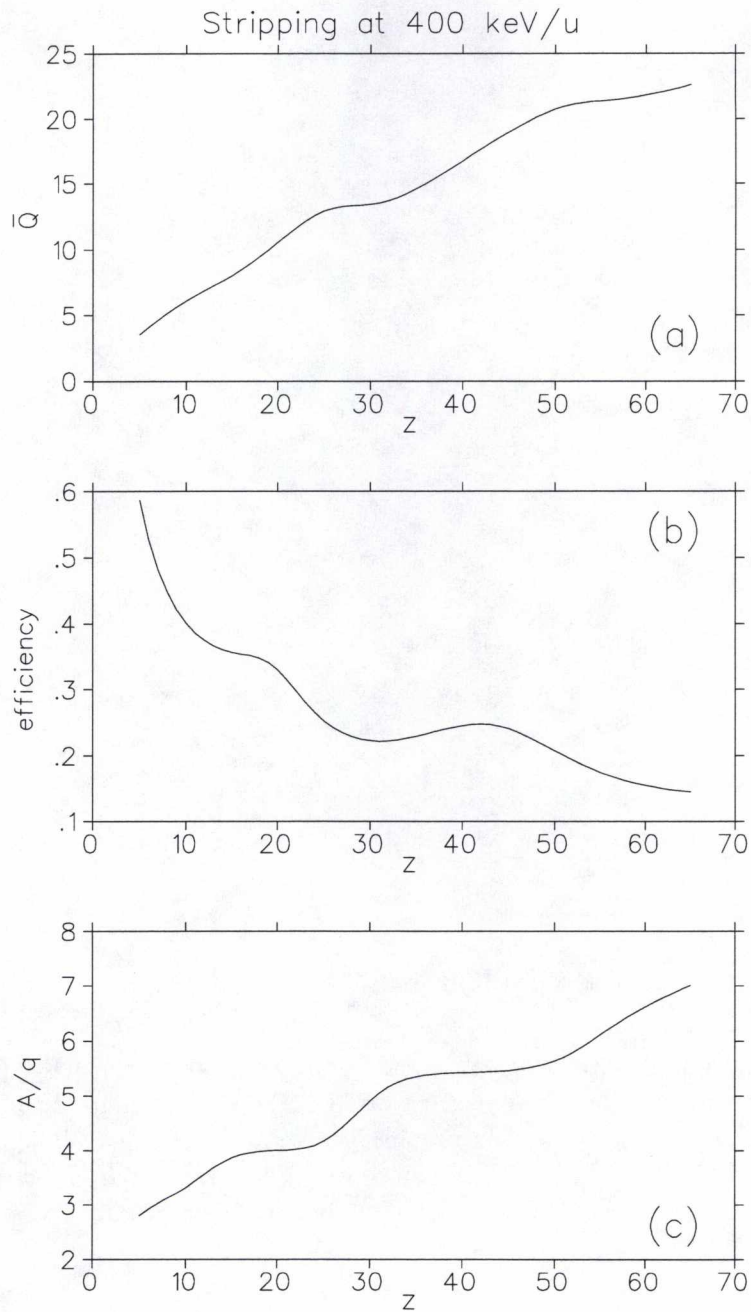
Figure 17: Data relevant to stripping heavy ions at 400 keV/u as a function of the proton number of the projectile. Plots include: *(a)* the most probable charge state $\overline{Q}$, *(b)* the efficiency of stripping into the most probable charge state, and *(c)* the mass to charge ratio of the projectile after stripping.

that will be installed in 2000. In this case the application is for a fixed final velocity, so long tanks each containing many drift tubes can be used to achieve the highest acceleration efficiency. Magnetic quadrupoles can be installed both in tanks and between tanks to provide periodic transverse
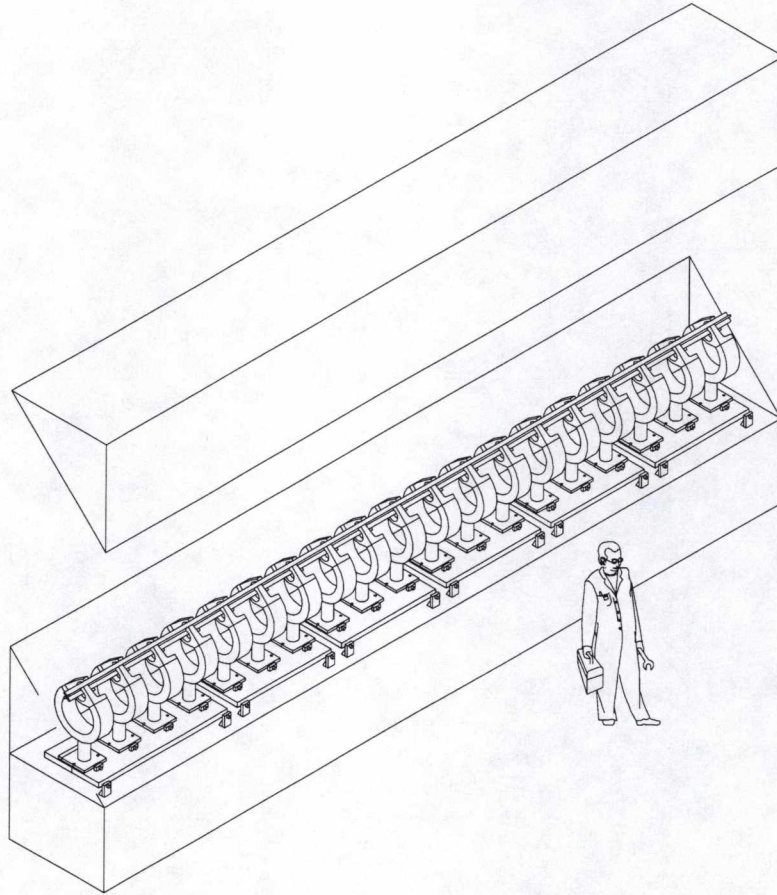
Figure 18: The ISAC 35 MHz RFQ.

focussing. The small longitudinal and transverse emittances from the RFQ ($\epsilon_z = 0.3\pi$ keV/u ns and $\beta\epsilon_{x,y} = 0.1\pi$mm mrad) allow a frequency of 70 MHz, double that of the RFQ frequency, reducing the size of the DTL tanks and improving the shunt impedance. The shunt impedance for the structure is estimated to be ~ 300 MΩ. In a cw DTL the dissipated power is a more limiting factor than the peak surface field in establishing the operating gradient. A power dissipation of 20 kW/m can be safely cooled. The relation

$$P_l = (\overline{E_oT})^2/Z,$$

where P_l is the power per unit length and Z is the shunt impedance then gives an average effective gradient $\overline{E_oT}$ of 2.4 MV/m.

In order to reduce the demands on the rf amplifier the DTL is divided into two tanks each with one quadrupole triplet inside roughly midway down the tank and one quadrupole triplet between tanks. Each triplet will require ~ 65 cm with gradients up to 60 T/m. A diagnostic box will also be added to the intertank region. The total length of the linac will be 5.8 m. The beam dynamics utilizes the method developed at GSI [34] where a short $-60°$ section is used after each magnet system for rebunching followed by an accelerating section at a synchronous phase of $0°$.

44
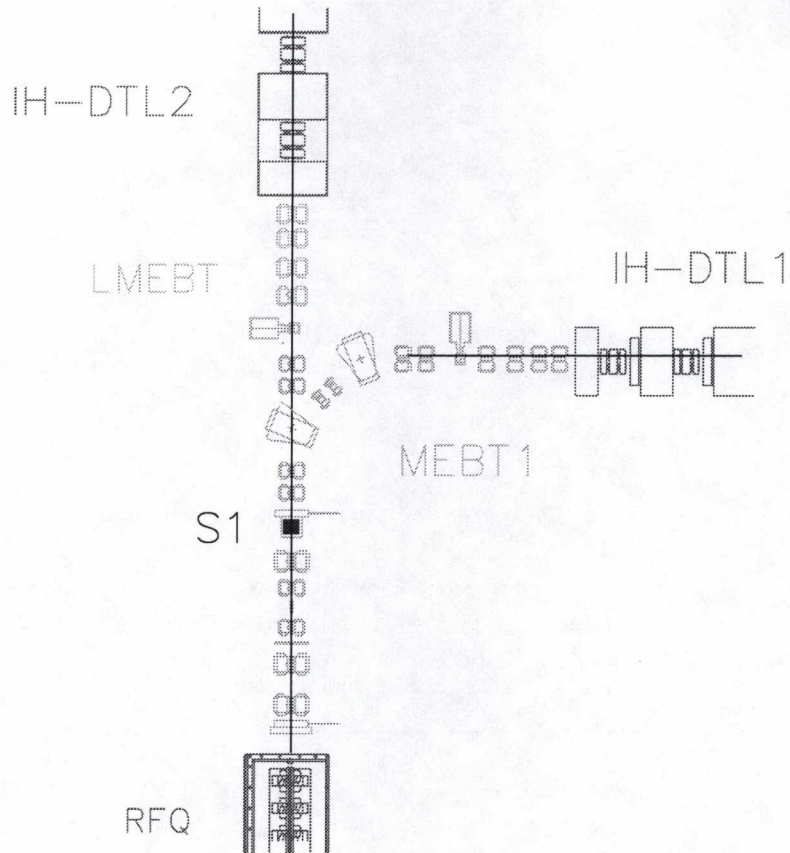
Figure 19: The LMEBT section matching the beam from the ISAC MEBT1 to the pre-stripper linac, IH-DTL2.

The acceptance of the linac is $\epsilon_z = 3.6\pi$ keV/u ns and $\beta\epsilon_{x,y} = 0.8\pi$mm mrad. With the expected beams from the RFQ the emittance increase during acceleration is calculated to be less than 5%.

A summary of the gross specifications for the linac are presented in Table VI and the specifications for each tank are given in Table VII. A schematic rendering of the DTL and associated beam envelopes is shown in Fig. 20.

Table VI: Gross specifications of the pre-stripper DTL.

Parameter	Value
Initial Energy	150 keV/u
Final Energy	400 keV/u
A/q	≤ 30
V_{eff}	7.5 MV
RF Frequency	70 MHz
Type	IH room temperature
Duty Cycle	cw
Length	5.8 m
Triplet Length	70 cm
Transmission	100%
Emittance Growth	$< 10\%$

Table VII: Specifications for each tank of the pre-stripper DTL.

Parameter	Tank 1	Tank 2
Energy Range	150-250 keV/u	250-400 keV/u
A/q	30	30
V_{eff}	3.0 MV	4.5 MV
No. of cells	13, 21	21, 20
E_g (MV/m)	2.7	2.7
Length (m)	2.2	3.0
Power (kW)	30	45
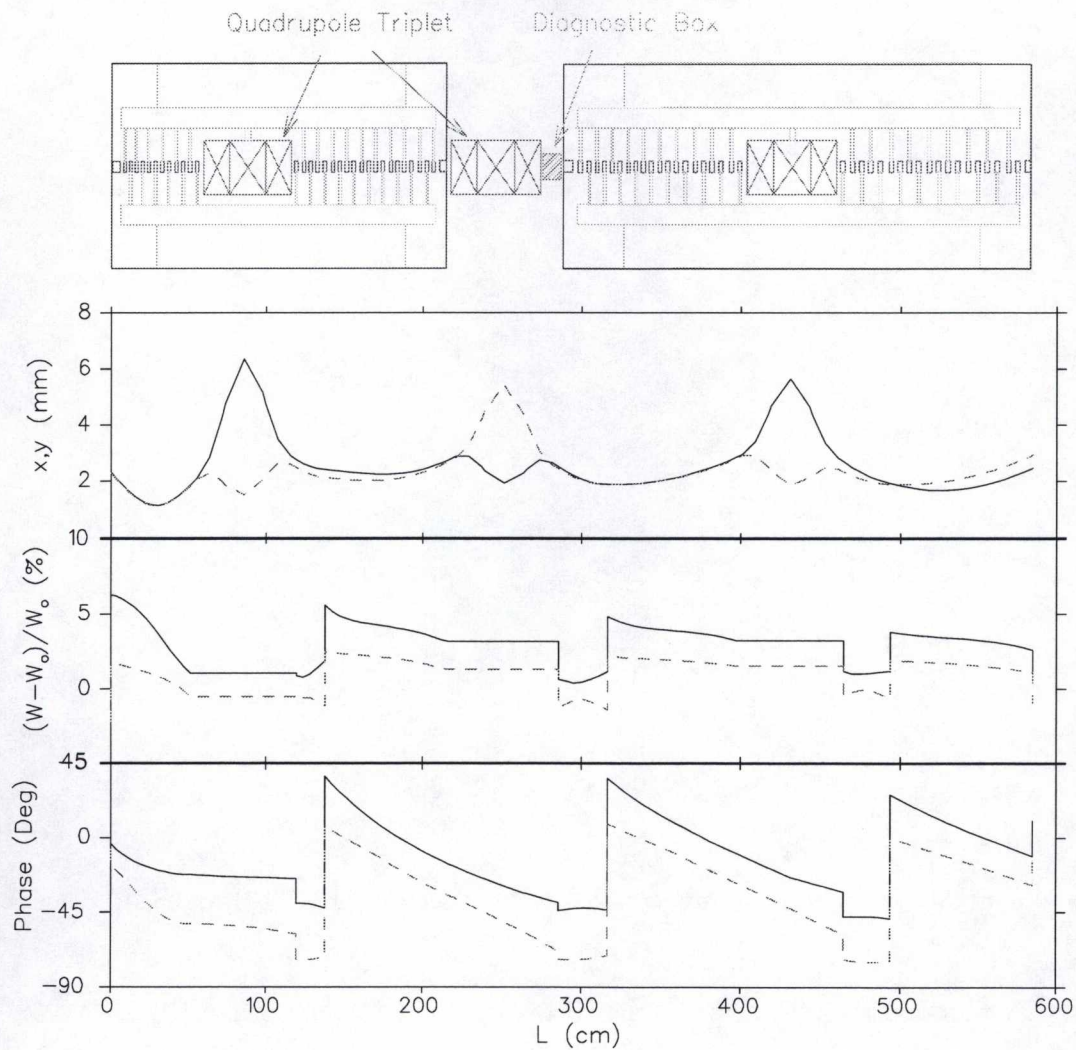
Figure 20: The pre-stripper IH-linac for ISAC-II and associated beam envelopes. In the top case the solid and dashed lines represent the x and y transverse beam envelopes. The bottom two figures show the minimum and maximum values of relative energy and phase respectively.

6.4.4 Medium-Energy Beam Transport (MEBT2)

The main function of the medium-energy beam transport (MEBT2) is to provide a means of stripping the ions to a higher charge state and to select the ion of choice. The design of MEBT2 is very similar to that of the existing MEBT for ISAC-I. Three sections are employed:

- Stripping foil matching section
- Charge selection section
- SC-DTL matching section

A schematic of MEBT2 is shown in Fig. 21.
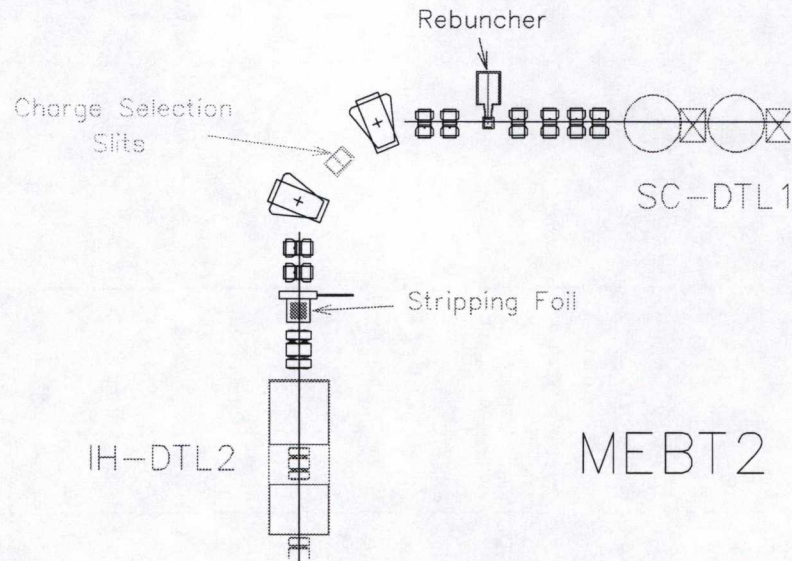
Figure 21: The medium-energy transport section (MEBT2) for ISAC-II.

In the first section the beam exiting the IH-DTL is collected and focussed transversely onto the stripping foil with a quadrupole triplet matching section to reduce the effects of multiple scattering. The section is kept short to minimize the debunching between IH-DTL2 and stripping foil so as to limit the longitudinal emittance growth due to energy straggling.

The charge selection section consists of an achromatic QQDDQQ 90° transport with charge selection slits at the dispersed focus in the symmetry plane.

The last section provides a three dimensional match to the following superconducting linac section. Four quadrupoles are used to match the beam transversely and a 35 MHz spiral buncher will be used to match the beam longitudinally.

6.4.5 Post-Stripper Linac

The gross specifications of the post-stripper linac are shown in Table VIII.

Table VIII: Gross specifications of the post-stripper linac.

Parameter	Value
Initial Energy	400 keV/u
Final Energy ($A/q = 7$)	6.5 MeV/u
A/q	$3 \leq A/q \leq 7$
V_{eff}	42.7 MV
Duty Cycle	cw

6.4.6 Superconducting Heavy-Ion Linacs

Recent improvements in accelerating gradient and simplification of fabrication procedures [42] plus flexible operation and excellent beam quality make a superconducting linac a favourable choice for the ISAC-II post-stripper accelerator. Superconducting technology is technically more difficult than the room temperature structures but the field of superconducting rf cavities for heavy ions is a mature one. The development of the SC accelerator technology started in the late 1960's leading to the funding of the heavy-ion linac at Argonne in 1975 with beam production in 1978 [35]. Since then many facilities have come on line, among them SUNY at Stony Brook, University of Washington, Oxford, Kansas State, Weizmann Institute, ANU-Canberra, JAERI-Tokai, and INFN-Legnaro.

Superconducting heavy-ion linacs are composed of several short (two- to four-gap), independently fed cavities arranged in a common cryostat with focusing magnets at periodic intervals down the length. The short cavities result in a broad velocity acceptance and consequently the acceleration does not have to follow a fixed velocity profile. For instance, lighter ions can be accelerated to a higher velocity than heavy ions. As well, resonator performance is not critical to the overall linac performance; that is, variation from the design gradients or even failure of a cavity are not catastrophic as in a fixed profile linac.
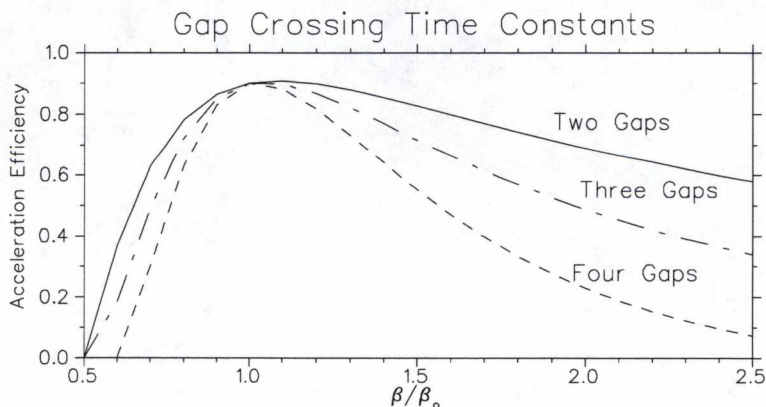

Figure 22: Transit time factors for a two-, three- or four-gap cavity as a function of relative ion velocity.

Two-gap cavities have been made in both a spiral [36] and QWR (quarter wave resonator) configuration [37]. Three-gap cavities have been made in a split-ring structure [38]. The four-gap cavities are constructed in a QWR interdigital geometry [39]. Two gaps give a larger velocity acceptance (Fig. 22) at the expense of a reduced voltage gain per cavity when compared to three- and four-gap cavities. Because of the very high electrical Q value it is necessary to reduce mechanical vibrations in the rf structures. The QWR shape is inherently more stable than the ring structures making three-gap cavities less attractive. Also in the case of ISAC-II, where there is a demand for accelerating ions with a wide range of A/q values, the advantage of the two-gap structure over the four-gap structure is clear as long as a stable low-β structure can be developed.

Another advantage of superconducting cavities is that high gradients can be achieved even in cw mode with relatively little rf power. Both lead and niobium have been used as superconducting materials in rf cavity construction. Because of the relative ease of manufacture and good heat dissipation lead plated onto copper was a popular choice in the early heavy-ion linac applications. However the higher critical temperature ($9.2°$K for Nb and $7.2°$K for Pb), higher critical magnetic field (1980 Oe for Nb and 800 Oe for Pb) and five times lower surface resistivity of Nb compared to Pb makes niobium a preferable superconducting material [40]. Developments in fabrication techniques have improved the ease of manufacture of niobium cavities. In the past ten years results at both JAERI and INFN-Legnaro have shown that niobium cavities either explosively bonded to copper as in the JAERI case [41] or bulk-machined or sputtered onto copper in the INFN case [42, 43] produce cavities that can operate with gradients consistently above 5 MV/m in the velocity range under discussion here. Gradients for lead-plated cavities, even with recent improvements in surface preparation, can only consistently reach levels of 3−3.5 MV/m [44]. While room temperature cavities operating in cw mode are capable of only 2.5 MV/m.

Cavity Specifications

A two-gap quarter wave structure is chosen for ISAC-II because of its high-velocity acceptance and inherent mechanical stability. The former is useful to accelerate the wide range of ions ($3 \leq A/q \leq 7$) efficiently with a minimum of cavity types and the latter is essential to produce high accelerating gradients. We choose a common linac geometry (INFN-Legnaro, JAERI-Tokai) having four resonators in a cylindrical cryostat with room-temperature quadrupoles between cryostats.

A cavity is identified by the ion velocity, β_o, required to traverse the distance between gap centers in half an rf oscillation. The distance between gaps is then $\beta_o\lambda/2$ where λ is the rf wavelength. The height of the cavity is $\lambda/4$. For the sake of economy of manpower and cost it is beneficial to limit the number of different cavity designs. Legnaro has reduced the design overhead required between different β_o values by maintaining a constant outer cavity diameter and changing the cavity frequency to alter β_o. Based on the same design principle, three cavity sizes, corresponding to low-, mid- and high-β_o cavities respectively, have been adopted for ISAC-II.

Overall acceleration efficiency plus practical concerns are responsible for the choice of cavity geometries. Any one cryostat will be outfitted with four identical resonators so the number of cavities of each type will be a multiple of four. A first stage of installation by 2003 (see Section 6.5) will consist of five cryostats loaded with twenty cavities delivering an effective voltage of $\sim$ 20 MV to a beam with an initial velocity of 5.6% (1.5 MeV/u). It was decided that in order to limit the early design work this stage should consist of only mid-β_o cavities designed for β_o =7.2%. The low-

and high-β_o values were chosen to optimize the acceleration efficiencies over the whole A/q range. Mass to charge ratios from $3 - 10$ were considered; the higher values may be possible direct from the CSB without stripping. In summary, the chosen cavity geometries correspond to particle velocities of 4.2%, 7.2% and 10.5% the speed of light with cavity quantities of 8, 20 and 20 for a total of 48 cavities. In the low-β_o section a gradient of 5 MV/m is assumed, while 6 MV/m is assumed elsewhere. The acceleration efficiency over the whole acceleration range is shown in Fig. 23(a,b,c) for various A/q values. The final acceleration efficiency as a function of mass to charge ratio is shown in Fig. 23(d).

Based on these voltages and the expected integrated time constant the final energy of the beam for different ions is shown in Fig. 24.

Cavity Dimensions

Once the design β_o is established the cavity dimensions are set by the rf frequency choice. The beam is bunched at 11.7 MHz and the lowest frequency accelerating device is the RFQ at 35 MHz. In choosing the linac frequency we have decided to retain the future possibility of bunching at 35 MHz for some applications. A lower frequency increases the cavity length, hence reduces the required number of cavities but requires a longer inner conductor where mechanical oscillations may be problematic. In Table IX the cell structure for each cavity type is given assuming rf frequencies of 70, 105 and 140 MHz, the 6th, 9th and 12th harmonics of the bunch frequency, for the low-, mid- and high-β_o linac sections respectively.

Table IX: Specifications for the two cavity types. The accelerating voltage assumes a gradient of 5 MV/m.

Parameter	Low-β_o	Mid-β_o	High-β_o
No. of Cells	2	2	2
β_o (%)	4.2	7.2	10.6
f_{rf} (MHz)	70	105	140
λ (cm)	428	285	214
$\beta_o\lambda/2$ (cm)	9.0	10.3	11.3
Cavity Inner Diameter (cm)	18.	18.	18.
Cavity Height (cm)	107	71.3	53.5
E_g (MV/m)	5	6	6
$V_{acc}T$/cav (MV)	0.85	1.0	1.0

The lower frequency is chosen to match the bucket size of IH-DTL2 taking into account the opposing effects of the reduced relative longitudinal emittance with acceleration and the increase in the longitudinal emittance due to energy straggling in the stripping foil. The rf frequency can be increased with ion energy as the relative longitudinal emittance is reduced through acceleration. The three cavity diameters are identical at 18 cm while the cavity heights vary with frequency. This gives a fixed outer cavity diameter of 20.5 cm, hence a common cryostat diameter for all sections of about 1 m.
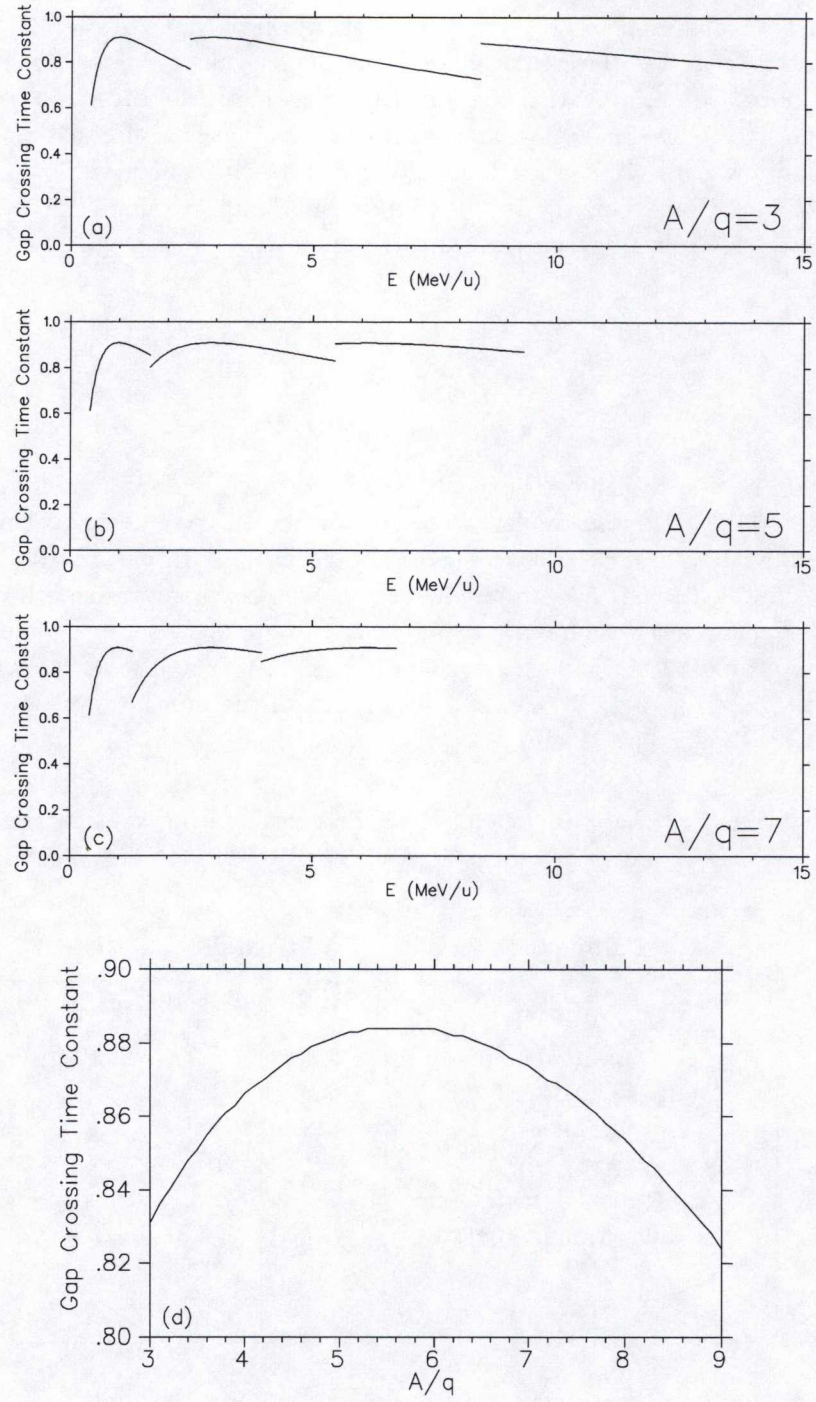
Figure 23: The acceleration efficiency as a function of particle velocity for various mass to charge ratios *(a,b,c)* using an optimized three-β_o accelerating scheme. In *(d)* the total acceleration efficiency is plotted as a function of A/q.
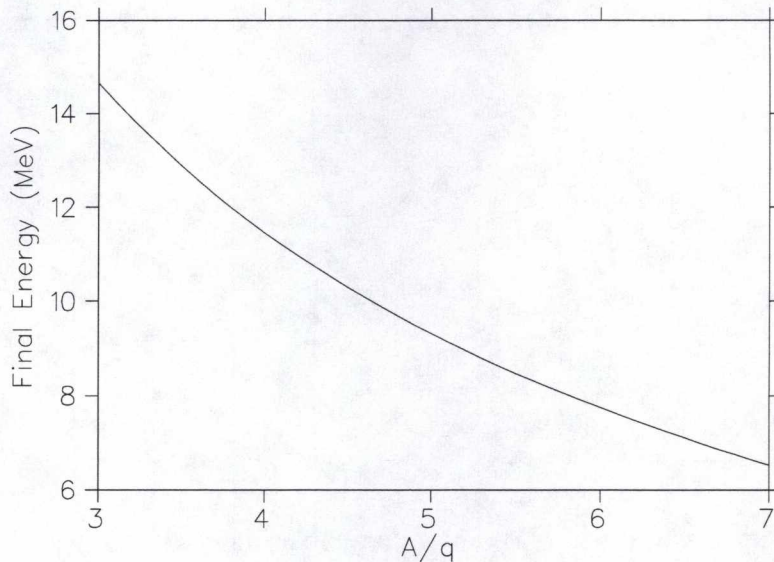
Figure 24: The final ion energy as a function of final mass to charge ratio.

Recent developments at Legnaro [42] (Fig. 25) have shown that cavities of bulk niobium or with niobium films sputtered on a copper substrate can deliver effective gradients consistently above 5 MV/m and in some cases as high as 8 MV/m with cooling loads of 7 W at 4°K. The ISAC-II design is based on effective gradients of 6 MV/m in the mid- and high-β_o sections and 5 MV in the low-β_o section. To allow for future developments the beam optics is based on gradients as high as 10 MV/m.

We opt for 8 low-β cavities (2 cryostats), 20 mid-β cavities (5 cryostats) and 20 high-β cavities (5 cryostats) for an effective voltage of 47 MV. The actual acceleration is normalized by the average synchronous phase; a synchronous phase of $-25°$ results in the required voltage gain of ~ 43 MV.

Linac Structure

Longitudinal focussing will be achieved by operating the cavities at a negative synchronous phase between -30° to -20°. This produces a net transverse defocusing due to the transverse fields near the entrance and exit of the acceleration gaps. Transverse stability will be maintained by periodic focussing between cryostats. Due to the strength of the accelerating fields and hence the rf defocusing, quadrupole triplets between each cryostat will be used to refocus the beam into the next cryostat. Beam transport using periodic triplets also has the advantage to keep the beam small in the accelerating sections. The beam size is maximum in the triplet and undergoes a waste in the center of the cryostat. This reduces emittance growth due to longitudinal-radial coupling. A schematic of one section of the superconducting linac is shown in Fig. 26.

The transverse focusing sections are 50 cm long for the low-β section and 60 cm long in the mid- and high-β sections with maximum gradients of 70 T/m. A short diagnostic box will be included in each inter-cryostat region. Even with a triplet every cryostat accelerating gradients are limited to 5 MV/m and 7.5 MV/m in the first two cryostats due to the large relative rf defocusing for the

Bulk niobium low beta cryostat n.6 - resonators performance <u>on-line</u>

Legend:
- Q1
- Q2
- Q3
- Q4
- 7W

Annotations on chart:
7 W

Alpi Design Requirements

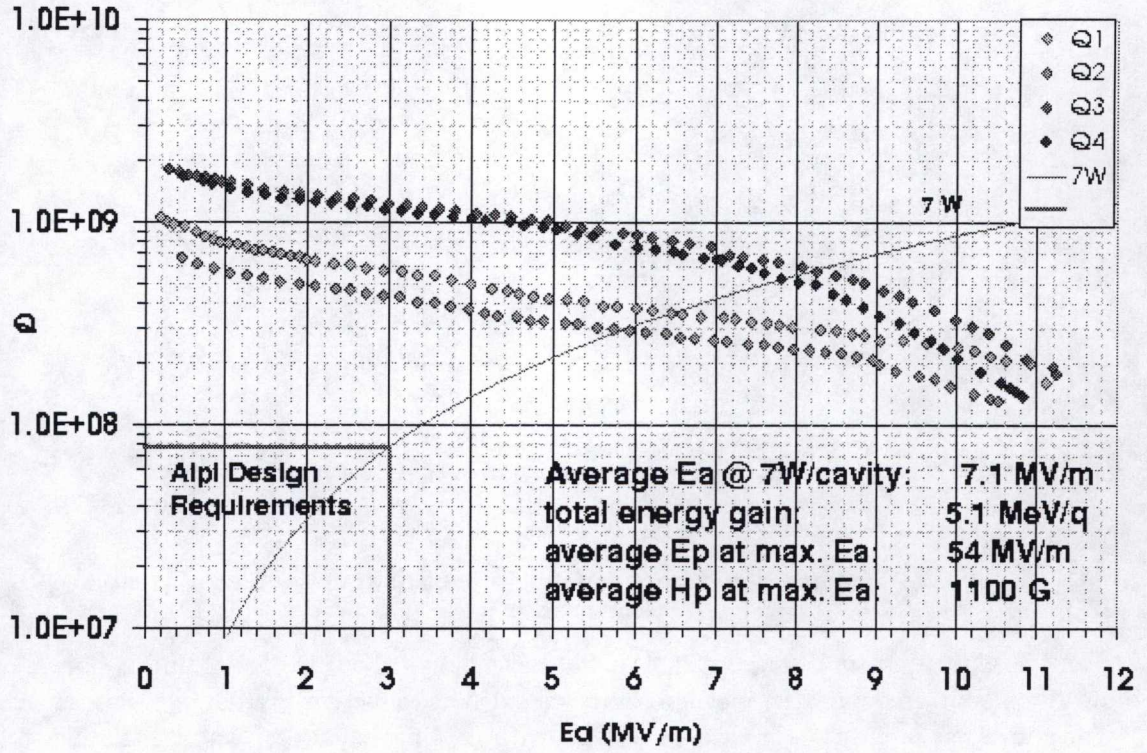|	
Average Ea @ 7W/cavity:	7.1 MV/m
total energy gain:	5.1 MeV/q
average Ep at max. Ea:	54 MV/m
average Hp at max. Ea:	1100 G

Figure 25: Recent accelerating gradients from the INFN-Legnaro low-beta bulk niobium cavities.

low velocity lighter ions. The lattice allows a gradient 10 MV/m in the remainder of the linac. A summary of the specifications for the post-stripper linac is given in Table X.

Table X: Specifications for each section of the post-stripper superconducting DTL.

Parameter	SC-DTL1	SC-DTL2	SC-DTL3
$E\ (A/q = 7)$	0.4-1.3 MeV/u	1.3-4.0 MeV/u	4.0-6.6
$E\ (A/q = 3)$	0.4-2.4 MeV/u	2.4-8.3 MeV/u	8.3-14.6
A/q	$3 - 7$	$3 - 7$	$3 - 7$
β_o	4.2	7.2	10.5
f (MHz)	70	105	140
N_{cav}	8	20	20
N_{cryo}	2	5	5
E_g (MV/m)	5	6	6
Length (m)	2.6	8	8
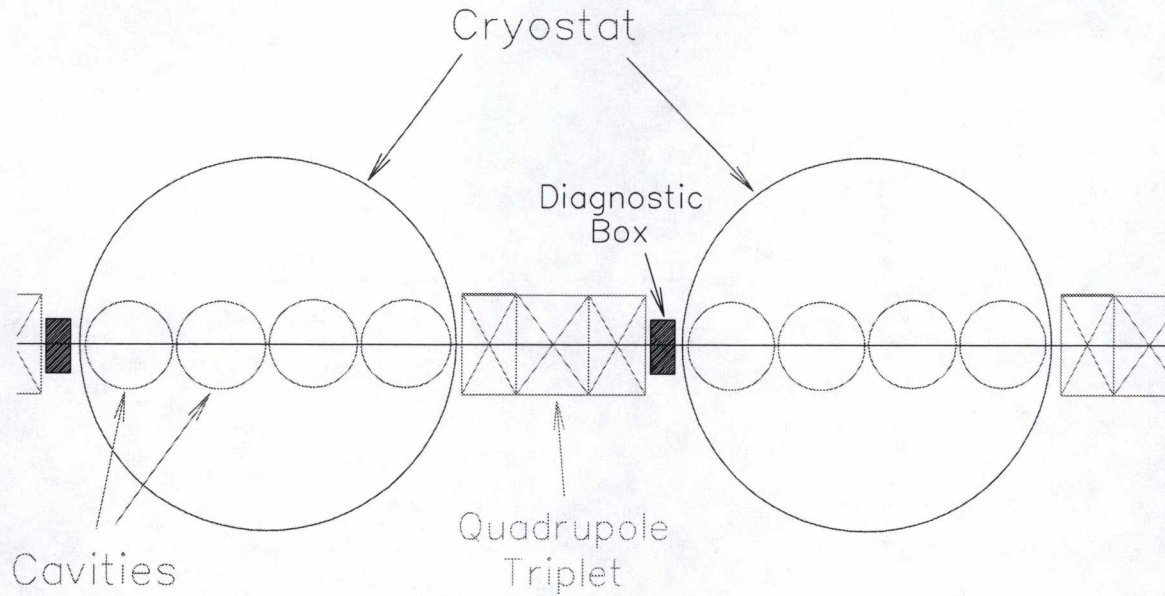
Figure 26: A schematic of a periodic section of SC-DTL1 and SC-DTL2.

Beam Simulations

Beams of initial emittance $\beta\epsilon_{x,y} = 0.2\,\pi$mm mrad and $1.6\,\pi$keV/u ns and for $A/q = 3$ and $A/q = 7$ were simulated in the linac code **LANA** [46] using a triplet every cryostat and a gradient of 5 MV/m. Growth in the transverse and longitudinal emittance was less than 5%. The longitudinal acceptance in both cases was 50π keV ns; 30 times larger than the design input beam. The transverse envelopes and beam energy for the two cases are shown in Fig. 27.

6.4.7 Cryogenic Loads

Judging by the experience at JAERI and INFN-Legnaro, modern cavities can operate at high gradient with reasonable loads on the cryogenic system. Cryogenic loads in these two laboratories have been based on cavity demands of $5-7$ W/cavity at 4°K. If the more conservative value is taken, a total cavity load of 340 W is obtained for 48 units. There is also substantial load in the transfer lines and cryostats of $10-15$ W/cryostat [47]. Therefore ISAC-II will require a refrigerator capacity of $\sim$500 W at 4°K. This is in a size range operating at many labs. Both over-capacity and redundancy are recommended in a linac cryogenic system. To this end two 500 W systems operating in parallel would be installed, one in the first stage (see Section 6.5) and the second during the second-stage installation.

The cryogenic system consumes approximately 500 W of wall power for each Watt at 4°K[48] for an expected power consumption of 500 kW for two 500 W systems.

6.5 Installation Procedure

The ISAC-II project requires a grade level addition to the ISAC experimental building to the north. The experimenters have requested some beam at an energy of $5-6$ MeV/u by 2003. This
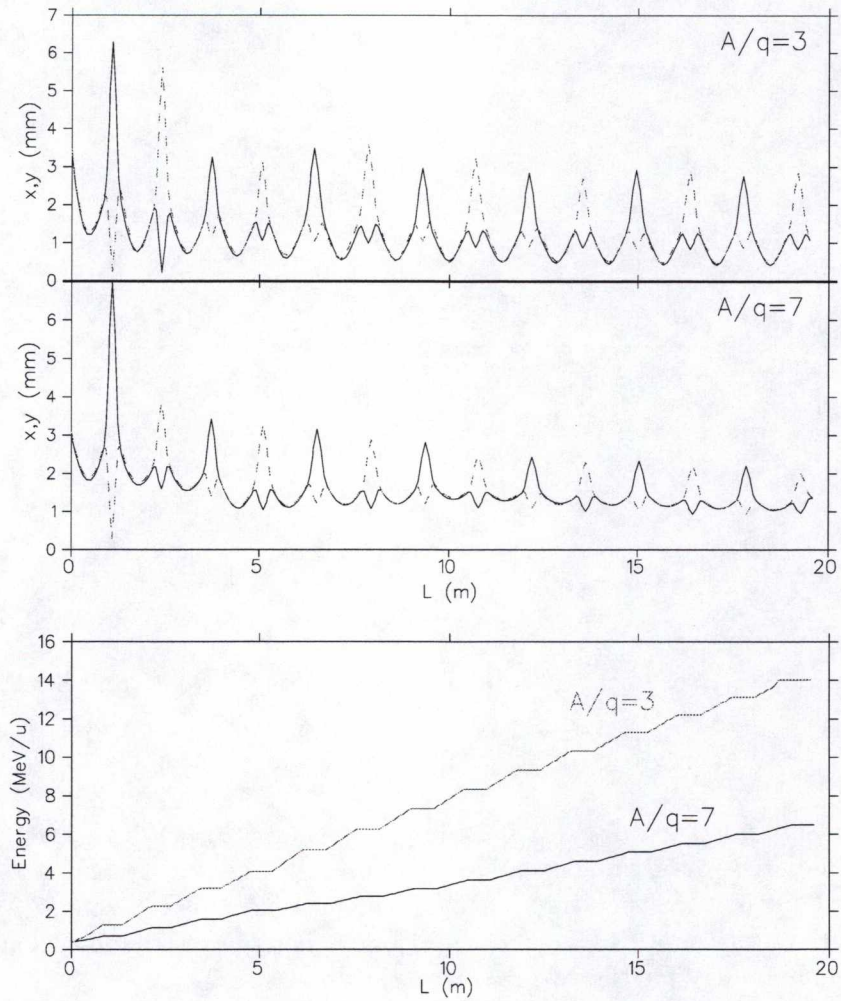
Figure 27: Beam envelopes (x is the solid line and y the dashed) and beam energy for the ISAC-II post-stripper linac for design particles of A/q of 3 and 7.

intermediate stage (termed Stage 1) is most easily realized by increasing the energy of the 1.5 MeV/u $A/q \leq 6$ particles from the ISAC-DTL with a booster linac of 20 mid-β cavities. The 20 MV of accelerating voltage would produce final energies from $4.5 - 7.5$ MeV/u for ions up to $A \leq 60$.

It is feasible to install this linac in a temporary location in the existing experimental hall with the idea to re-locate the linac in the final location after the building is complete. However, the most efficient way to satisfy the 2003 beam requirement would be to complete the new building addition by April 2002 and install the Stage 1 linac in the new ISAC-II building. Such a construction milestone is feasible given clearance from the regulatory authorities to proceed. A transfer line from the ISAC DTL to the new building would be required but it is only slightly more involved than the transport line that would be required downstream of DRAGON to supply the temporary linac position. In this scenario, beam could be delivered to users by June 2003. The remainder of the linac including IH-DTL2 and low- and high-β sections of the linac could be installed for full operation in April 2005. A schematic of the proposed staging is shown in Fig. 28.

ISAC-II — 2001

ISAC-II — 2003
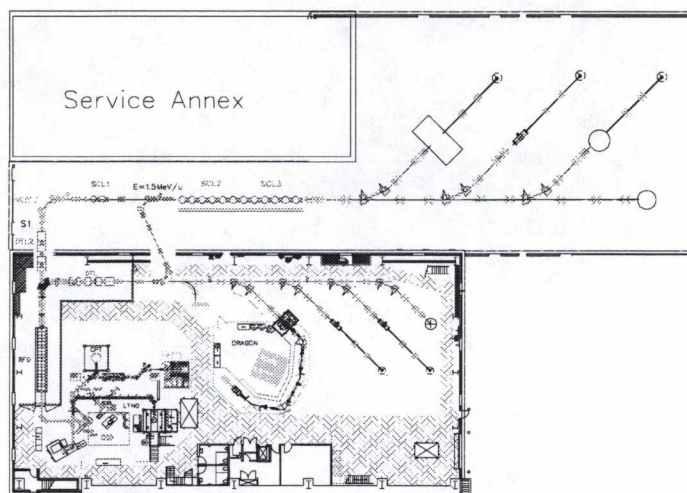
Service Annex

ISAC-II — 2005

Service Annex
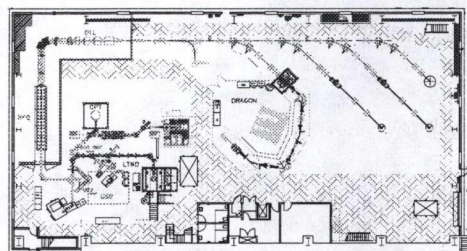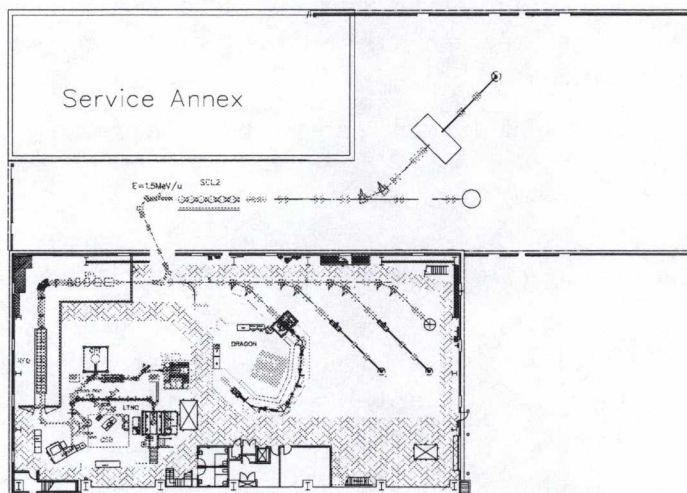
Figure 28: An installation scenario to satisfy an experimental program as early as 2003.

57

Design of the new building must begin by April 2000 with construction 10 months later. A test cryostat and resonator preparation and assembly area should be readied by the end of 2000. Design of a new mid-β cavity should begin as soon as possible with prototyping to begin Feb. 2000. The prototype would be tested in the test cryostat facility a year later. Once tests prove successful an order would be placed for 20 mid-β cavities. It seems reasonable that the five assembled cryostats of mid-β cavities could be ready for installation in the new building beginning June 2002. A transfer line connecting the existing ISAC IH-DTL1 and the new SC-DTL2 would be installed simultaneously.

To achieve the final ISAC-II specifications the IH-DTL2, MEBT2, two low-β cryostats and five high-β cryostats of the superconducting linac would be added to reach the final design. The installation of the low-energy portions of this line could be done with only minor interference with high-energy beam delivery to the experimenters. The five high-β cryostats could be installed during a shutdown of the high-energy line.

Final energy and acceleration efficiency plots are given for the two configurations in Fig. 29(a,b). The acceleration efficiency is defined as the fraction of ions from the ion source (or charge-state booster) reaching the highest energy. The total efficiency including the efficiency of the charge-state booster is given in Fig. 29(c). This plot assumes: *(a)* 100% CSB efficiency, *(b)* CSB efficiencies of 25%, 20%, 15%, 10% for $q = 2, 3, 4, 5$ respectively, and *(c)* CSB efficiencies of 10% for all charges.

In general, higher energies and intensities can be obtained for lower masses. There are tradeoffs possible between energy and intensity. For example, a maximum energy of 10 MeV/u even for mass 150 would be available in the completed ISAC-II, albeit at a considerably reduced intensity, with the addition of a second stripping foil before the high-β section.

The projected beam intensities at ISAC-II can be obtained by multiplying the ISAC-I beam intensities given in Table I by the appropriate transmission and charge-state booster efficiencies of Fig. 29(c).

6.6 Building/Infrastructure Upgrades

To deliver the ISAC scientific program for the next five-year plan requires extensions to the present building and infrastructures and upgrades of some of the existing facilities. The building upgrade plan includes an expansion to the north in the lower parking lot outside the current TRIUMF perimeter. This land is part of the UBC Discovery Park reserve. As a preliminary estimate approximately 70,000 ft^2 of land space is required for the conventional facilities. A proposed building arrangement is shown in Fig. 30.

The building addition includes a new, high-bay experimental hall at the same grade level and alongside the ISAC-I hall and ancillary buildings to house services and staff.

The experimental hall will house the superconducting linear accelerator, the experimental beam lines and stations, and support/auxiliary services.

It is anticipated that the following services will be housed in the ISAC-II experimental hall:

- counting rooms for experimenters,

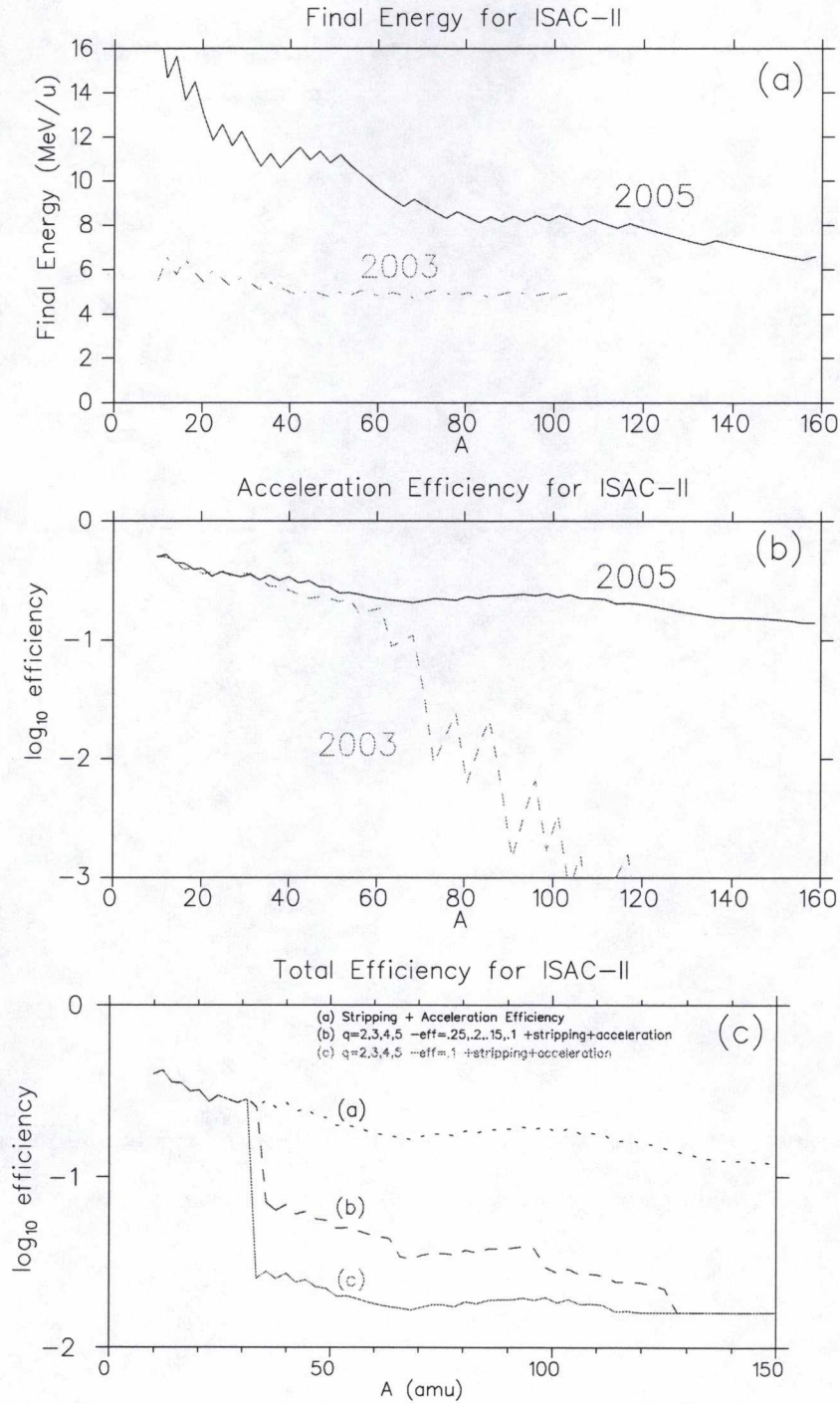- cryogenic systems and associated controls,

Figure 29: *(a)* Final energy and *(b)* acceleration efficiency for the two stages of ISAC-II construction shown in Fig. 28. Plot *(c)* shows the estimated total efficiency of the final stage including the conversion efficiency of the CSB.
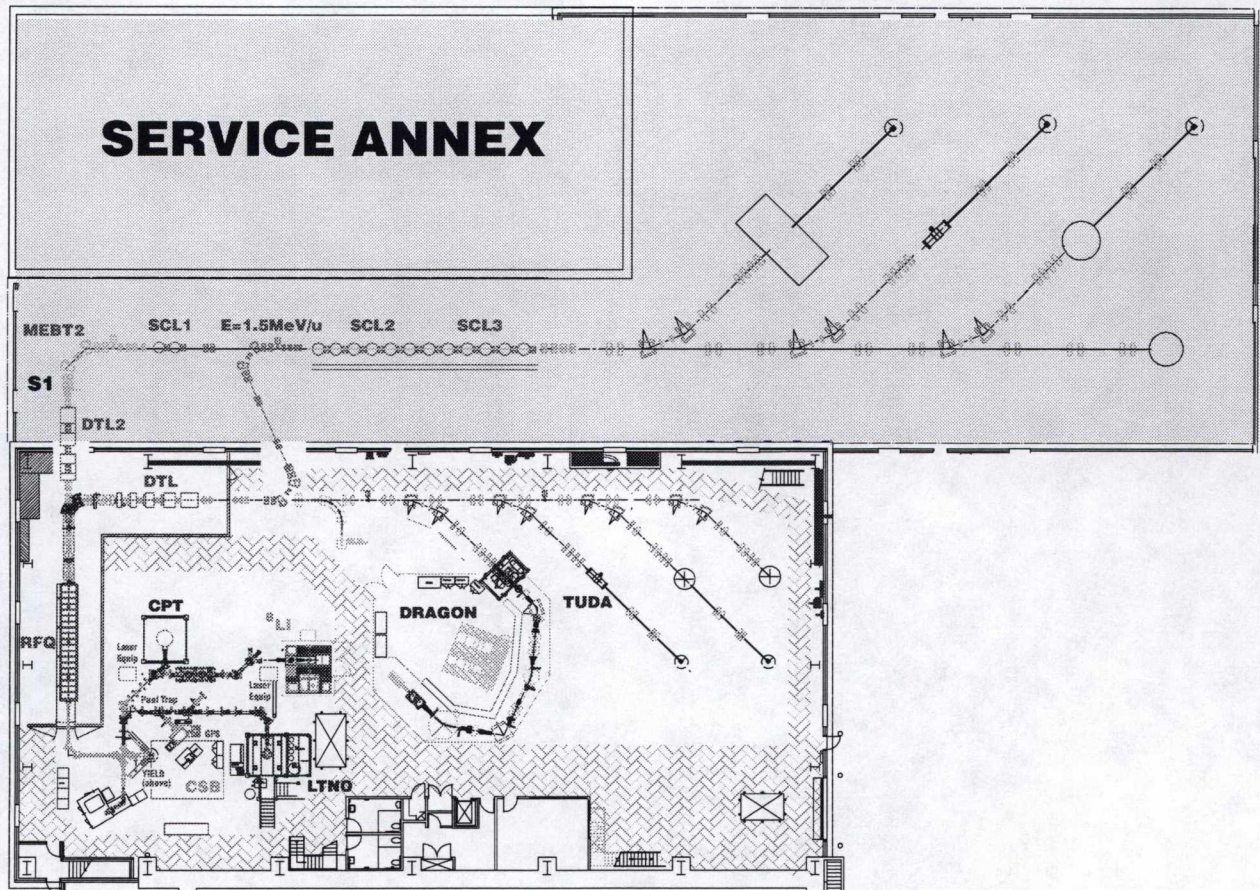
ISAC II - 2005

Figure 30: Building layout.

- technical support services for the experimental facilities (assembly and machine shop),

- decontamination facilities and storage for radioactive material,

- beam line shielding,

- electrical and mechanical services for beam lines,

- overhead cranes,

- other services (meeting rooms, storage, toilets, showers, etc.).

Some services must be housed in dedicated buildings adjacent to the experimental hall:

- the Helium compressor stations, as close as practical to the superconducting LINAC,

- the experimental gas storage and handling facility,

- offices for approximately 70 staff,

- laboratory space for assembling and testing of new accelerator components,

- general building services.

A necessary infrastructure for the ISAC science program is a "hot" chemistry laboratory for the development of new targets and processing of radioactive material. Other systems requiring upgrade include the ISAC-I data and voice networks, mechanical and electrical infrastructures to serve ISAC-II.

The conventional facility plan also includes modifications to the present access raodway, the addition of a ring road around the new buildings and fire lanes around the new and existing buildings.

It is anticipated that the shipping and receiving service will have to be relocated to TRIUMF's west entrance.

The building upgrade can be completed in approximately 24 months from the date the funds are available.

7   Safety Issues

The safety issues relevant to ISAC-II will, for the most part, be no different from those already encountered during the operation of ISAC-I. For example, the radiation fields generated by the decay of deposited radioactive ions will be similar to those in ISAC-I. However, the ISAC-II accelerator will be capable of accelerating ions to an energy of approximately 10 MeV per nucleon and up to 15 MeV per nucleon for very light ions. As the ions are accelerated to an energy above the Coulomb barrier, they will, on collision with targets, collimators and beam stops, give rise to nuclear reactions that will produce neutrons.

The highest intensity ion beams will be obtained with stable ions during development and tuning. There may also be some interest in experiments using beams of accelerated stable ions. The highest intensity to be considered for *radioactive* ions is the same as for ISAC-I, i.e. 4×10^{10} s^{-1}. For *stable* ions the maximum intensity available will be much greater. Up to 2 particle μA (1.2×10^{13} s^{-1}), at an energy of 10 MeV/u, may be used for some experiments. It is the operation with stable ions which will set the requirements for shielding against neutrons. The accelerator and at least one beam line will therefore be shielded to allow operation at this level.

7.1   Source Term

Until recently shielding for heavy-ion accelerators has been only of academic interest as the beam intensities and energies available did not require a large investment in shielding. Often existing proton accelerators have been modified to accelerate heavy ions at a great penalty in beam intensity so that existing shielding was more than sufficient.

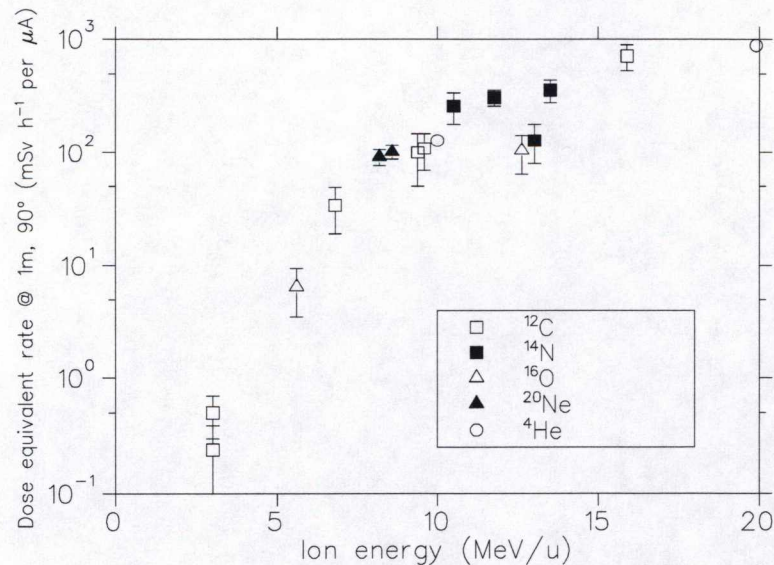Measurements by Ohnesorge *et al.* [49] of the neutron dose equivalent rates at 1 m and 90°

Figure 31: The fast neutron equivalent dose rates per particle μA 1 m from thick targets of iron, nickel or copper and 90° from the incident heavy-ion beam direction.

from the incident ion beam direction are reproduced in Fig. 31. The dose rate for ions incident on thick targets of iron, nickel or copper is seen to vary quite smoothly with energy and is more or less independent of ion species, at least for light ions. At an ion energy of 10 MeV/u the source term at 90° is 100 mSv h^{-1} per particle μA of ions stopped. For the maximum *radioactive* ion beam intensity of $\sim 4 \times 10^{10}$, the neutron dose rate from the stopped beam would be ~ 600 μSv h^{-1}. For the maximum *stable* ion beam of 2 particle μA, the neutron dose rate would be 200 mSv h^{-1} at 90°.

Aleinikov *et al.* [50] have measured the angular dependence of the neutron dose equivalent rate for 6.6 MeV/u ^{58}Ni ions bombarding a thick Cu target and Bertini *et al.* [51] have calculated double differential production cross sections for neutrons produced by 16 MeV/u ^{12}C ions on ^{56}Fe. Both find that the neutron production in the forward direction is approximately an order of magnitude greater than at 90°.

7.2 Shielding

The attenuation of neutron dose equivalent in concrete for source neutrons of 1 and 10 MeV is shown is Fig. 32. The energy spectrum of the neutrons generated when stopping heavy ions will be a typical evaporation spectrum although it may extend to energies 2 to 3 times that of the average kinetic energy of the nucleons in the incident ion (Bertini *et al.* [51]). Neutrons with $E_n \leq 0.1$ MeV do not contribute very much to the dose equivalent and therefore the attenuation of the neutron dose rate can be characterized by those with energy of a few MeV. The thickness of shielding needed depends on the fraction of the ion beam stopped at any given point, the mean energy of the neutrons produced and the source to shield distance. The losses in the accelerator are expected to be $< 1\%$ in total and hence for chronic losses the lateral shielding may be fairly light, i.e. less than about 1 m of concrete.
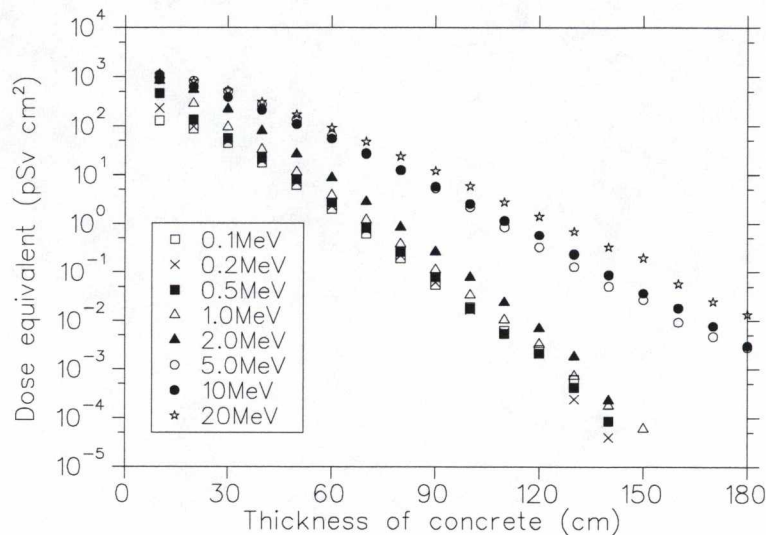

Figure 32: Attenuation of neutron dose equivalent in concrete for neutrons of energy 0.1 and 20 MeV.

63

For more significant loss points, e.g. collimators, experiment interaction regions and beam dumps, of the order of 1 m concrete will be required laterally and about 2 m in the forward direction.

Any field point in direct, unshielded view of the source produced by stopping the entire 2 particle μA of ion beam, even at distances of the order of the dimension of the building that will house the facility $(10-30$ m), would be exposed to a neutron dose equivalent rate of $1-0.1$ mSv h^{-1}. Therefore, in order to avoid undesirable restrictions on accessibility to mezzanines and cranes, it will also be necessary to install roof shielding over these source points.

8 Manpower, Costs and Schedule

It will be necessary to expand the ISAC floor space. Most of the expansion will be a high-bay grade-level construction along the north and east of the present experimental hall. A multi-level office wing will be required along the West wall of the building to accommodate the displaced trailer offices. The estimated cost is approximately $15M, which would come from the Provincial Government of British Columbia. The building would be available for occupancy in 2002.

A task-by-task manpower and cost estimate has been done for the ISAC-II project. For sake of example we present here the installation scenario presented in Section 6.5. In year 1 and 2 the charge-state booster, (CSB) and associated LEBT will be assembled in the experimental hall. Work will also proceed on the mid-β superconducting rf cavities. A prototype of the cavity will be fabricated and tested in the first year while in years two and three 20 (5 cryostats) mid-β cavities will be received and installed in the completed ISAC-II hall along with a short transport section (HEBT Transfer) to permit experiments by year end. The low- and high-β cavities room temperature IH linac and MEBT2 components would be procured in year 4 for assembly and installation in year 5.
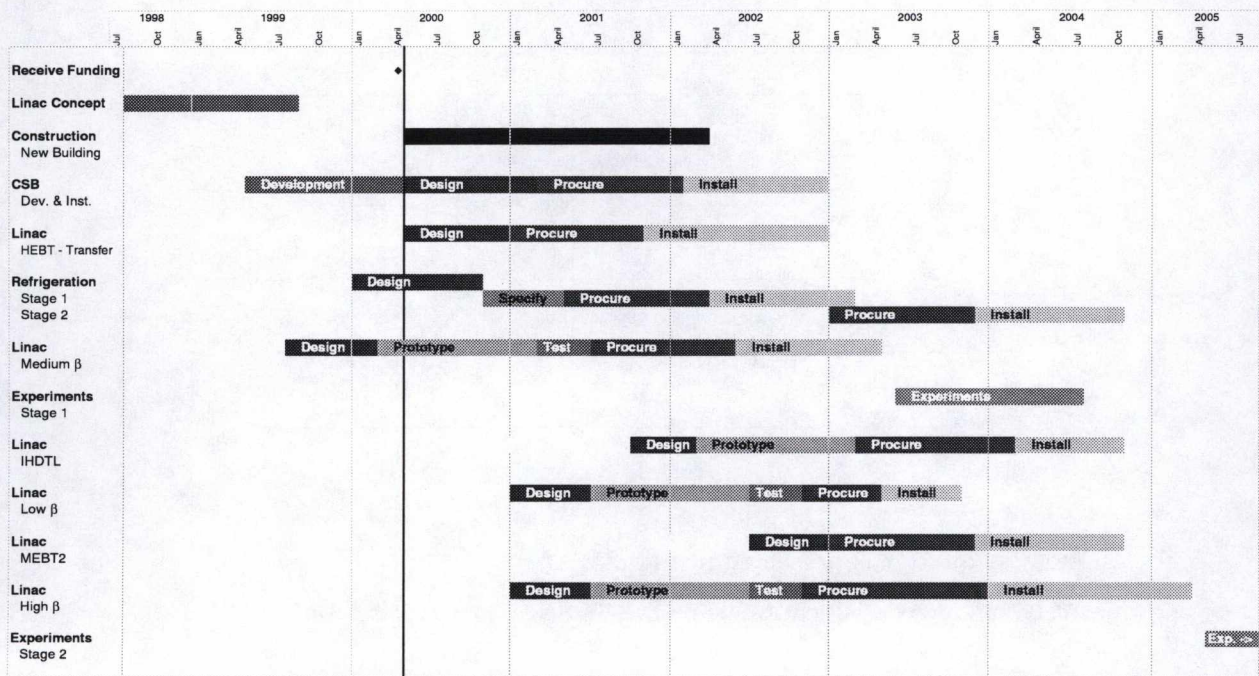

Figure 33: Gant chart of ISAC-II major milestones.

A summarized Gant chart of the installation is shown in Fig. 33. This schedule forms the basis of a more detailed task-by-task Gant chart, which is used to chart manpower and cash flow.

Each main device (i.e., IH-DTL2) is broken down into components, then sub-components, then tasks. Each task is fixed with a manpower allocation using the following categories: physicist, engineer, rf engineer, mechanical technician, electrical technician, rf electrical technician, control technician, vacuum technician, electrician and plumber. Each item is fixed with an estimated cost including capital costs, fabrication and installation costs and associated overhead (i.e., controls,

safety, services etc.). In all cases the internal manpower cost is not included. The cost of the building is also not included.

In some cases, where strategies are not presently well defined, a bulk cost estimate is used with a conservative contingency. This is especially true in the case of the charge-state booster where a definite solution has not yet been chosen. A budget amount of $2M has been allocated to develop, procure, install and commission the CSB. In the case of the superconducting linacs the costs have been gathered by talking with many existing laboratories: Argonne, New Delhi, Legnaro and JAERI. In particular, recent numbers for cavity fabrication in North America have been used. The cost of the refrigeration units has been estimated from North American labs, who have recently purchased systems of the scale required by the ISAC-II project. Finally the costing of the standard beam line and IH-DTL components comes from our experience with ISAC-I.

The results of the estimations are shown in Figs. 34–37. We present the expected accumulated expenditure in Fig. 34. The total estimated cost of $18M is broken down by project.

Costs and performance of ISAC-II are summarized in Table XI.

Table XI: Cost summary for ISAC-II.

Components	A_{max}	E_{max} MeV/u	ΔCost ($M)	ΣCost ($M)	Year
ISAC-I	30	1.5			1
Stage 1	60	4.8	9	9	2.5
Stage 2	150	6.5	9	18	5

The cash flow by quarter is presented in Fig. 35.

The quarterly manpower allocation is shown in Fig. 36 by job type and then by project in Fig. 37.

The peaks in the plot will be averaged out in practice as the quarter-by-quarter activities are shifted for most efficient use of personnel. In general, some 30 fully-employed people are required over most of the project. Some overlap with ISAC-I completion can be done in the first year.
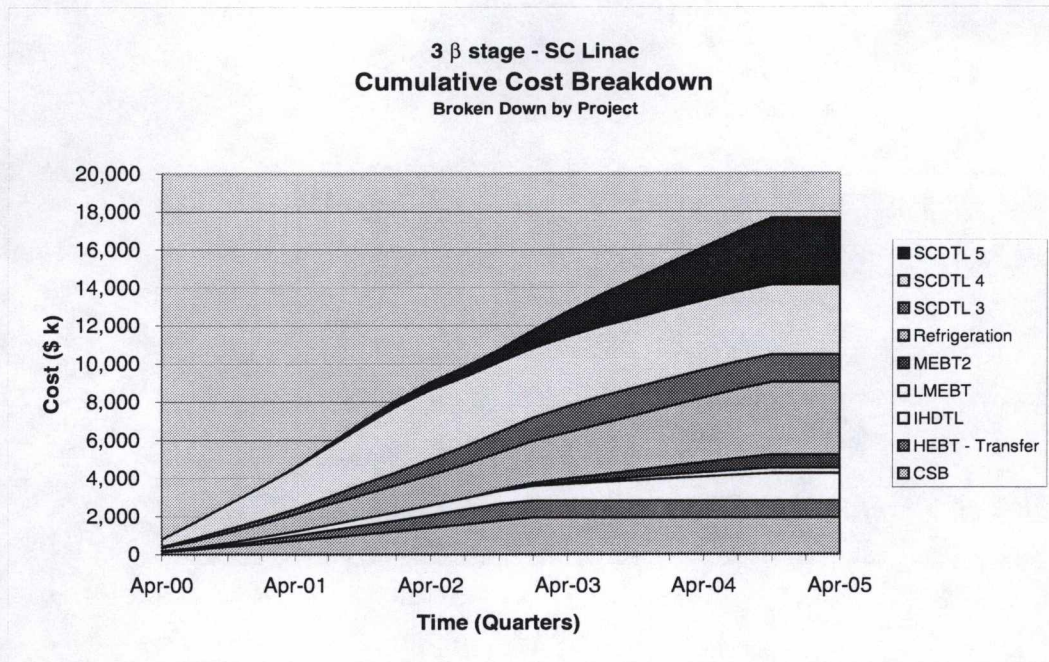
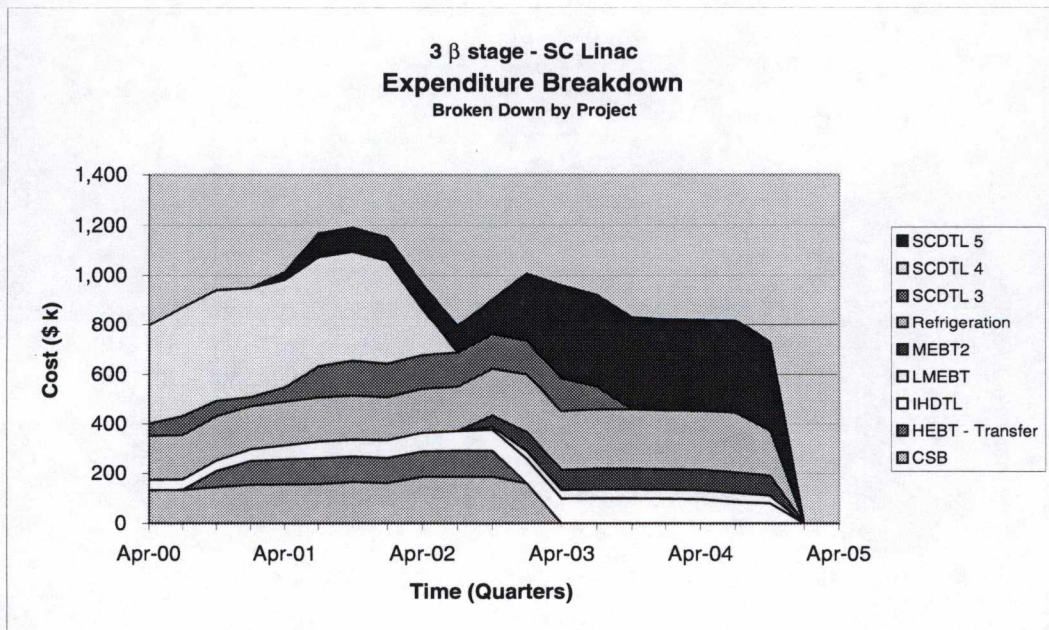Figure 34: Accumulated expenditures by project.

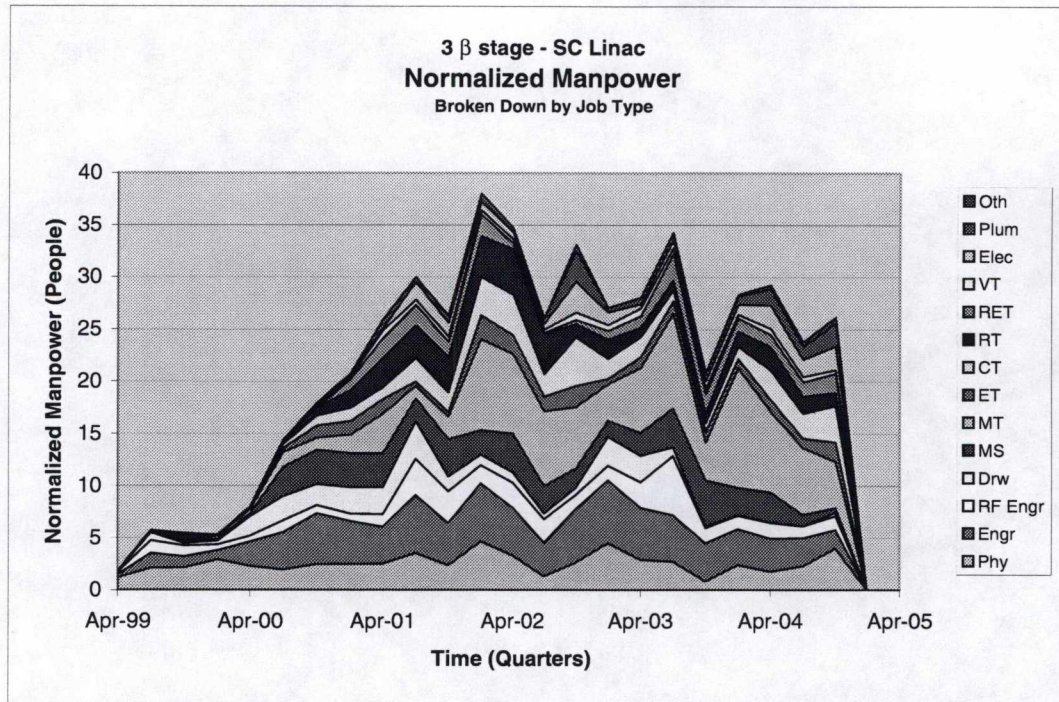Figure 35: Expected cash flow in each quarter by project.

67

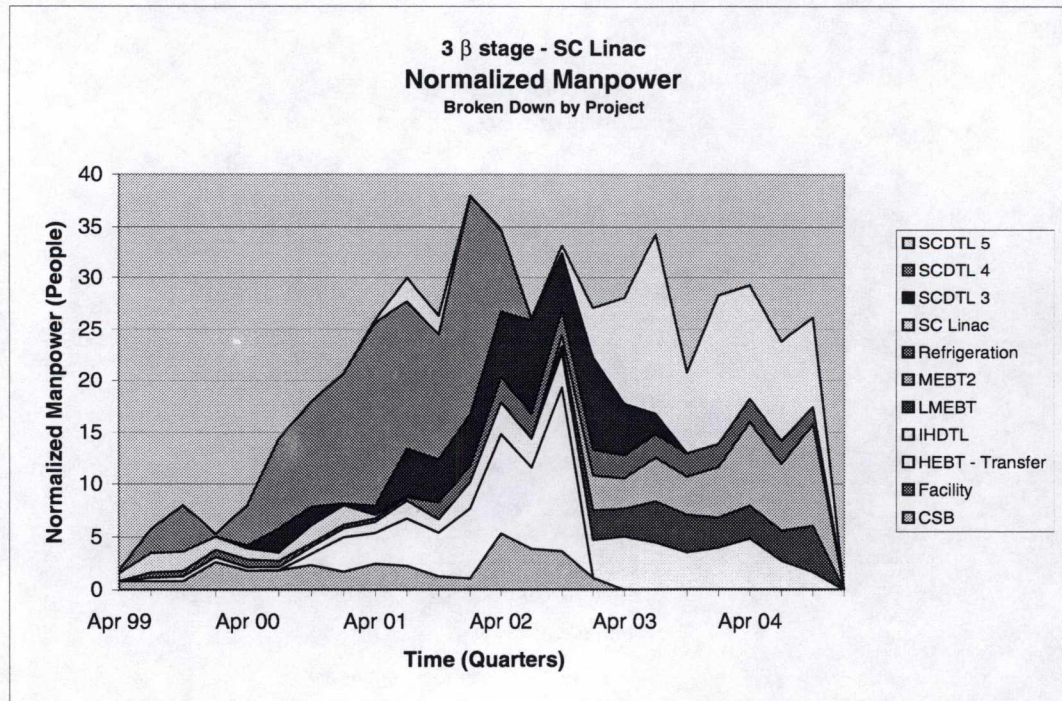Figure 36: Manpower allocation as a function of job type.

Figure 37: Manpower allocation as a function of project.

68

9 Future Considerations

9.1 Higher Energy Operation

The flexibility of the super-conducting linac structure also allows further expansion capabilities well into the future. There is considerable interest in exploiting the high quality beams typical of ISOL based facilities at energies associated with fragmentation facilities. A stripping stage at $1.5-3$ MeV/u could be added yielding almost fully stripped ions, $A/q \leq 3$, for lighter masses. Future cavity development and an upgraded refrigerator system could result in accelerating gradients approaching 10 MV/m yielding final energies of 20 MeV/u with no additional cavities. The addition of 6 cryostats of high-gradient cavities with a $\beta_o=16\%$ would give an additional voltage gain of ~ 30 MV and final energies near 30 MeV/u. The length of the linac addition would be ~ 8 m and is compatible with the layout of the proposed ISAC-II building extension.

9.2 Thoughts on Simultaneous User Modes for ISAC

The switchyard in the LEBT of the ISAC Experimental Hall has been designed to permit simultaneous independent beams to the LE and HE areas. The goal was to have a radioactive beam in one area and a stable beam from the off-line ion source in the other area. To make ISAC more cost effective the goal could be to make the two areas have simultaneous (but different) radioactive ion beams. If one of the areas uses a longer half-life (say hours or days, such as ^{7}Be), then the longer lived product can be transferred in batch mode to the off-line ion source on the experimental floor [or a second ion source in the same region]. Another approach would be to use a He gas jet as was done, quite successfully for certain materials, at TASCC, LAMPF and TRIUMF. The gas jet technique is used to transport recoiling reaction products from a thin target to some location far from the high radiation area. Since there are a number of elements that are not released efficiently from a thick ISOL target, such as group-6 and -7 elements, the gas jet approach could be used to transport such reaction products from a thin production target located near the ISAC target to an ion source located at a considerable distance from the target. The ion source could be located in the mass separator pit with a second mass separator and LEBT bringing the beam near the off-line ion source, or the ion source could be the off-line ion source with a slightly improved mass separator. Our target modules are large enough to support a gas jet target either in front of or behind the ISAC targets. Another approach might be to build another driver. Louvain-la-Neuve has shown that certain light elements can be produced very efficiently with a high current 30 MeV cyclotron. For DRAGON, ^{15}O is required at high intensities. This and certain other light isotopes can be produced very efficiently with a 30 MeV cyclotron. A new vault could be built to the west of the target cave to house a 1 mA, 30 MeV TR30 cyclotron. The cyclotron, vault, ion source and mass separator would be less than about $8M. Finally, one could contemplate extracting a dual beam down BL2A with a split foil (experimentally demonstrated in BL1A). A magnetic septum could divert the beams towards the East and West targets simultaneously. It would be convenient for the beams to have slightly different vertical elevations at the targets, since then the radioactive ion beams would also be at different elevations. In the present scheme the pre-separator allows one to choose only one target at a time. A second pre-separator could be mounted above it if the beams were sufficiently separated.

References

[1] Report of the Study Group on Radioactive Nuclear Beams (OECD Megascience Working Group on Nuclear Physics, 1999).

[2] ISAC – a proposal for an intense radioactive beams facility, TRI-95-1, October 1995.

[3] J-M. Poutissou, Nuclear Physics News, Vol. **8**, No. 3 (1998) 11.

[4] L. Buchmann, Physics in Canada, Vol. **22**, No. 2 (1999) 53.

[5] ISAC-I proposal, Submissions to the Long Range Planning Committee of TRIUMF, (Canada, 1993).

[6] RI Beam Factory: Basic Science, RIKEN Accelerator Research Facility Report, (August 1994).

[7] Long Range Plan of the Nuclear Science Advisory Committee (USA, 1996).

[8] *"Scientific Opportunities with an Advanced ISOL Facility"*, OSC Symposium White Paper, November 1997, available from http://www.phy.ornl.gov/nisol/nisol_ref.html.

[9] *"Proposal for Japan Hadron Facility"*, KEK Report 97-3, (Japan, 1997).

[10] *"Nuclear Physics in Europe: Highlights and Opportunites"*, report from the Nuclear Physics European Collaboration Committee (Europe, 1997).

[11] SIRIUS Science (CLRC, U.K., 1999).

[12] Physics Today, **52**, No. 4 (1999) 21.

[13] W. Satula, D.J. Dean, J. Gary, S. Mizutori and W. Nazarewicz, Phys. Lett. B **407** (1997) 103.

[14] R. Coszach *et al.*, Phys. Rev. C **50** (1994) 1695.

[15] D.R. Tilley, H.R. Weller, C.M. Cheves and R.M. Chasteler, Nucl. Phys. A **595** (1995) 1.

[16] P. Decrock *et al.*, Phys. Rev. C **48** (1993) 2057.

[17] K.E. Rehm *et al.*, Phys. Rev. Lett **80** (1998) 676.

[18] R.F. Casten, J. Phys. G: Nucl. Part. Phys. **24** (1998) 1409.

[19] C.J. Barton, R.F. Casten *et al.*, Letter of Intent, (1998).

[20] M. Wiescher, Int. Conf. on Exotic Nuclei and Atomic Masses (ENAM), Michigan, (1998).

[21] S. Hofmann *et al.*, Z. Phys. A **354** (1996) 229.

[22] N. Takigawa, M. Kuratani and H. Sagawa, Phys. Rev. C **47** (1993) R2470.

[23] K.E. Zyromski *et al.*, Phys. Rev. C **55** (1997) R562.

[24] L. Gingras *et al.*, Proc. of the XXXVI Int'l. Winter Nucl. Phys. meeting, Bormio, (1998).

[25] J.P. Martin *et al.*, Nucl. Inst. and Meth. **A257** (1987) 301.

[26] V. Ninov, P. Armbruster, F.P. Hessberger, S. Hofmann, G. Münzenberg, Y. Fujita, M. Leino and A. Lüttgen, Nucl. Inst. and Meth. **A357** (1995) 486.

[27] K.E. Rehm, C.L. Jiang, M. Paul, D. Blumenthal, J. Gehring, D. Henderson, J. Nickles, J. Nolen, R.C. Pardo, A.D. Roberts, J.P. Schiffer and R.E. Segel, Nucl. Inst. and Meth. **A370** (1996) 438.

[28] M. Paul, B.G. Glagola, W. Henning, J.G. Keller, W. Kutschera, Z. Liu, K.E. Rehm, B. Schneck and R.H. Siemssen, Nucl. Inst. and Meth. **A277** (1989) 418.

[29] R. Geller, *"Development of ECR Plasmas for Radioactive Ion Beams"*, Proceedings of HIAT98, Argonne Nat. Lab. 1998, to be published.

[30] E. Baron and Ch. Ricaud, *"Beam Foil Interaction Studies for the Future Stripper of GANIL"*, EPAC'88.

[31] K. Shima, N. Kuno, M. Yamanouchi and H. Tawara, Atomic Data and Nuclear Data Tables **51** (1992) 173.

[32] E. Nolte *et al.*, Nucl. Inst. and Meth. **158** (1979) 311.

[33] R.E. Laxdal, *"The Separated Function Drift Tube Linac for ISAC"*, TRIUMF Design Note TRI-DN-97-04 (April, 1997).

[34] U. Ratzinger, *"A Low Beta RF Linac Structure of the IH type with Improved Radial Acceptance"*, Proceedings of 1988 Linear Accel. Conf., Newport News, Virginia (June, 1989).

[35] L.M. Bollinger *et al.*, Proc. 1976 Proton Linear Accel. Conf., Chalk River, AECL-5677 (1976) 95.

[36] G.J. Dick and K.W. Shepard, Appl. Phys. Lett. **24** (1974) 40.

[37] I. Ben-Zvi and J.M. Brennan, Nucl. Instr. and Meth. **212** (1983) 73.

[38] K.W. Shepard, J.E. Mercereau and G.J. Dick, IEEE Trans. Nucl. Sci. **22** (1975) 1179.

[39] K.W. Shepard, IEEE Trans. Nucl. Sci. **32** (1985) 3574.

[40] L.M. Bollinger, Ann. Rev. Nucl. Part. Sci. **36** (1986) 475.

[41] S. Takeuchi, T. Ishii and H. Ikezoe, Nucl. Inst. and Meth. **A281** (1989) 426.

[42] A. Facco, *"Superconducting Cavity Development at Legnaro"*, Proceedings of HIAT98, Argonne Nat. Lab. (1998) to be published.

[43] V. Palmieri, Part. Accel., **53** (1996) 217.

[44] A. Lipski *et al.*, *"An Environment-Friendly Method for Resonator Surface Fabrication"*, Proceedings of the HIAT98 Conference, Argonne Nat. Lab. (1998) to be published.

[45] S. Takeuchi, T. Ishii, H. Ikezoe and Y. Tomita, Nucl. Instr. and Meth. **A287** (1990) 257.

[46] D.V. Gorelov and P.N. Ostroumov, *"The* LANA *Computer Code for the Beam Dynamics Simulation in Multi-Cavity Linacs"*, INR Internal Report (1993-1994).

[47] I. Ben-Zvi, Nucl. Instr. and Meth. **A287** (1990) 216.

[48] D. Storm, private communication.

[49] W.F. Ohnesorge *et al.*, Health Physics, **39** (1980) 633.

[50] V.E. Aleinikov *et al.*, Radiation Protection Dosimetry, **11** (1985) 245.

[51] H.W. Bertini, R.T. Santoro and O.W. Hermann, Phys. Rev. **C14** (1976) 590.